Studies on enzymes involved in dissimilatory nitrogen metabolism in *Aspergillus oryzae*

(麹菌の窒素異化代謝に関わる酵素の研究)

東京大学大学院農学生命科学研究科応用生命工学専攻
平成 18 年度博士課程　　進学
氏名　　周勝敏
指導教員　祥雲　弘文

Table of contents

Abbreviations

FHb	flavohemoglobin
NOD	NO dioxygenase
FHP	*Alcaligenes eutrophus* FHb
YHB	*Saccharomyces cerevisiae* FHb
HMP	*Escherichia coli* FHb
Fre	*E. coli* flavin reductase
NRase	nitrate reductase
Nas	bacterial cytoplasmic assimilatory nitrate reductase
NarG	bacterial membrane-bound respiratory nitrate reductase
NapA	periplasmic nitrate reductase
dNar	dissimilatory nitrate reductase
dNir	dissimilatory nitrite reductase
P450nor	P450 type nitric oxide reductase
N2Or	nitrous oxide reductase
CYP55A5	*A. oryzae* P450nor encoding gene
NOC-18	1-Hydroxy-2-oxo-3,3-bis(2-aminoethyl)-1-triazene; NO generator
GSNO	S-nitrosoglutathione, NO generator
IPTG	isopropyl-1-thio-Д-D-galactopyranoside

Introduction

1. The biological nitrogen cycle

Nitrogen is a basic element for life because it is an essential component of most bio-organic substances, such as amino acids, proteins, vitamins and nucleic acids. It exists in the biosphere in several redox states, ranging from N (+V) (in nitrate) to N (–III) (in ammonia). Interconversions of these nitrogen species constitute the global biogeochemical nitrogen cycle (Figure 1). These processes are in principal based on the redox reactions of nitrogen compounds catalyzed by microorganisms. Briefly, inorganic nitrogen is converted to a biologically useful form by dinitrogen fixation or nitrate assimilation and the further incorporation of ammonia. Nitrogen is removed from the environment by both nitrification, the oxidative conversion of ammonia to nitrate, and denitrification, a respiratory process whereby nitrate is successively reduced to nitrite, N oxides (NO and N_2O), and dinitrogen (N_2).

2. The assimilatory and dissimilatory nitrogen metabolisms

The nitrogen metabolisms can be categorized into two types, assimilatory and dissimilatory metabolism, according the process and purpose in organisms.

In assimilatory pathway, nitrogen is incorporated into cell mass. This process is usually repressed or quantitatively insignificant in anaerobic environments due to the usual presence in anaerobic environments of large concentrations of ammonia and organic nitrogen compounds. It is not affected by oxygen status, but inhibited by reduced nitrogen compounds.

In dissimilatory pathway, oxidized nitrogen used as electron acceptor for cell's

metabolic processes. It results in greater ATP yield/substrate oxidized than fermentation. The nitrogen is not incorporated primarily into cells. This pathway occurs in anaerobic environments and is often inhibited by oxygen.

Denitrification is a typical form of dissimilatory nitrogen metabolism, which is catalyzed by distinct enzyme species: NO_3^- reductase (Nar), NO_2^- reductase (Nir), nitric oxide (NO) reductase (Nor), and nitrous oxide reductase (N_2Or) and involves NO_2^-, NO, and N_2O as intermediates (Figure 1). Denitrification is a part of the bio-energetic metabolism of microbial cells in which these nitrogen oxide compounds serve as terminal electron acceptors fro the respiratory chain instead of dioxygen (O_2) (22, 88). Extensive studies of bacterial systems have shown that some contain the full process of denitrification, whereas many lack part of the reducing steps (1). Since denitrification would be defined as a process containing the key reaction of N-N bond formation that yields N_2O or N_2 (88), microbes that reduce NO_2^- to N_2O are also classified as denitrifers.

The process of ammonification is another form of dissimilatory NO_3^- reduction that is distinguishable from denitrification as it produces NH_4^+ instead of gaseous nitrogen compounds. Physiologically, it acts as an electron sink in the absence of NO_3^- reduction to NO_2^- and NO_2^- reduction to NH_4+ catalyzed by Nar and Nir (NH_4^+ forming), respectively. The Nar of some enterobacteria are membrane-bound complexes that generate a proton electrochemical gradient, and functions in anaerobic (NO_3^-) respiration. In contrast, ammonification by obligate anaerobes such as clostridia is not linked to the respiratory chain and occurs in the cytoplasm (30). The reaction is slower than that by the enterobacteria and since it is coupled to substrate level phosphorylation, it might be a fermentative metabolic system (ammonia fermentation) (30).

3. Denitrification by fungi.

For more than a century, denitrification has been considered a prokaryotic process and it was assumed that the mass transfer of fixed nitrogen back to N_2 exclusively proceeds through bacterial activities. Nevertheless, over the years, fungi have had an intermittent record of denitrification. N_2O formation was found in the genera *Fusarium*, *Giberella*, *Trichoderma*, *Cylindrocarpon*, and *Chaetomium* and in a considerable number of other members of the fungi and yeasts (70, 71, 78). Several bacterial systems are comprised of four successive reducing steps, namely, reduction of NO_3^-, NO_2^-, nitric oxide (NO) and N_2O. Each step is associated with the electron transport chain in the cellular membrane to support anaerobic respiration by which the cells obtain energy for growth. Denitrification is generally accepted as an adaptation system that works in anoxic environments. Usually, expression of the genes encoding the denitrifying enzymes is strictly repressed under oxic conditions where the bacteria can obtain sufficient energy through oxygen (O_2) respiration. In addition, the activities of most enzymes involved in denitrification are sensitive to dioxygen (O_2).

Denitrification by the fungus *Fusarium oxysporum* and *Cylindrocarpon tonkinense* first reported by Shoun *et al* (70, 71, 78), catalyzes the conversion of NO_3^- or NO_2^- to N_2O under O_2-limited conditions (Figure 2). *F. oxysporum* does not seem to have N_2O-reducing activity, and thus the final product of the fungal denitrification is N_2O. Cell-free NO_3^- reductase (dNar) and NO_2^- reductase (dNir) activities can be reconstituting bacterial enzyme activities. The fungal denitrification system is located in the respiring organelle mitochondrion and is coupled to the mitochondrial electron transport chain to produce ATP. Fungal NO reductase (Nor) is unique in that it is a

cytochrome P450 and it has been designated as P450nor. P450nor is an essential component of denitrification that is located in the cytosol and in mitochondria. Unlike mitochondrial dNar and dNir activities that are associated with the respiratory chain, NO reduction by P450nor does not seem to link to ATP synthesis as it is not associated with the electron transport chain but receives electrons directly from NADH (42, 57, 69).

4. Nitric oxide (NO) is ubiquitous and requires detoxification

Nitric oxide (NO, nitrogen monoxide) is a signaling and defence molecule of major importance in biological systems (14). It is a common product of enzymic and nonenzymic oxidation of reduced nitrogen compounds and of reduction of nitrogen oxides. In mammals, NO is produced by arginine-oxiding NO synthases (47). At low concentration, NO controls blood pressure in mammals and it is a messenger in the central and peripheral nervous systems. During responses to infection, foreign bodies, or tissue injury, toxic amounts of NO are produced by an inducible NO synthase isoform presumably to help kill or inhibit the growth of invading microorganisms or neoplastic tissue (21). In microorganisms, the metabolic reduction of nitroganic nitrate (NO_3^-) or nitrite(NO_2^-), such as denitrification, is also an important source of toxic NO (29) (Figure 1). NO can damage DNA (80), initiate lipids peroxidation (62), exacerbate peroxide-induced damage and inhibit critical enzymes, including the citric acid cycle enzyme aconitase (20) and terminal respiration oxidases (8). NO also has the potential to damage a variety of biomolecules by forming the more indiscriminate toxin and oxidizing agent peroxynitrite (4). So NO is ubiquitous and requires detoxification for microorganisms.

5. The strategies of NO detoxification

Organisms have evolved mechanism for NO metabolism and detoxification.

Under anaerobic conditions, inducible nitric-oxide reductases (NORs) are produced by denitrification bacteria, nitrogen-dissimilating fungi, and pathogenic microorganisms. NORs reduce NO to N_2O, an intermediary metabolite, for NO detoxification.

It is now evident that many organisms employ flavohemoglobin (FHb) to metabolize NO and moreover, that the enzymes form the first line of defense against NO toxicity under aerobic conditions. FHb-deficient mutant of *E. coli*, *Saccharomyces cerevisiae*, *Cryptococcus neoformans* and *Candida albicans* each lack significant aerobic NO metabolic activity. (18, 26, 31, 74) . Further, FHb protein or FHb gene transcription has been shown to be induced by submicromolar to 20 μM NO in *E. coli*, *C. albicans* and *B. subtilis*. (25, 50, 60) and by NO generating agents in *S.typhimurium*, *E. coli, C. albicans* and *B. subtilis* (16, 56). Furthermore, FHb expression protects microbes against the toxicity of NO and NO generators (44, 49). *Dictyostelium discoideum* expresses two FHbs that protect against aerobic growth inhibition by NO generators, GSNO and sodium nitroprusside (34).

6. Aerobic detoxification of NO by FHb

FHb detoxify NO in an aerobic process, which protects the host from various noxious nitrogen compounds, was termed nitric oxide dioxygenase reaction (NOD) by Gardner *et al*. (26). The reaction mechanism is shown in Figure 3. NO detoxification consumes O_2 and NAD(P)H and converts NO and O_2 in equistoichiometric amounts to nitrate (26). The reaction has been suggested to proceed via a heme-bound peroxynitrite

($^{-}$OONO) (55) (Figure 3 B). The possible model of electron transfer and ligand reduction reactions in FHb was shown in Figure 3A. Electrons from NAD(P)H are passed to FAD and then to reduce the single heme. Under aerobic condition, O_2 is bound in the distal heme pocket to form Fe^{+2}-O-O and then reacted with nitric oxide (NO) to give nitrosylation of flavoHb (Fe^{3+}-$OONO^{-}$). At last, the reactive and toxic intermediates (-OONO) is released as the nontoxic NO_3^{-}. Then NO was oxidized to NO_3^{-} by flvoHb. The resulted Fe (III) heme can be re-reduced in the presence of NAD(P)H via the "on-board" FAD.

7. Anaerobic detoxification of NO by FHb ?

O_2-independent NORs (NO reductase) can supplant or complement the NOD function of FHb in microbial NO detoxification. Functional complementation or replacement may be especially significant in microaerobic and anaerobic environments of infect tissues. But recent researches showed that FHb also be conferred to protect the anaerobic growth of *S.typhimurium* and *S.cerevisae* against NO or NO generators (16, 44). It suggested an O_2-independent NO detoxification function mechanism of FHb. Poole and co-workers have repeatedly suggested that *E. coli* FHb, and other microbial FHbs, function as anaerobic NORs by avidly binding NO and reducing NO to form N_2O in solution (39, 83). *R. eutropha* FHb deficient mutant strain did not accumulate N_2O during denitrification with nitrite as electron acceptor, which also implicated a NOR function of FHb. So there is a view that FHbs can also prevent NO poisoning to cells with the functions of NOR. However, FHbs showed a very poor anaerobic NO metabolic activities, which is several magnitudes lower than the rate under aerobic conditions (39). Thus the anaerobic NO detoxification of FHb became argued.

8. Other enzymatic functions for FHb

Before the NO detoxification role of FHb was revealed, many hypothesis had been proposed for the physiological functions of FHb. The observation that *E. coli* FHb is a NADH oxidase, and is thereby able to generate superoxide radicals and H_2O_2, was used to suggesting that FHb might be involved in the oxidative stress response in *E. coli* (51). *A. eutrophus* and *Bacillus subtilis* FHbs are increased dramatically in response to oxygen limit, which has led to the concept that FHb may serve as oxygen stores (38), though each globin molecule could presumably store only one oxygen molecule. The expression of *Saccharomyces cerevisiae* FHb is optimal in hyperoxic conditions and is reduced under hypoxic or anaerobic conditions. Additionally, the expression level is enhanced in the presence of reagents which can promote oxidative stress. These finding suggest *S. cerevisiae* FHb plays a role in the oxidative stress response in yeast (87). In another side, the expression of *E. coli* FHb gene is not markedly affected by oxygen supply. The maintenance of expression under both conditions appeared to be coffered the FHb as an oxygen sensor , in which continual presence in the cell of the sensor molecule would be required (61).

To verify these hypothesis, a large amount of experiments remain to be carried out.

9. The aim of this study.

Extensive studies of flavoHbs from bacteria and yeast have revealed many details of the structure, function, and reaction mechanism of FHb. To date, the sole flavoHb from a fungi, *Fusarium oxysporum*, was isolated and characterized the spectra and prosthetic groups only. It is insufficient to elucidate the property and the

physiological function of the flavoHb in fungi. Additively, Blast research of the completed fungal genome database with bacterial flavoHb, multiple flavoHb genes homologies were frequently discovered in one cell genome. So we are interested in knowing the characters of the fungal flavoHbs and whether the multiple flavHbs from the same cells share the identical properties. In this work, we studied two flavoHbs from *Aspergillus oryzae in vitro* and *in vivo* to elucidate physiological functions of fungal FHb.

On the other hand, by blast search of the *A. oryzae* genome database with the *E. coli* periplasmic nitrate reductase (NapA), a dissimilatory nitrate reductase, a *napA*-like gene was found. To date, no eukaryotic type dissimilatory nitrate reductase was reported. So in this study, I tried cloning a eukaryotic dissimilatory nitrate reductase-like gene from *A. oryzae* for the first time.

Denitrifying fungi can reduce nitrate (NO_3^-) or nitrite (NO_2^-) to nitrous oxide (N_2O) by dissimilatory nitrate reductae (dNar) or dissimilatory nitrite reducase (dNir) and nitrous oxide reductase (P450nor). The acitivities of the enzymes involved in denitrification process were detected in some denitrifying fungi. However, the corresponding genes have not been identified and isolated except the sole one encoding p450nor. To well understand the denitrification of fungi, the molecular genetic analysis are required. My predecessor, Master Nakanishi, isolated a copper-containing dNir (NirK) gene from *Aspergillus oryzae* (*A. oryzae*) and gave a characterization of its recombinant protein for the first time. In this study, I kept on the study of NirK to investigate the relation between NirK and denitrification.

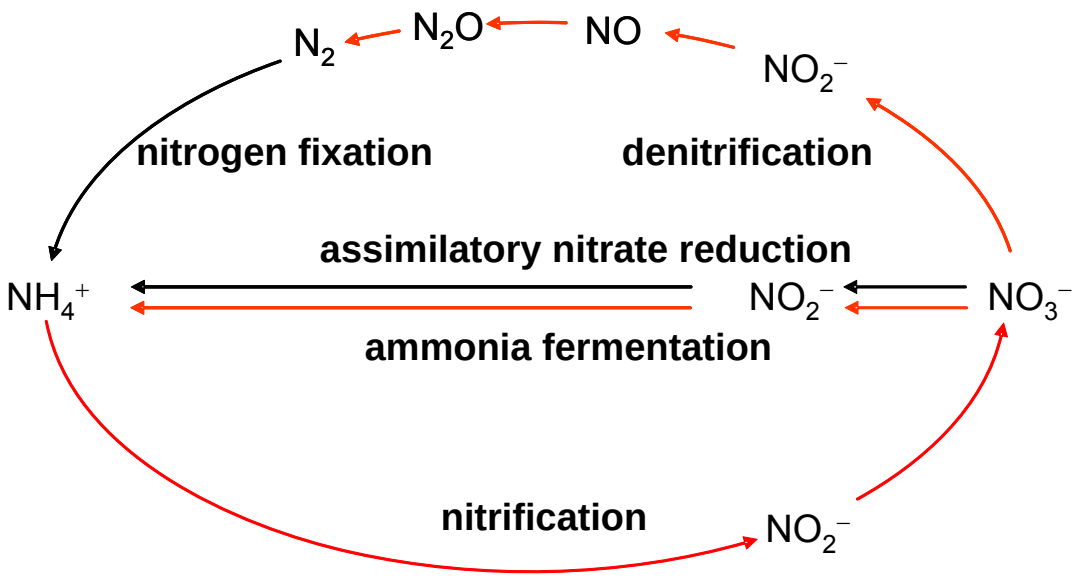

Figure 1 The biological nitrogen cycle.

The arrows in red showed the dissimilatory nitrogen metablisms (denitrification, ammonia fermentation and nitrification)

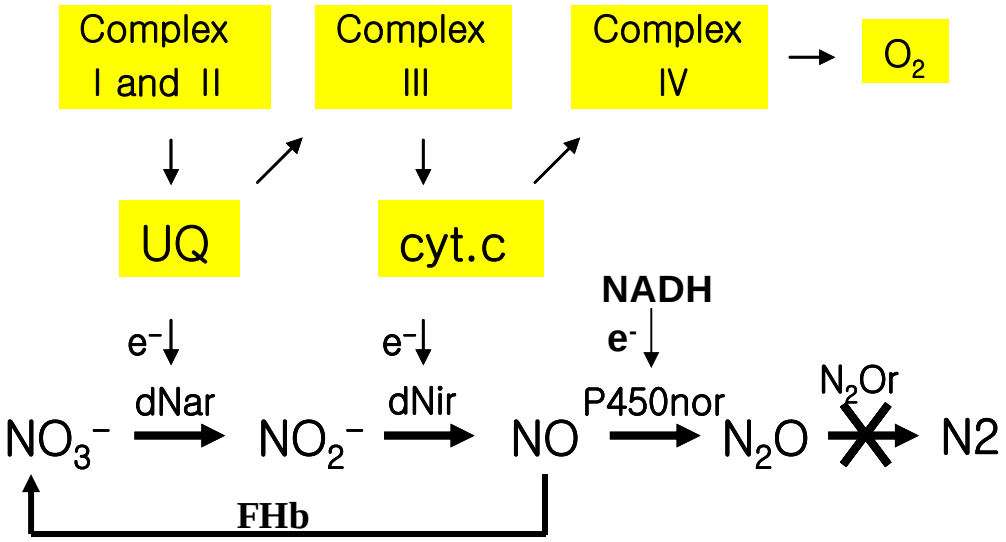

Figure 2 Deduced denitrification pathway in fungi.

dNar : dissimilatory nitrate reductase

dNir : dissimilatory nitrite reductase

P450nor : nitric oxide reductase

N_2Or : nitrous oxide reductase

FHb : flavohemoglobin, NO dioxygenase

A

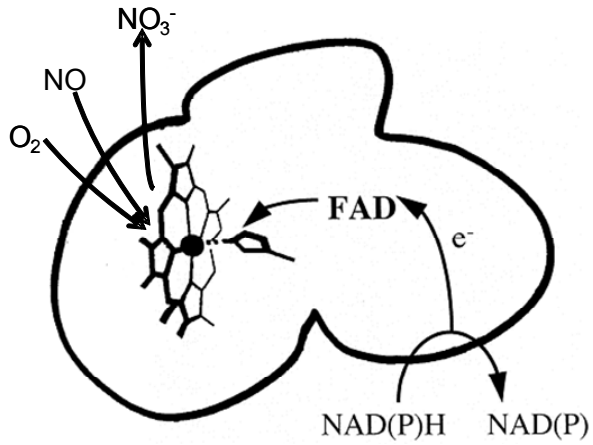

B

$$Fe(III) + e^{-} \rightarrow Fe(II)$$

$$Fe(II) + O_2 \rightarrow Fe(II)O_2$$

$$Fe(II)O_2 \rightarrow Fe(III)^{-}O_2$$

$$Fe(III)^{-}O_2 + NO \rightarrow [\, Fe(III)^{-}OONO] \rightarrow Fe(III) + NO_3^{-}$$

Figure 3. NO dioxygenase (NOD) activity of flavohemoglobin (FHb).

A. Electron transfer and NO dioxygenation in FHb.
Electrons from NAD(P)H are passed to FAD and then to the active site –heme.

B. The NOD mechanism of FHb.
The reaction has been suggested to proceed via a heme-bound peroxynitrite.

Chapter 1 Cloning, recombinant expression, and characterization of two flavohemoglobins (FHb) from *A. oryzae*

Aspergillus oryzae is an important filamentous fungus in the Japanese fermentation industry, such as sake, soy sauce, and miso manufacture, as well as in commercial enzyme production. *A. oryzae* also has been widely used as a host for the production of homologous and heterologous proteins because of its great productive capacity with respect to the secretion of proteins (40). Very recently, the genome sequencing project was completed, which will allow the molecular genetic analysis in more details. With the extreme study on *A. oryzae* recently, abundant information about this fungi was discovered, which make it easier to handle *A. oryzae* as a laboratory organism. Though *A. nidulans* has considerable advantages as a laboratory model organism, it is not a denitrifying fungus. So we selected *A. oryzae* to investigate the enzymes involved in dissimilatory nitrogen metabolism.

FHb of bacteria or yeast had been demonstrated to be a NO dioxygenase (NOD) which catalyzes the oxidation of NO to NO_3^-. So FHb is not seemed to be directly involved in denitrification, but its substrate, NO, is an intermediary metabolite in the denitrification pathway.

In this chapter, I cloned and characterized two fungal FHbs from *A. oryzae* in vitro. This would be the first to show that a microorganism contains two isozymes of NO dioxygenase FHb and that intracellular location of the isozymes possibly differs.

1-1 Materials and methods

1-1-1 Strains and plasmids and culture conditions

! Wild-type *Aspergillus oryzae* RIB40 was used to isolate the *fhb* genes. *Escherichia coli* DH5α was used for DNA multiplication and *Escherichia coli* BL21

(DE3) Condon plus was used as the host for expression of proteins. pT7Blue2 (Novagen) was used for the cloning of the PCR products and pET28b (+) was used for the over-expression of N-terminal 6-Histagged proteins. *A. oryzae* was grown on DPY agar medium with 10mM $NaNO_2$ at 30℃ for 3 days. All *E. coli* was grown in LB medium at 37℃ added the corresponding antibiotics. The media used in these experiments were shown in Table 1-1.

1-1-2 Cloning of the the cDNAs encoding FHb-homolog genes

For isolation of *A. oryzae fhb* genes, *E. coli* FHb (HMP) was as a query sequence to blast search the genome database of *A. oryzae* (DOGAN). The two identified *fhb* genes (*fhb1*, *fhb2*) were chosen to be cloned. Total RNA was isolated from *A. oryzae* grown on YPD agar plate at 30℃ for 3 days, using TRIZOL Reagent (Invitrogen) following its manual. Full-length cDNAs were obtained by 5'-3' RACE using the GeneRacer™ Kit (Invitrogen) following the supplier's protocol. To obtain 5' end, cDNA was amplified using *fhb* reverse gene specific primers, GeneRacer™5' primer (Table 1-2). To obtain 3' ends, cDNA was amplified using *fhb* forward gene specific primers, GeneRacer™ 3' primer (Table 1-2). Amplified 5'- and 3'- Race DNA was cloned using pT7Blue T-Vector (TaKaRa), separately. The sequencing reaction were performed with CEQ Dye Terminator Cycle Sequencing with Quick Start Kit (BECKMAN COULTER), and sequenced with a sequencer (CEQ2000XL; BECKMAN COULTER).

1-1-3 Subcloning, expression, and purification of the recombinant FHbs.

fhb1 gene was subcloned using the sense primer, *fhb1*-ORF-F (*Nde I* site

shown in capital), and the antisense primer, *nirK*-ORF-R (*Not I* site shown in capital) (Table 1-2), to express the full-length FHb1. *fhb2* gene lacking the predictive mitochondrial targeting signal, in which the sequence was predicted to encode the N-terminal 30 amino acid residues was truncated, was amplified from the fungal cDNAs using the sense primer, *fhb2*-ORF-F (*EcoR* I site shown in capital), and the antisense primer, *fhb2*-ORF-R (*Xho* I site shown in capital) (Table 1-2). The PCR products were digested with the corresponding restriction enzymes, and they were inserted into pET28b (+) (Novagen) to construct the over-expression plasmids for N-terminal hexahistidine-tagged proteins. The constructions of plasmids for expression of *fhb1* and *fhb2* were shown in Figure 1-4. *E. coli* BL21-CondonPlus(DE3)-RIL (Stratagene) cells harboring the vectors were grown in LB medium containing 20 μg/ml kanamycin and 100 μg/ml chloramphenicol at 37°C to the OD of 0.5. Recombinant protein expressions were induced at 20°C by 0.1 mM isopropyl-1-thio-β-D-galactopyranoside (IPTG) with the addition of 0.8 mM $FeCl_3$ and 0.5 mM aminolevulinic acid hydrochloride for 16 h. Harvested cells were resuspended in 20 mM K-phosphate buffer (pH 7.2), 0.3 mM phenylmethylsulfonyl fluoride, 0.5 mM dithiothreitol, 0.5 M NaCl and 10 mM imidazole, and then sonicated. The broken cells were centrifuged, and the resulting supernatant was applied to affinity chromatography with HiTrap Chelating HP (GE Healthcare). The column was washed with 20 mM Na-phosphate buffer (pH 7.2) and 10 mM imidazole, and the bound proteins were eluted with a gradient of 10–500 mM imidazole. Fractions containing FHbs were applied to gel filtration using HiLoad 16/60 (GE Healthcare) in 20 mM K-phosphate buffer in 0.15 M NaCl at a flow rate of 1 ml/min.

1-1-4 Identification and determination of prosthetic groups

Flavins were extracted and determined by the method described in (27) with a little modification. The FHb proteins or the flavin standard solutions (100 μl) were mixed with 190 μl of methanol-methylene chloride (9:10, v/v) and vortexed for 60 s. After addition of 90 μl of 0.05 M ammonium acetate buffer (pH 6.0), the mixture was additionally vortexed for 60 s and then centrifuged for 20 min at 17,400×*g* at 4°C. The upper phase was filtered through a 0.45 μm filter and immediately injected into a Waters Model 600E HPLC System (Waters) equipped with a PEGASIL ODS column (4.6 × 250 mm**,** Senshu Kagaku). The samples were protected against light during the whole procedure. For separation and identification of flavins, the following elution method was performed. Methanol–0.05 M ammonium acetate buffer, pH6.0, in the isocractic mode at 20:80 (v/v) methanolammonium acetate for 1 min, and then in linear gradient from 20:80 (v/v) to 90:10 (v/v) within 10 min at the flow rate 1 ml/min.

Heme content was determined by the pyridine ferrohemochromogen method employing the molar absorption coefficient of the chromogen of the protohemes as 34.4 mM^{-1} cm^{-1} at 557 nm (58).

1-1-5 NO dioxygenase (NOD) activity.

NOD activity was measured in under room temperature with an ISO-NO MARK II-type NO electrode (World Precision Instrument, USA). The reaction mixture contained 2ml of 50mM citrate-NaOH buffer (pH5.5), 100μM NAD(P)H, 1μM flavin, purified FHbs and the necessary concentration of NO-releaser, 1-Hydroxy-2-oxo-3,3-bis(2-aminoethyl)-1-triazene (NOC-18).

1-1-6 Other analytical methods

Alignment of amino acid sequence was done with CLUSTALW (http://clustalw.genome.jp/). Prediction of mitochondrial targeting signal was performed with iPSORT (http://hc.ims.u-tokyo.ac.jp). Protein concentration was determined by BCA Protein Assay Reagent Kit using the bovine serum albumin as a standard. UV-visible absorption spectra were recorded at room temperature with a Jasco V-550 spectrophotometer.

1-2 Results

1-2-1 Identification and clone of two FHb homologue genes from *A. oryzae*.

By BLAST search on *A. oryzae* genome database (DOGAN) using *E. coli* FHb (HMP) as a query sequnce, two FHb-like genes (AO090011000202, AO090012000171) were identified. We named them *fhb1* and *fhb2*, respectively. The two homologue genes were located in chromosome 7, and chromosome 4, respectively.

The full length cDNAs of the two genes were cloned and sequenced as described in materials and methods. Sequences analysis revealed intron exists in neither of the genes. The two cDNAs contains 1251 bp and 1311 bp, respectively. Figure 1-1 shows the deduced amino acids sequences of the two FHb genes. FHb1 consists of 416-amino acids and FHb2 consists of a putative mitochondrial targeting signal peptide of 30-amino acids and a mature 436-amino acids. The deduced fungal FHb proteins were compared with two bacterial FHbs, *E. coli* HMP and *A. eutrophus* FHP, which are the best-characterized members of the FHb protein family. FHb1 shows 41 % homology with HMP and 47 % homology with FHP. FHb2 shows 40 % and 51 % homology with

HMP and FHP, respectively. FHb1 and FHb2 share 44% homology to each other. As shown in the alignment (Figure 1-2), the catalytic triad formed His-F8, Tyr-G5 and Glu-H23 at the proximal site of heme in the bacterial FHbs are completely conserved in either of FHb1 or FHb2. Tyr-B10 and Gln-E7, which are suggested to be essential for high O_2 affinity, involved in heme ligand stabilization and important to efficient NOD function are also highly conserved in FHb1 and FHb2. The RQYS motif essential for FAD binding in the bacterial FHbs (24) are completely conserved in both of FHb1 and FHb2 sequences. So the feature of the two proteins in their sequences might allow them to act as a NO dioxygenase.

The phylogenetic comparison (Figure 1-3) shows the relationship between the two *A. oryzae* FHbs with FHbs from various prokaryotic and eukaryotic microbes. It is consistent with the view that FHbs does not follow a discernible evolutionary pattern (6).

1-2-2 MW determination of the recombinant FHbs.

The FHbs were expressed and purified according to the methods described in "Materials and Methods". The full length FHb1 was expressed favorably in *E. coli* but not for FHb2 (data not shown). The predicated mitochondrial targeting signal sequences at the N-terminus of FHb2, which may affect the posttranslational modification of the peptides, was truncated to make the expression efficiently.

The His_6-tag carried in the N-terminal amino acid sequence of both FHb1 and FHb2 made it convenient to be purified with the His-tag affinity column. The purification process could be monitored and controlled by the red color of FHb. FHb1 was eluted from 0.1M to 0.2M of the imidazole concentration (Figure1-5 A); FHb2 was

eluted from 0.16M to 0.22M imidazole(Figure1-6 A). The expression level of FHb2 was significantly lower than FHb1. The result of SDS-PAGE showed that the His-tag affinity column had made the target proteins purified efficiently (Figure1-5 B, Figure1-6 B). The followed Gel filtration column conferred the further purification of the proteins . The elution Volume (Ve) of FHb1 and FHb2 were 81.81ml and 73.84ml, respectively. The results were shown in SDS-PAGE (Figure 1-7 A,B; Figure1-8A,B).

The purified enzymes appeared as single bands on SDS-PAGE (Figure1-9 A.), and the apparent molecular mass of FHb1 and FHb2 are estimated to be 51,000 and 50,000 Da, respectively. the molecular mass of FHb1 and FHb2 in solution was approximately 51,000 and 98,000 Da, respectively, as estimated by calibrated gel filtration chromatography (Figure 1-9 B). These results suggested that FHb1 and FHb2 exist as a monomer and a dimmer in solution, respectively.

1-2-3 Absorption spectra of FHbs and prosthetic groups.

UV-visible absorption spectra of purified FHb1 and FHb2 in resting (Fe^{3+}), dithionite-reduced (Fe^{2+}), dithionite-reduced plus CO (Fe^{2+}–CO), and NADH-reduced (Fe^{2+}-O_2) forms are shown in Figure 1-10, and their peak maxima are summarized in Table 1-3. The characteristics of the absorption spectra of both FHbs are basically similar to those of previously reported spectra of other FHbs (72). Unlike FHb1 and other FHbs, however, the Soret peak maximum of FHb2 did not show red-shift from the resting form to the NADH-reduced one (Figure 1-10 B), suggesting that the heme of FHb2 can not accept electron from NADH via the flavin cofactor. The type of flavin in purified FHbs was analyzed by TLC using FMN and FAD as standard samples. The bound heme was indentified as protoheme by the pyridine ferrohemochrome method,

which gave the characteristic spectra with peaks as 419, 525, and 557nm (Figure 1-12). The contents of heme in the proteins were estimated by the method described in materials and methods. The flavin in FHb1 was identified to be FAD (Figure 1-11). The contents of FAD and heme in the purified preparation of FHb1 were estimated as 0.30 mol/mol protein and 0.39 mol/mol proteins, respectively. On the other hand, we could not detect any flavin in the purified FHb2, but its heme content was estimated as 0.89 mol/mol protein. It has been shown that the heme and FAD cofactors are often partially dissociated from FHb during the purification procedures (36). When the absorption spectra of FHb2 were measured after incubation of 16 μM FHb2 protein with 32 μM FAD for 5 min at room temperature (Figure 1-10 C), a spectral shift of the Soret peak maximum and appearance of visible peak at 580 nm were observed (Table 1-3), indicating that the electron transfer from NADH to heme was restored.

1-2-4 Nitric oxide dioxygenase (NOD) activities of FHb1 and FHb2

NOD activities of the purified FHbs were measured by an NO electrode (Figure 1-13). FHb1 exhibited robust NOD activities either in the absence or presence of externally added FAD (Lane 2 and Lane3). In contrast, FHb2 required external FAD for its NOD activity (lane 4 and Lane 5). This result is in consistent with the quantitative analysis of the FAD contents of these FHbs. It has been shown that FHbs from various microorganisms largely differ in their preference for the reducing substrate of NOD activity. For example, *A. eutrophus* FHb (FHP) does not utilize NADPH as an electron donor, whereas *S. cerevisiae* FHb (YHB) and *E. coli* FHb (HMP) utilize either NADH or NADPH (35). The dependencies of the NOD activities of FHb1 and FHb2 on the reducing substrates (NADH and NADPH) and the flavin cofactors (FAD and FMN)

were compared (Table 1-4). Addition of flavin cofactors had no large effect on the NOD activity of FHb1, but FAD gave a slight activation effect. This result is consistent with the FAD to heme ratio (3:4) contained in the purified FHb1 protein. In contrast to the cases of YHB and HMP, FHb1 showed slightly higher activity against NADPH than NADH. As to FHb2, addition of both FAD and NADH was required for the full NOD activity, but FMN and NADPH were not effective. Steady-state kinetic parameters of the NOD activities of the two FHbs were measured with various NO concentrations at room temperature (25°C). The K_m and V_{max} values of FHb1 in the presence of 100 ¶M NADPH were 2.0 ¶M and 8.3 s^{-1}, and the K_m and V_{max} values of FHb2 in the presence of 100 ¶M NADH and 1 ¶M FAD were 2.4 ¶M and 6.9 s^{-1}(Figure 1-14). The V_{max} values are within the range of reported V_{max} values of other FHbs at 37°C (76) or at room temperature . The K_m and the V_{max} values of two FHbs against NO were not largely different.

E .coli FHb (HMP) exhibited highly sensitive to cyanide. Imidazole, cyanide, azide can apparently bind to ferric HMP. So, here I tested the inhibition effects of imidazol, azide and cyanide on NOD activity of FHb1 and FHb2 (Figure 1-15). As the data shown, both of FHb1 and FHb2 are sensitive to cyanide but not to imidazol and azide.

1-2-5 Crystallization of FHbs

The two FHbs show 44% homology to each other in their primary amino acid sequence. But they still exhibit many differences in prosthetic groups binding and in the dependencies of the NOD activities on the electron donors (NADH and NADPH). To elucidate these difference clearly, the structure studies are necessary. So I have tried crystallizing the two FHb2. Abundances of crystallization

screening conditions were performed, but only FHb2 was succeeded (Figure 1-16). It is unfortunate that the crystals obtained in both of the conditions did not exhibited good resolutions.

1-3 Discussions

Eukaryotic microorganisms often have multiple genes for FHb homologues in their genomes. For example, two FHb genes of *Dictyostelium discoideum* lie close to each other in the genome. Both of their gene products are responsible for NO stress resistance, indicating that they have the same function in a co-operative manner. On the other hand, the *Candida albicans* genome contains three FHb homologue genes, but only one of them (*CaYHb1*) is responsible for NO detoxification . Essential amino acid residues for the NOD activity are not conserved in the other two genes (*CaYHb4* and *CaYHb5*). In our study, both of the two FHb homologues from *A. oryzae* have been shown to exhibit robust NOD activities. One of the unique characteristics of FHb2 is its possible N-terminal mitochondrial targeting signal, since no typical signal sequence was found in other FHbs to date. The *S. cerevisiae* FHb (YHb), which is encoded by the nuclear gene *YHB1*, is located in both the cytosol and mitochondrial matrix although no targeting signal sequence is present in this enzyme . How it is exported into mitochondria is unclear and its physiological function in mitochondria hasn't been elucidated. The production of NO in mitochondria has been estimated to occur in several eukaryotes. Dissimilatory nitrite reductase in mitochondria produces NO in the denitrifying fungi, *F. oxysporum* and *Cylindrocarpon tonkinense* (41). Additionally, in the mitochondria of *S. cerevisiae*, NO is produced by cytochrome oxidase under hypoxic conditions (13). Therefore, the presence of mitochondrial FHb in eukaryotic

cells may respond to the mitochondrial NO stress.

The purified recombinant FHb1 and FHb2 proteins were estimated as monomer and dimer in solution, respectively. To our knowledge, all bacterial and yeast FHbs isolated so far are monomeric. However, it is proposed that HMP might exist as a dimer in vivo due to the observed cooperativity in cyanide binding.

FHbs prepared from bacteria and yeast contained only 24–44% FAD due to dissociation from the protein during the purification procedures. In our preparation from recombinant *E. coli* cells, FHb1 contained 30% FAD, whereas FHb2 released it completely. The FAD binding domain of the FHb family is highly conserved, but FHb2 exhibits some differences in this region. Pro232, Tyr235 and Val236 in FHP are responsible for binding the pyrophosphate and adenosine moieties of FAD . These residues are conserved in FHb1 (Pro231, Tyr239 and Val240), but not in HMP and FHb2 (Figure 1-2). A Tyr residue, which is located 5 Å from the isoalloxazine ring of FAD , is conserved in HMP (Tyr188), FHP (Tyr190), and FHb1 (Tyr187), but it is replaced by Phe in FHb2.

As to the reducing substrate specificity, FHb1 showed slight preference to NADPH over NADH, but FHb2 was highly specific to NADH. Interestingly, two P450nor isozymes in *C. tonkinense* have similar characteristics; one isozyme with a mitochondrial targeting signal (P450nor1) is specific to NADH, whereas the other without a signal (P450nor2) utilizes both NADH and NADPH and prefers the latter. Such preferences for reducing substrates may be related to the predicted cellular distribution of these enzymes. NADH is present in both of the cytosol and mitochondria because it is produced from the glycolysis and the citric acid cycle. In contrast, the major source of NADPH is the oxidative phase of the pentose phosphate pathway in

cytosol, and the NADPH level is usually very low in mitochondria.

We will discuss the cellular localization and physiological functions of FHb1 and FHb2 in *A. oryzae* in the next chapter.

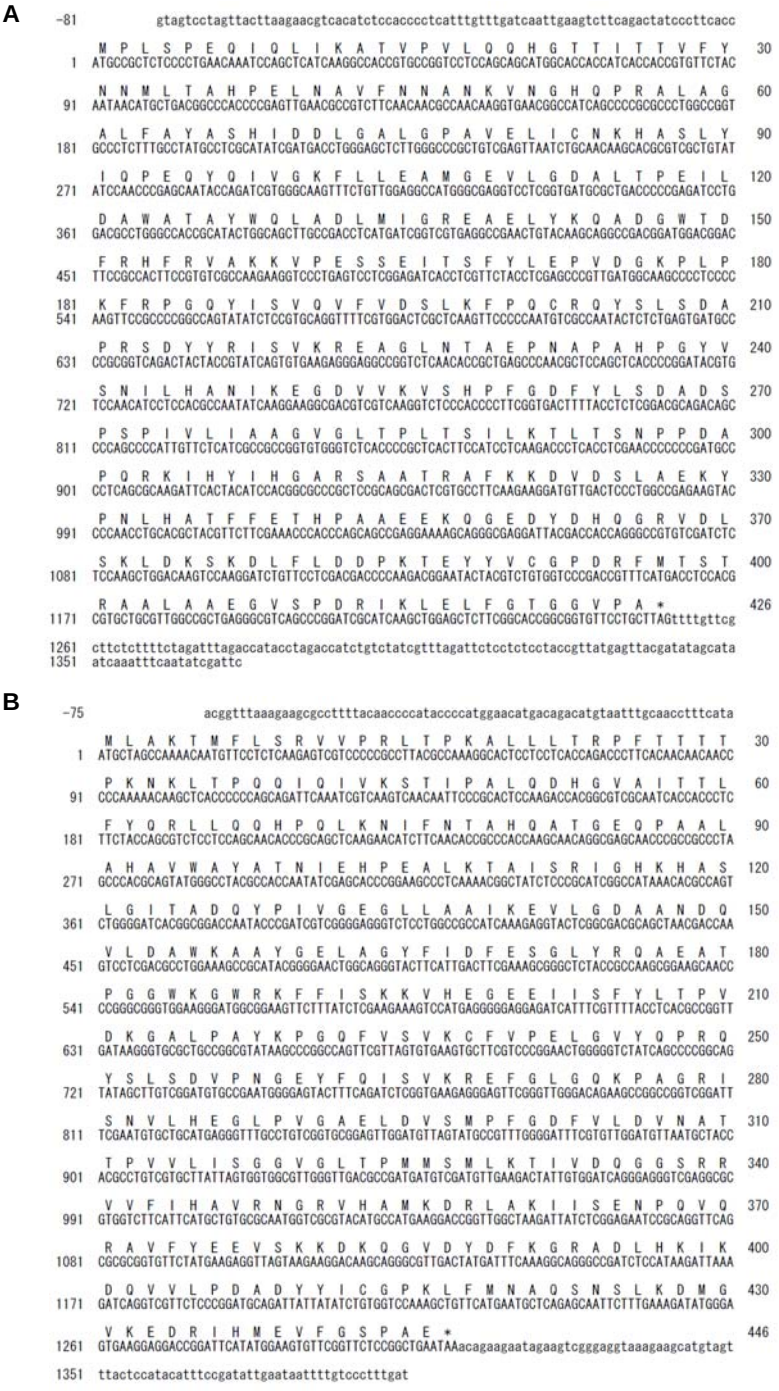

Figure 1-1. Nucleotide sequence and deduced amino acid sequence of cDNAs of *A. oryzae fhb1* (A) and *fhb2* (B).

The numbers on the left refer to the positions of nucleotides (bottom lines).
The number on the right refer to the position of amino acid residues (top lines)
The stop codons is indicated by asterisk.

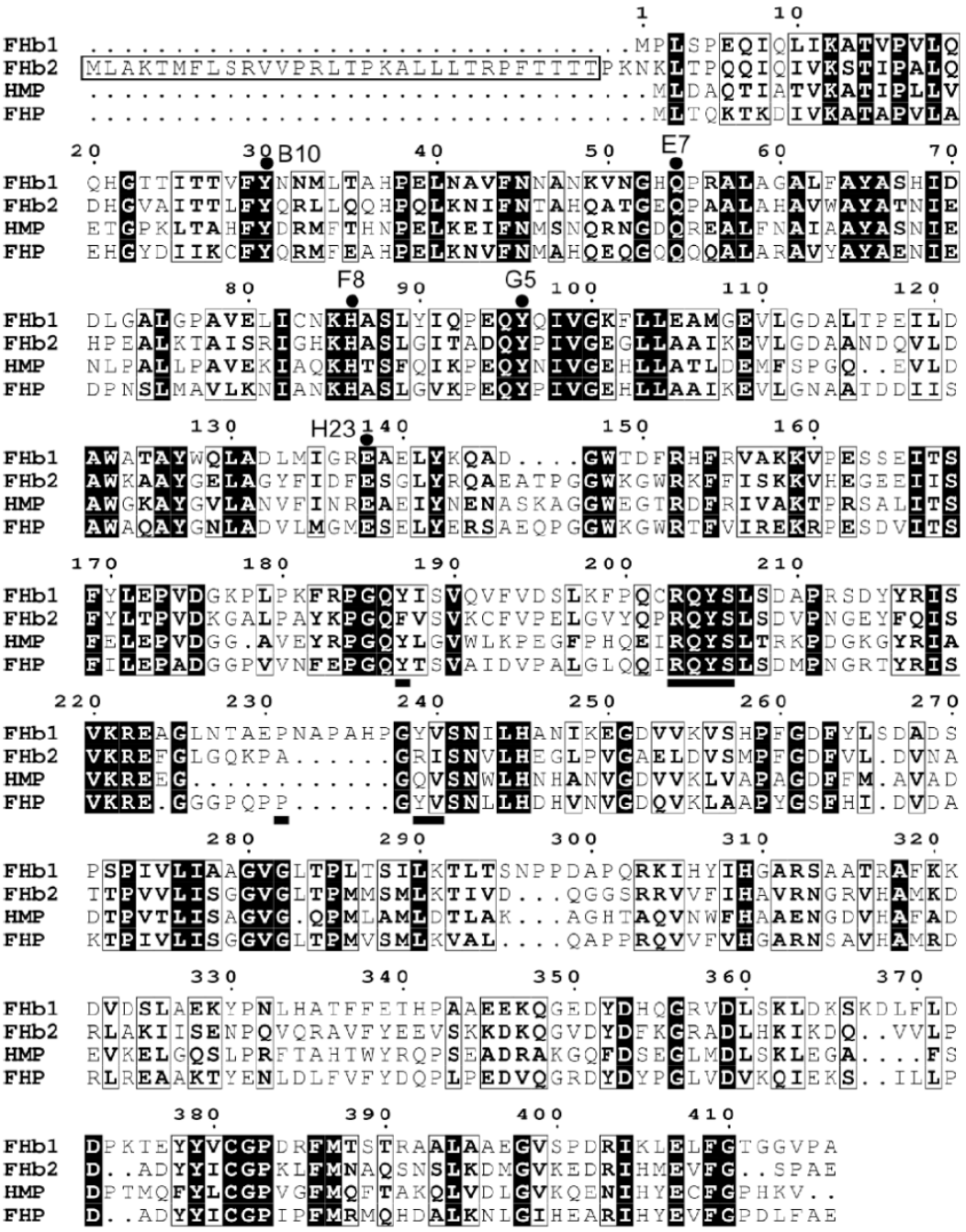

Figure 1-2. Amino acid sequence alignment of FHb1, FHb2, *E.coli* FHb (HMP), and *A. eutrophus* FHb (FHP).

The predicted N-terminal mitochondrial targeting signal sequence of Fhb2 is shown in a box. Essential residues for heme binding and NO dioxygenase activity are indicated by closed circles above the sequences. Residues responsible for FAD binding in FHP are indicated by bars under the sequences.

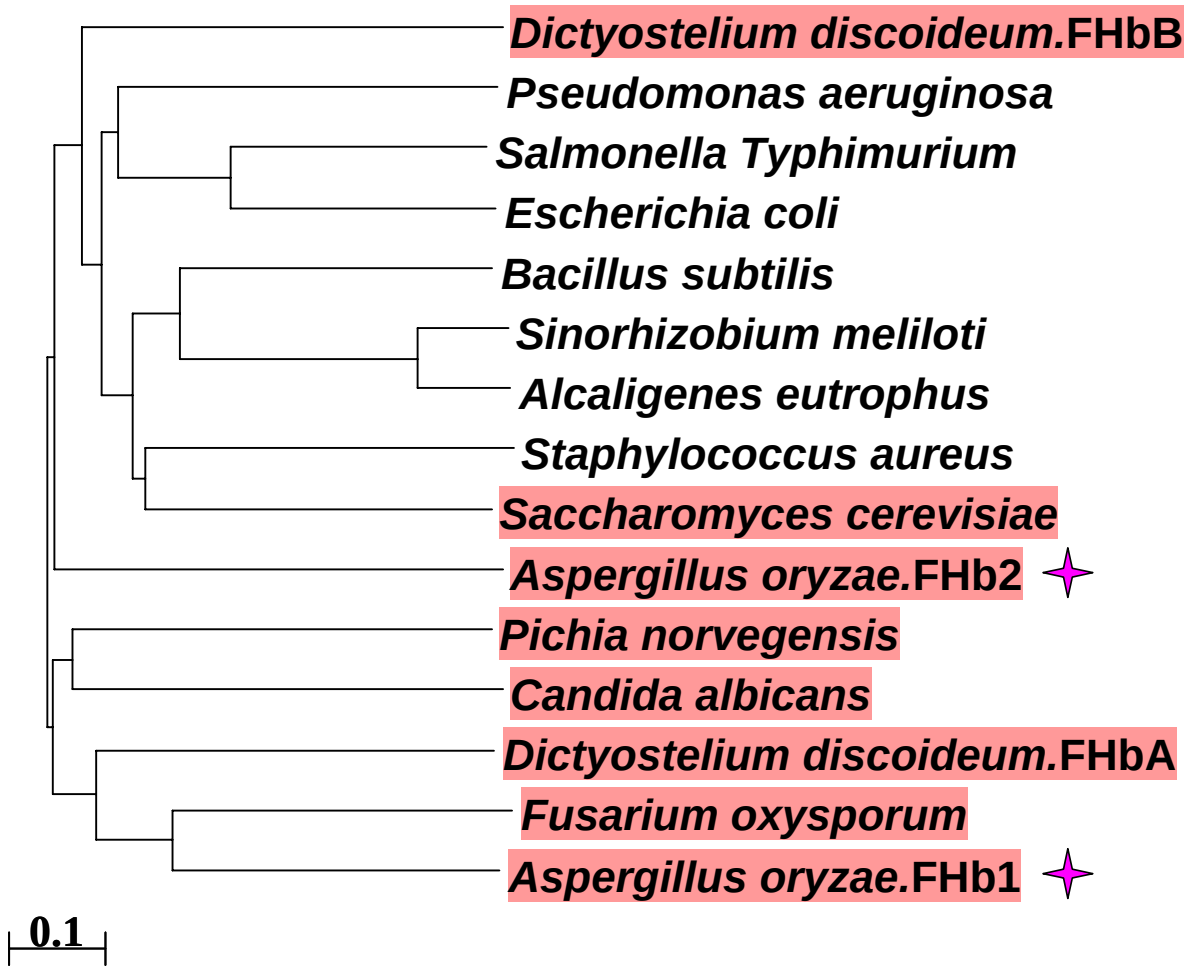

Figure 1-3. Phylogenetic tree of the microbial FHbs

Eukaryotic FHbs are shown in red background;
The rest ones are prokaryotic FHbs.

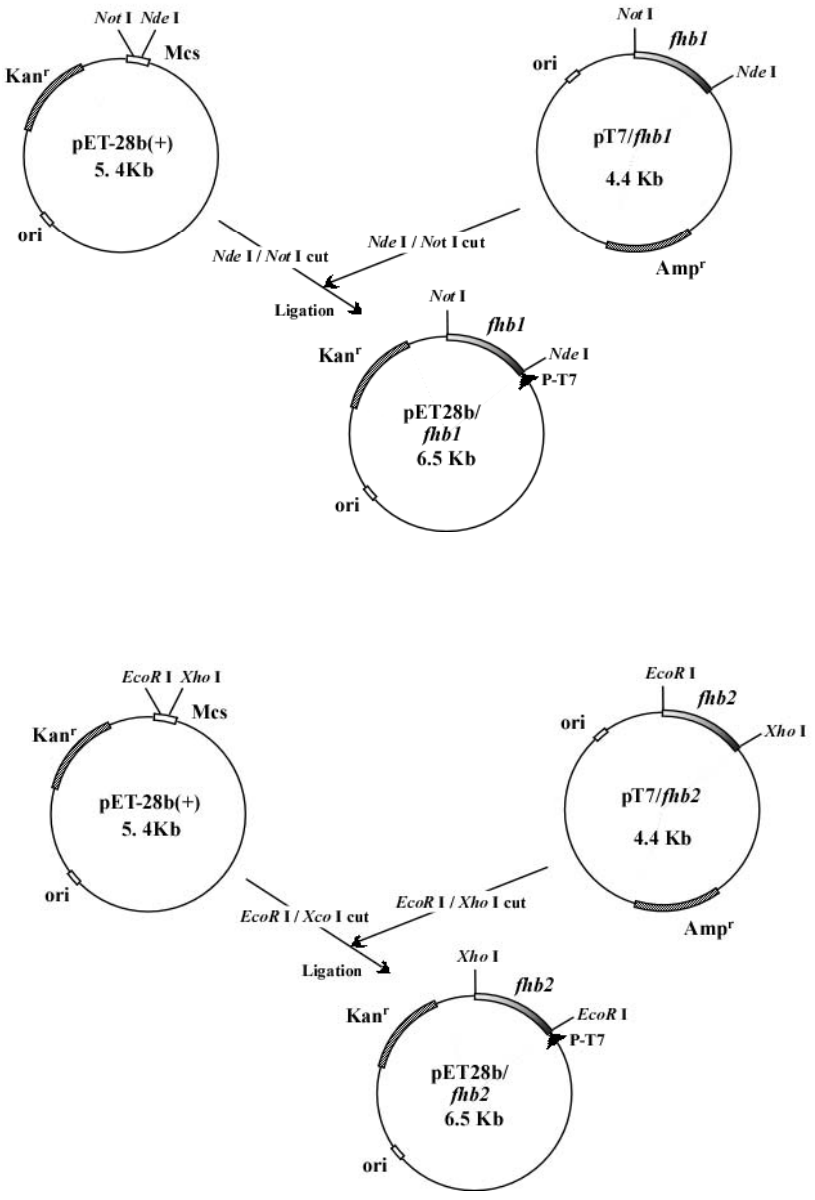

Figure 1-4 Constructions of plasmids pET28b/*fhb1* and pET28b/*fhb2* for production of the full length FHb1 and FHb2 without the putative mitochondrial targeting signal in *E. coli.*

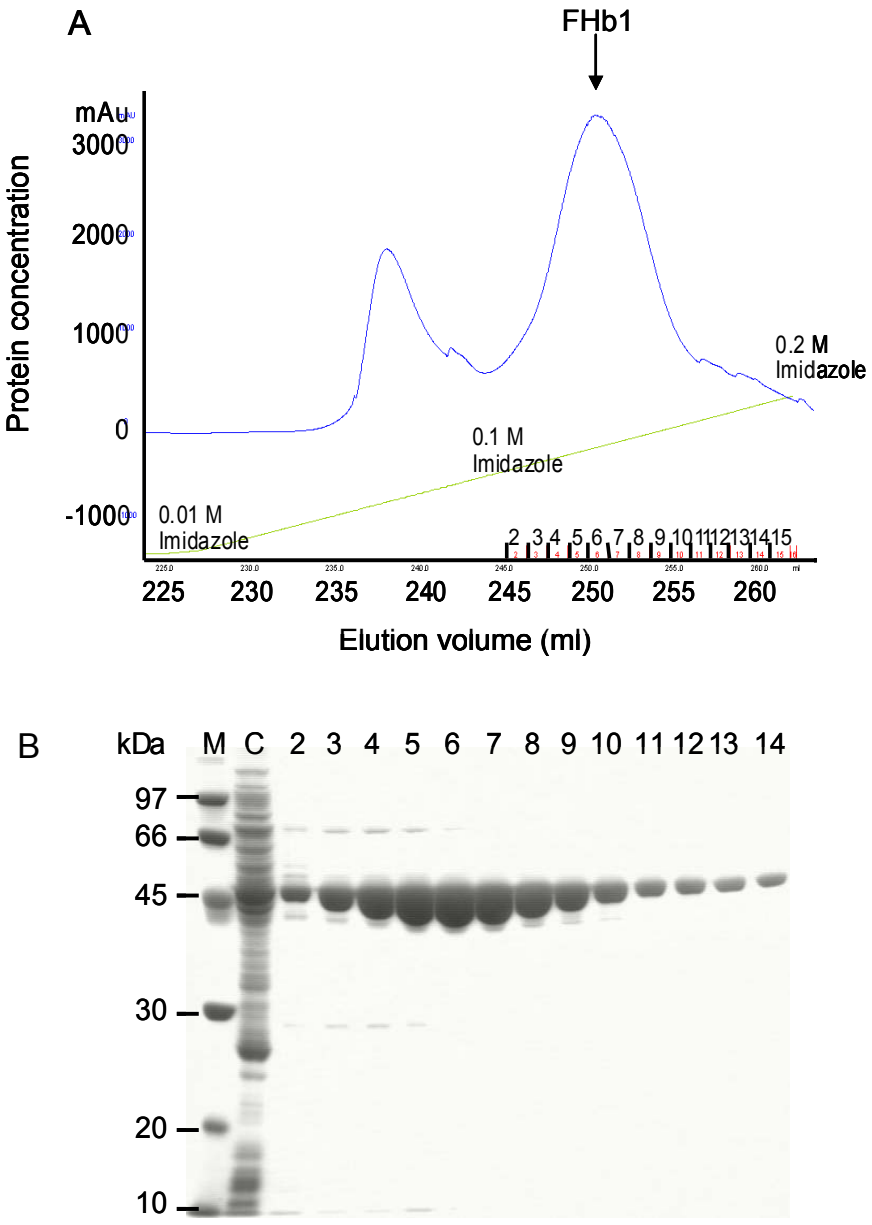

Figure 1-5. Purification of FHb1 by His-tag affinity column
A. Purification chart .
Elution of FHb1 was monitored by its red color
B. SDS-PAGE
Gel concentration was 12%;
M: protein maker; C: cell extract from *E.coli*;
2~14 were corresponding to fractions of purification chart

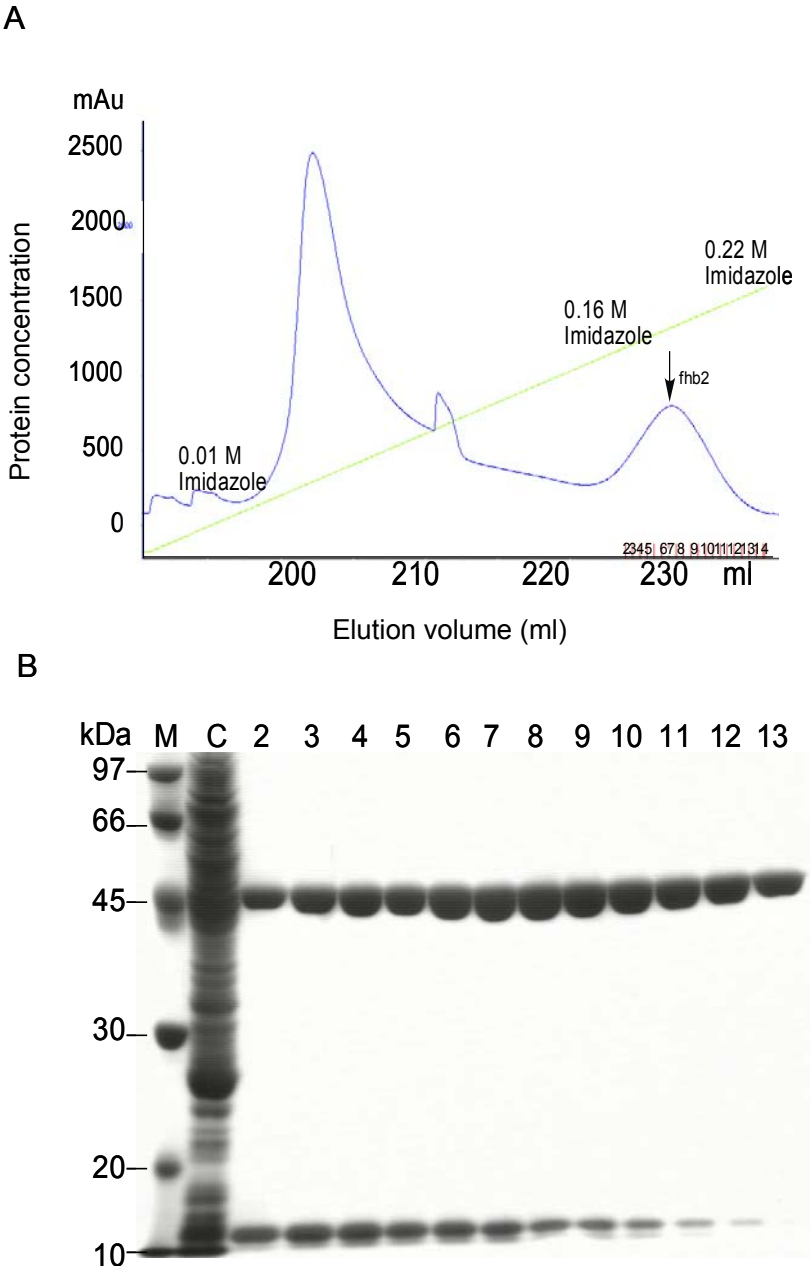

Figure 1-6. Purification of FHb2 by His-tag affinity column
A. Purification chart .
Elution of FHb2 was monitored by its red color
B. SDS-PAGE
Gel concentration was 12%;
M: protein maker; C: cell extract from *E. coli*;
2~13 were corresponding to fractions of purification chart

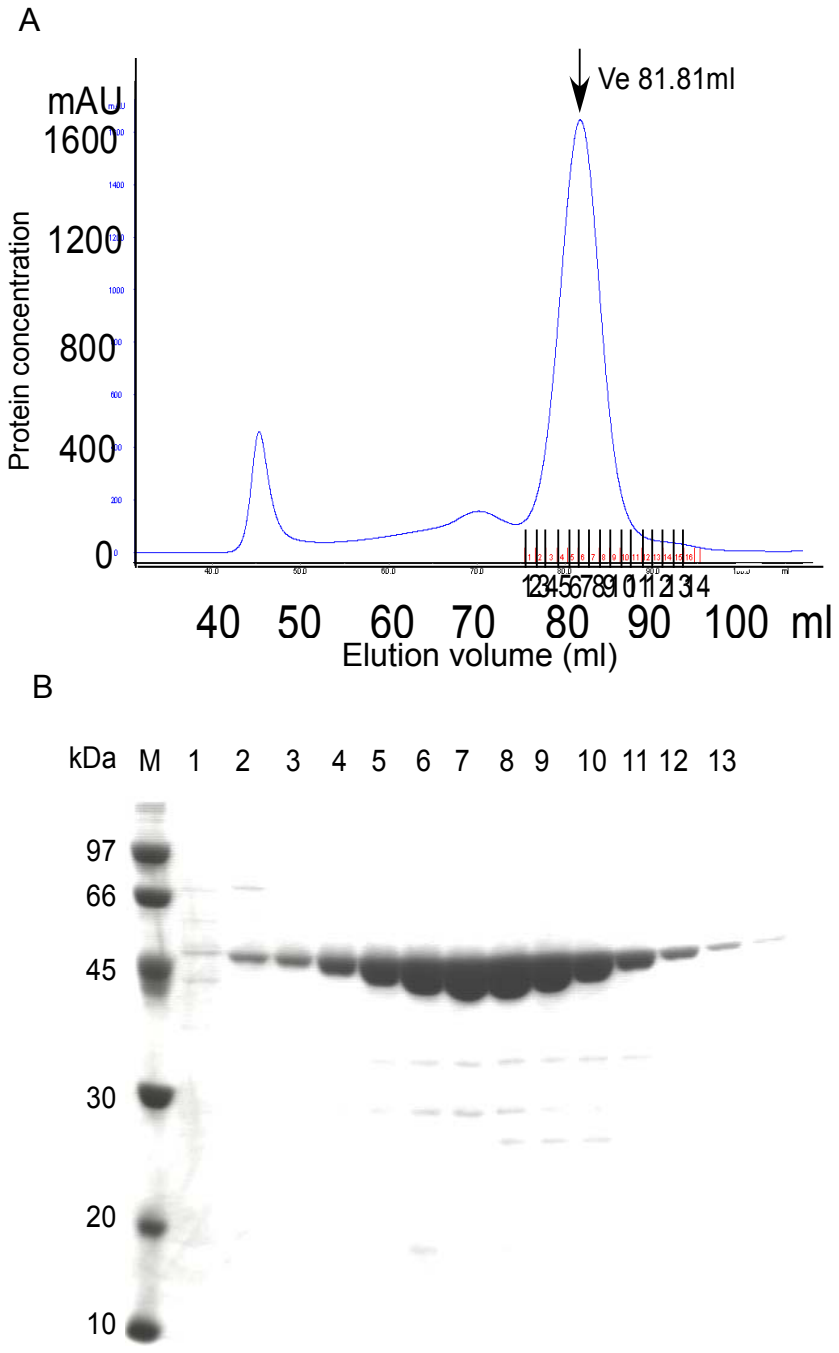

Figure 1-7. Purification of FHb1 by gel filtration chromatography

A. Elution chart .

Elution of FHb1 was monitored by its red color

B. SDS-PAGE

Gel concentration was 12%;

M: protein maker; 1~13 were corresponding to fractions of elution chart

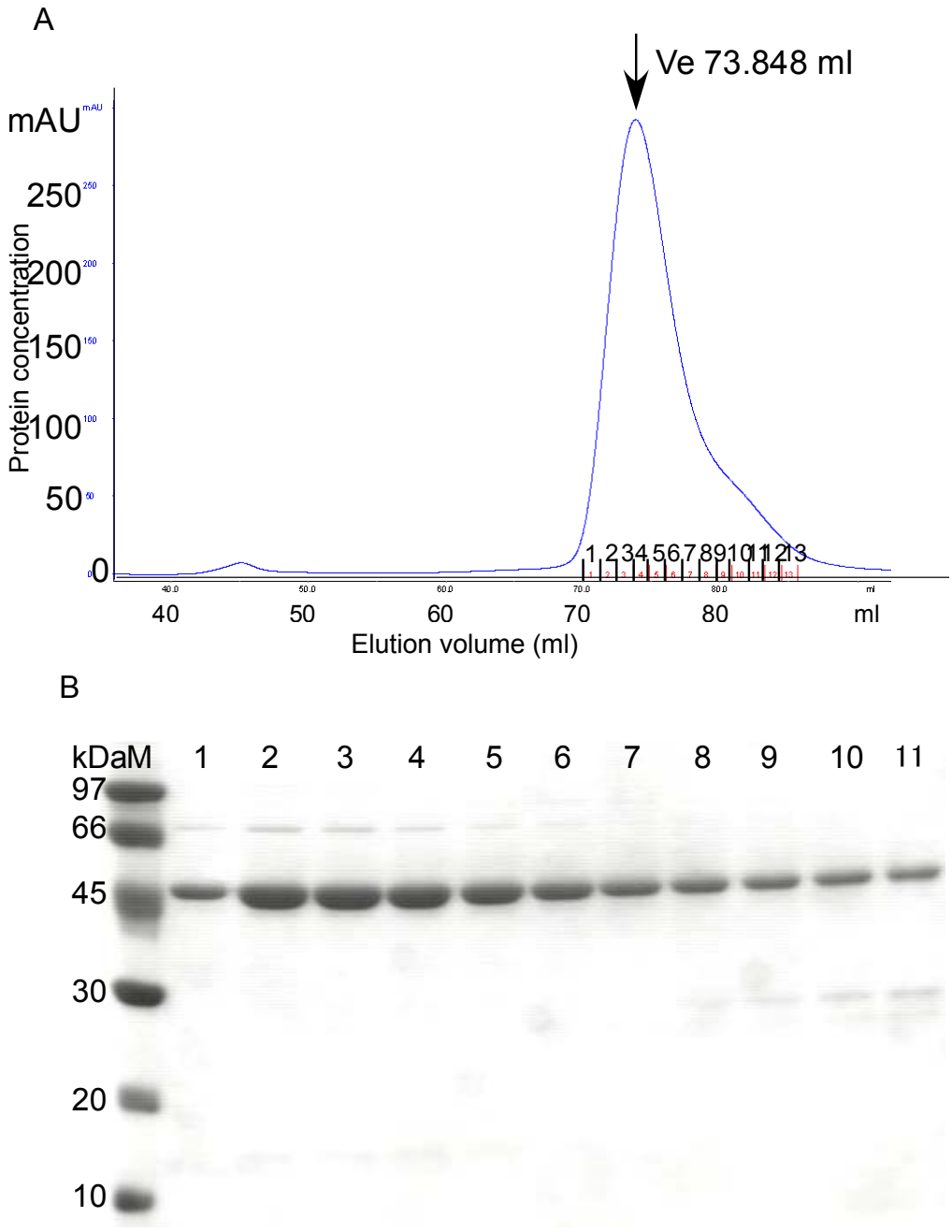

Figure 1-8. Purification of FHb2 by gel filtration chromatography

A. Elution chart .

Elution of FHb2 was monitored by its red color

B. SDS-PAGE

Gel concentration was 13%;

M: protein maker; 1~11 were corresponding to fractions of elution chart

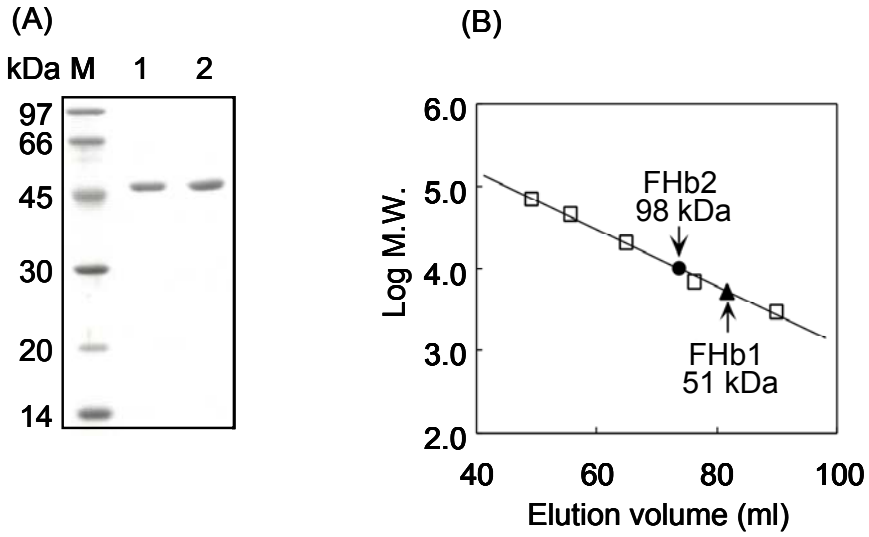

Figure 1-9. Molecular weight determination of purified recombinant FHb1 and FHb2.

(A) Samples purified by two step as shown in materials and methods were subjected to SDS-PAGE on a 12% gel, followed by Quick CBB staining. Lane1 and lane 2 showed FHb1 and FHb2, respectively.

(B) Determination of the MW of FHb1 and FHb2 by gel filtration chromatography (HiLoad 16/60 column). The following protein standards were used for the calibration curve: thyroglobulin (669 kDa), apoferritin (443 kDa), β-amylase (200 kDa), albumin bovine serum (66 kDa) and carbonic anhydrase (29 KDa). The flow rate was 1ml/min.

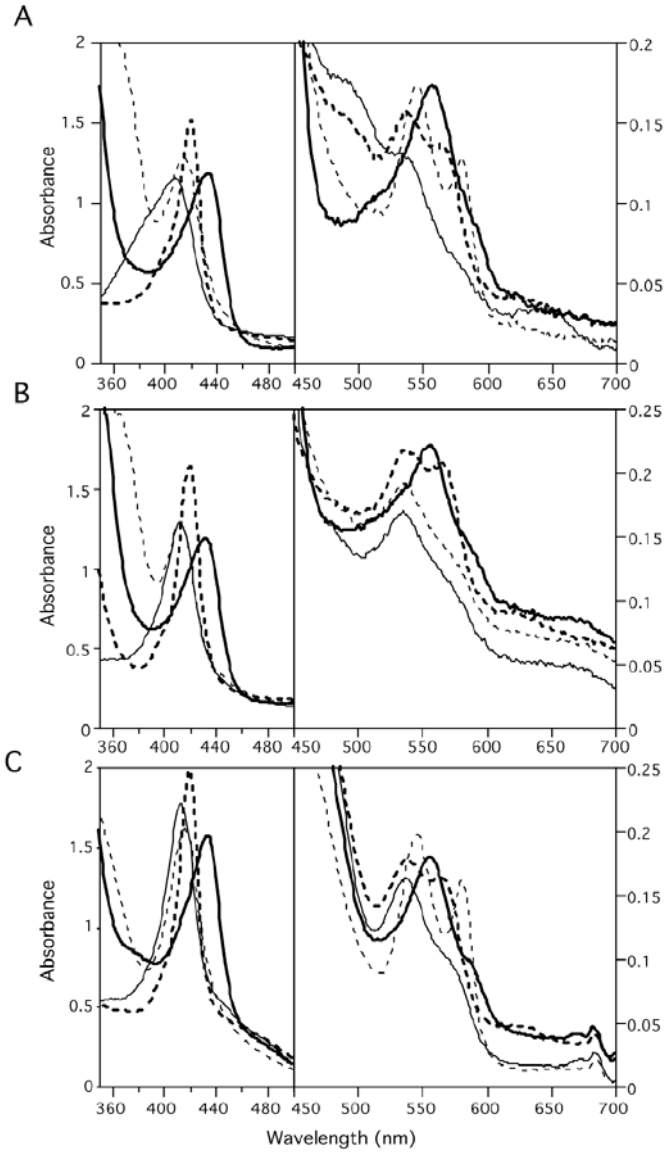

Figure 1-10. UV-visible absorption spectra of purified FHb1 (A), FHb2 (B), and FHb2 after incubation with FAD (C).
Left, g-(Soret) band region; right, visible region.
(——, thin), resting (Fe^{3+}); (——, thick), dithionite-reduced (Fe^{2+});
(– – –, thick), dithionite-reduced plus CO (Fe^{2+}–CO); (– – –, thin), and NADH-reduced (Fe^{2+}–O_2).
The spectra were measured for 0.7 mg/ml FHb1 or 0.5 mg/ml FHb2 in 20 mM Na-phosphate buffer (pH 7.2) at room temperature.

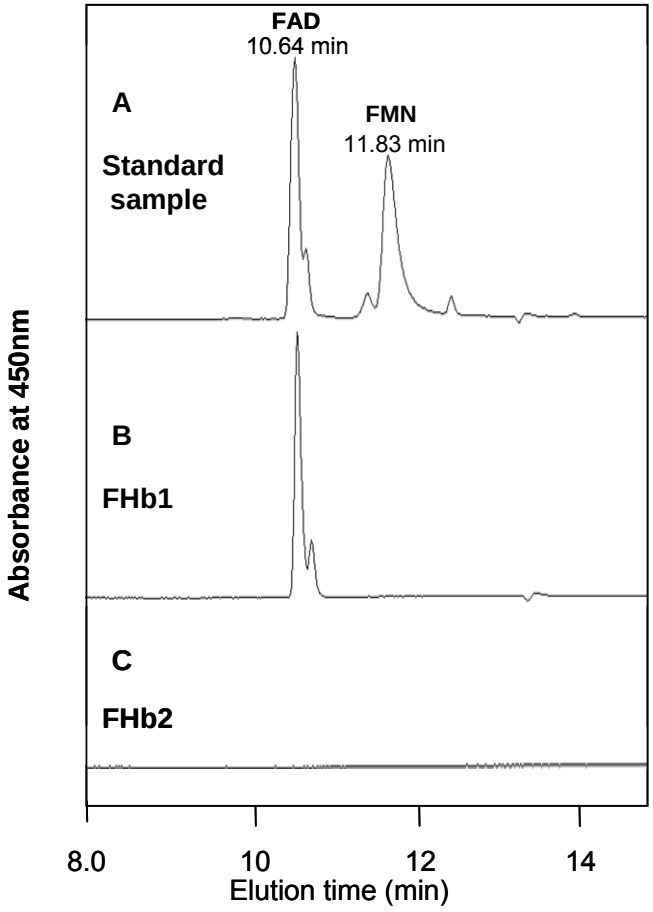

Figure 1-11. HPLC chromatogram of Flavin (FAD and FMN) extracted from FHb1 and FHb2.

Flavin extracted from proteins was identified and determined by the standard curves prepared with the stock solutions of FAD(50 μ M) and FMN (50 μ M).

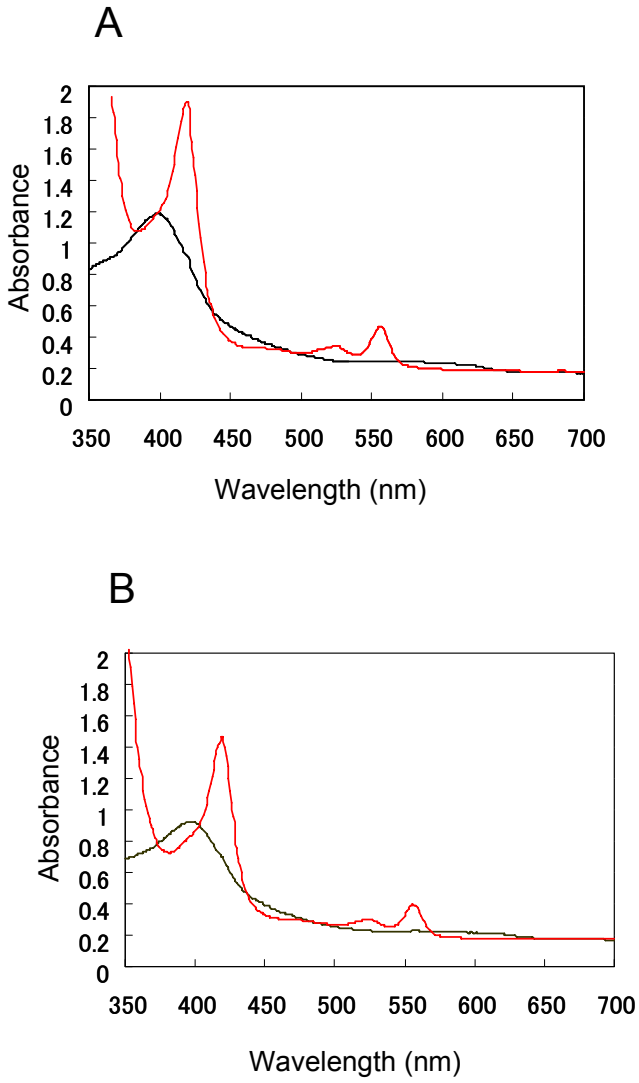

Figure 1-12 Spectra of Pyridine ferrohemochromegen of FHb1 (A) and FHb2 (B).

50 μl FHb (10.4mg/ml FHb1 or 3.4mg/ml FHb2) was dissolved into 100 μl of 1N NaOH, adding 120 μl of 60% pyridine, and diluting to 600 μl with H_2O; after recording a baseline, sodium dithionite was added to the sample cuvette, and spectra was recorded.
To compute the heme concentrations,the extinction coefficient 32.4$mM^{-1}cm^{-1}$ was used for reduced (red) minus oxidized (black) pyridine ferrohemochromegen between 557nm and 575nm.

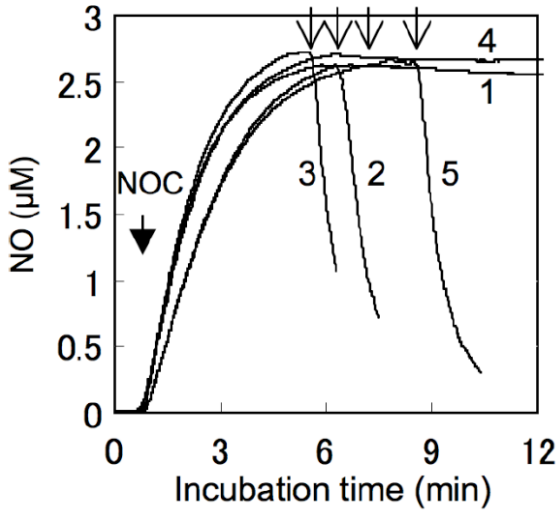

Figure 1-13. NOD activities of FHb1 and FHb2.

Details are described in Materials and Methods. In all systems, 3 μM NOC-18 (NO donor) was initially added and the activities were measured at room temperature. Enzyme was added at the time indicated by the arrow.
Line 1, no enzyme;
Line 2, FHb1; line 3, FHb1 plus 1 mM FAD;
Line 4, FHb2; line 5, FHb2 plus 1 mM FAD.

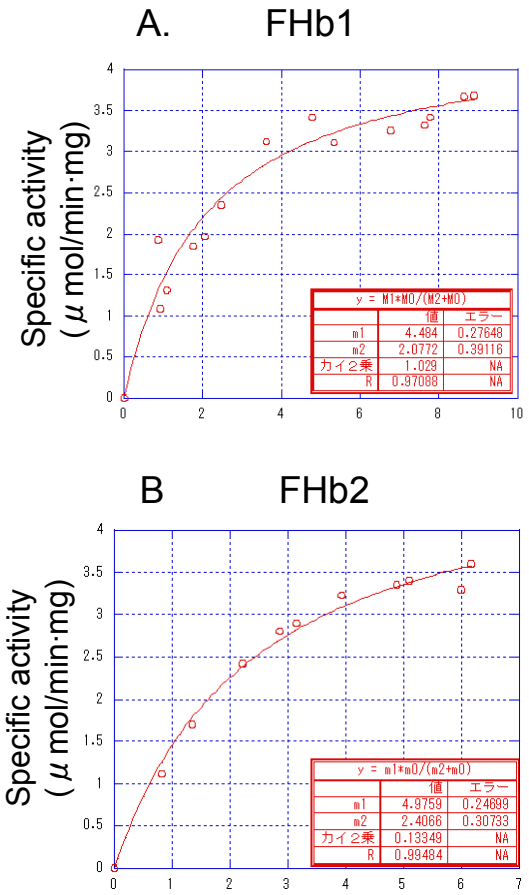

C summary

NOD	Vmax (NO heme^{-1}s^{-1})	Km (μ M)
FHb1(NADPH+FAD)	8.3	2.0
FHb2 (NADH+FAD)	6.9	2.4

Figure 1-14. Steady-state Kinetics of nitric-oxide dioxygenase (NOD) kinetics of FHb1 and FHb2.

NOD activity were measured with 100 μ M NAD(P)H, 1 μ M FAD, and FHb (FHb1=3.3 μ g or Fhb2=2.5 μ g) under room temperature.

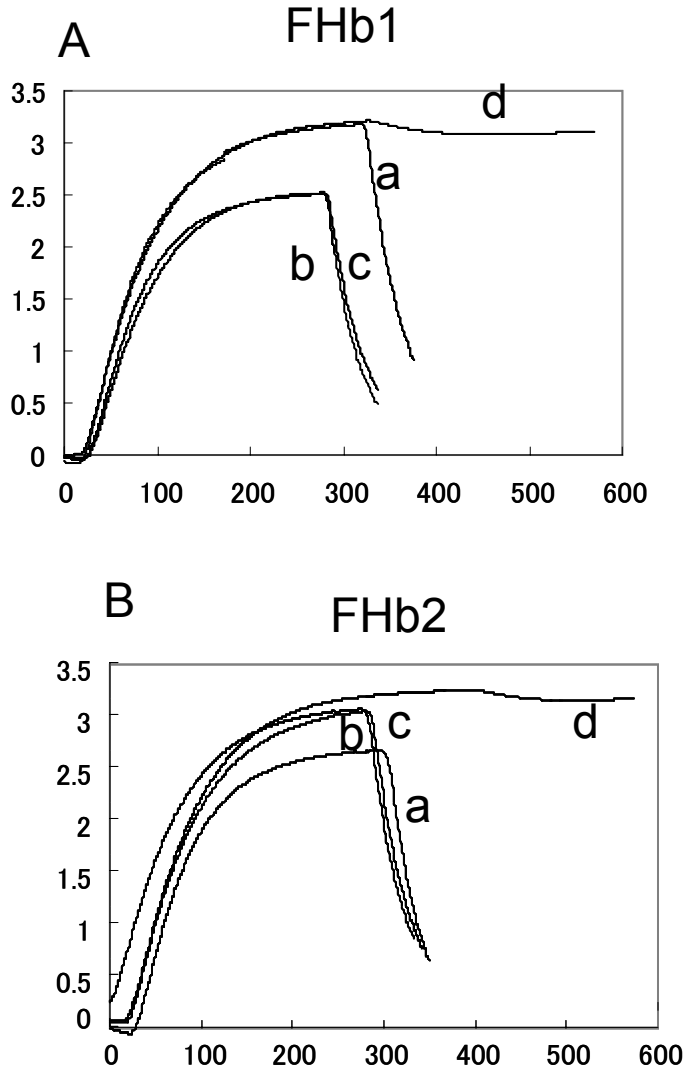

Figure 1-15 Effect of inhibitor on the NOD activity of FHb1 (A) and FHb2 (B).

a: without inhibitor
b: Imidazole 2mM
c: azide 2mM
d: cyanide 2mM
Inhibitors were added prior to the enzymes addition to assure inhibitors binding to ferric FHbs.
The reaction conditions were same to Figure 1-13 with the external FAD.

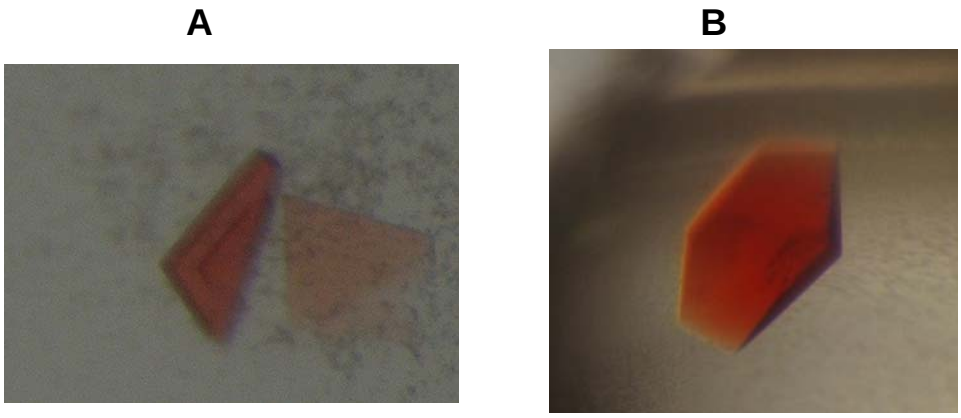

Figure 1-16 Crystallization of FHb2.

Crystallization condition:
A. 1.4 M Sodium/Potassium Phosphate, pH 8.2, FHb2: 5mg/ml.
B. 0.1M Citrate buffer, pH 5.5 + 15% PEG3350
FHb2: 5mg/ml
Incubation temperature: 25℃.

Potato Dextrose Broth（Difco）	24 g
INA AGAR	15 g
DW	1000 ml
	pH 5.1-5.2

Potato Dextrose Agar（PDA）medium

Dextrin（KOKUSAN）	20 g
POLYPEPTON	10 g
Yeast Extract（BD）	5 g
KH_2PO_4	5 g
$MgSO_4 \cdot 7H_2O$	0.5 g
DW	1000 ml
	pH 5.5

DPY medium

SOB medium (BD)	28 g
20% glucose	20 ml
DW	1000 ml

SOC medium

LB broth, Miller (BD)	25 g
DW	1000 ml

LB (Luria-Bertani) medium

Table 1-1 Media used in this work

Name	Sequence(5' → 3')
fhb1 reverse GSP primer	gccgtggatgtagtgaatcttgcgc
fhb1 forward GSP primer	ccggccagtatatctccgtgcagg
fhb2 reverse GSP primer	gcacgacaggcgtggtagcattaac
fhb2 forward GSP primer	ggccagttcgttagtgtgaagtgc
fhb1- ORF-F	CATATGatgccgctctcccctgaacaaatcc
fhb1- ORF-R	GCGGCCGCctaagcaggaacaccgccg
fhb2- ORF-F	GAATTCaagctcacccccagcagattc
fhb2- ORF-R	CTCGAGttattcagccggagaaccgaac

Table.1-2. Nucleotide sequences of primers used in this work.

Restriction endonuclease cleavage sites are shown in capital.

Peak maxima of UV-visible spectra.

FHb	Form	Soret maximum	Visible maxima
FHb1	Fe^{3+}	407	540, 645
	Fe^{2+}	434	558
	Fe^{2+}–CO	421	538, 565
	Fe^{2+}-O_2	414	545, 579
FHb2	Fe^{3+}	412	535
	Fe^{2+}	432	556
	Fe^{2+}–CO	420	537, 560
	Fe^{2+}-O_2	412	535
FHb2 after incubation with FAD[a]	Fe^{3+}	412	535
	Fe^{2+}	434	556
	Fe^{2+}–CO	420	539, 565
	Fe^{2+}-O_2	416	546, 580

[a] **See text for details.**

Table 1-3. Peak maxima of UV-visible spectra.

FHb	Additives[a]	NOD activitiy (s^{-1})
FHb1	NADH	1.71 ± 0.17
	NADH + FAD	2.26 ± 0.15
	NADH + FMN	2.04 ± 0.25
	NADPH	2.43 ±0.10
	NADPH + FAD	2.66 ± 0.15
	NADPH + FMN	2.63 ± 0.12
FHb2	NADH	ND[b]
	NADH + FAD	2.92 ± 0.23
	NADH + FMN	0.74 ± 0.11
	NADPH	ND[b]
	NADPH + FAD	0.34 ± 0.08
	NADPH + FMN	0.08 ± 0.02

[a] See Materials and Methods for details.
[b] Not detected.

Table 1-4 Dependencies of the NOD activities on the reducing substrates and the flavin cofactors.

Chapter 2 Transcriptional responses of *fhb* genes to NO stress and effects of *fhb* genes deletions on NO resistance

！ For a long term, the function of FHb was obscure. FHbs have been suggested to function in oxygen sensing (61), storage and delivery (77, 81) as prototypes of hemoglobin in high organisms. However, other evidences suggested that FHb was involved responses to oxidative stress (87). Moreover, some bacterial FHbs are shown involved in denitrification (15). In the past decade, a role in NO detoxification was regarded as the key physiological significant in microorganisms. The first indication that FHb might be involved in NO biochemistry was the up-regulation of the *E. coli hpm* gene by NO or nitrosating agents (60). The role of NO detoxification were supported by the experiments that *hmp* knockout mutants of *E. coli* and *S. typhimurium* are severely compromised for survival in the presence of NO (16, 49). It has been demonstrated for several microorganisms including bacteria and yeast that FHb has an important role in protection against nitrosative stress.

In chapter 1, studies of the purified recombinant FHb1 and FHb2 suggested both of them may act as the NO detoxification enzymes in cytosol and mitochondria, respectively. In this chapter, I studied the physiological functions of the two FHbs, FHb1 and Fhb2, in vivo.

2-1. Materials and methods

2-1-1. Strains, media, and culture conditions.

A. oryzae RIB40 and RIB40 Δ*ku70*Δ*pryG* were used as the over-expression host strain and the gene-deletion parent strain, respectively (73). YPD was used as a complete medium and Czapek-Dox (CD) medium was used as a minimal medium. The RIB40 Δ*ku70*Δ*pryG* was maintained by culture on medium with 5mM uracil and

5mM uridine. 10 mM $NaNO_2$ or 100 ΟM NO was added to cause NO stress. Aerobic condition was performed by incubating the cultures with a cotton plug on the shaker at 150 rpm. Anaerobic condition was obtained by being degassed for 5min and bubbled with Ar gas for 5min prior to being incubated with a rubber stopper at a milder agitation (150rpm). All the cultivations of *A. oryzae* were performed under 30Ⅲ. *E. coli* DH5α was used for DNA multiplication, which has been described in chapter 1 in details.

2-1-2 Transcription analysis of *fhb1* and *fhb2* in *A. oryzae*.

Quantitative real-time PCR (Q-RT-PCR) was used to examine the transcription levels of *fhb1* and *fhb2* in *A. oryzae* under various conditions. Total RNA were isolated as described in chapter 1. The total RNA was treated with DNase I (TaKaRa) and cDNAs were synthesized using ReverTra Ace® (ToYoBo) with an oligo(dT) primer. Primer pairs, qRT-PCR-*fhb*-F and qRT-PCR-*fhb*-R, qRT-PCR-γ-*actin*-F and qRT-PCR-γ-*actin*-R (Table 2-1), were used to amplify 200-300bp DNA fragments of *fhb*1, *fhb*2 and γ-*actin,* respectively. Real-time PCR was performed with SYBR® Premix Ex Taq (TaKaRa). Reactions were performed in the Light Cycler 330 (Roche Diagnostics). The relative mRNA levels were normalized to that of γ-*actin* as a reference gene.

2-1-3 Construction of *fhb* over-expression strains

Pyrithiamine (PT) resistant gene (*ptrA*) was used as a selectable marker gene to construct the *fhb1* and *fhb2* over-expression strains. PT is a potential antagonist of the thiamine. PT can inhibit the growth of wild-type *A. oryzae* efficiently.

As shown in Figure 2-6, the vector p*NGA* 142 containing the improved

glucoamylase prompter (P*glaA142*) and the Γ -glucosidase terminator (T*agdA*) and the p*PTRI* vector (TaKaRa) containing the *ptrA* gene were cleaved by *Pst I* and *Sma I*. Then the *ptrA* gene was introduced into p*NGA* 142 to construct the over-expression vector p*PTGA*. The subcloned *fhb1* and *fhb2* with the corresponding primers (*A.o.FHb1*-F, *Not* I site shown in capital; *A.o.FHb1*-R, *Spe* I site shown in capital) shown in Table 2-1 were cleaved by *Not* I and *Spe* I and inserted into p*PTGA* vector which also has been treated with *Not* I and *Spe* I. Then the over-expression plasmids, *pPTGA / fhb1* and *pPTGA / fhb2*, were obtained.

The over-expression plasmids were transformed into *A. oryzae* RIB40 and the transformants were selected by PT resistant gene *ptrA* on the CD plate containing 0.1 O g/ml pyrithiamine. The transformants were sub-cultivated for 3 times to stabilize the plasmid. Then the over-expression strains of *fhb1* and *fhb2* were prepared.

2-1-4 **Construction of *fhb1* and *fhb2* single disruption strains.**

The strategy for constructing the *fhb1* and *fhb*2 single gene disruption cassette by fusion PCR is shown in Figure 2-2. All the primers were listed in Table 2-1.Using the genome DNA of *Aspergillus nidulans* as a template, the selectable maker gene *pryG* was amplified with the primers: *pryG* primer7 and *pryG* primer8. Using the genome DNA of *Aspergillus oryzae* RIB40 as a template, upstream(1kb) of the *fhb1* ORF were generated using the primers: *⊿fhb1* primer1 and *⊿fhb1* primer3; downstream(1kb) of the *fhb1* ORF were generated using the primers: *⊿fhb1* primer4 and *⊿fhb1* primer6. The sequences shown in capital in primer3 were designed to complementarily overlap the 5' terminal sequences of marker gene *pyrG*. The sequences shown in capital in primer4 were designed to overlap the 3' terminal sequences of marker gene *pyrG*. The

three DNA fragments were then mixed and amplified by fusion PCR with LA Taq DNA polymerase (TaKaRa) to create the *fhb1* disruption cassette. The fusion PCR conditions were as following: heating to 94℃ for 2 min; 30 cycles of 94℃ for 30 s, 55℃ for 30 s and 72℃ for 4 min; followed by a final extension for 5 min. *fhb2* disruption cassette was created by the same methods using the corresponding primers shown in Table 2-1. The amplified *fhb* disruption cassettes was purified by PCR purification Kit (LaboPass) and then transformed into *A. oryzae* Δ*ku70*Δ*pyrG*, respectively. The transformants were selected on the CD plate as the candidate strains of Δ*fhb1* and Δ*fhb2*.

2-1-5 Gene deletion verification by Southern blot analysis

The genome DNA from the host strain and the candidate Δ*fhb1* and Δ*fhb2* were separated on 0.8% agarose gel by electrophoresis after digestion with the corresponding restriction enzymes as shown in Figure 2-3, and then transferred to Hybond N^+ membrane (Amersham Biosciences, USA). Dig-labeled probes were constructed using a DIG PCR labeling kit with the corresponding primers shown in Table 2-1. Hybridization and detection of signals were carried out using DIG system (Roche).

2-1-6 Transformation of *A. oryzae*

The transformation of *A. oryzae* was performed by the method of Gomi et al (28), except that Yatalase (Takara, kyoto) was used as a mycelial spheroplast preparation.

2-2 Results and discussions

2-2-1 Transcriptional responses of *fhb1* and *fhb2* genes to NO stress.

To examine whether both of the two *A. oryzae* FHb genes are respond to NO stress like the bacteria and yeast FHb genes, I investigated their transcriptional level under the NO stress conditions. As shown in Figure2-1, compared with the untreated cells, *fhb1* from the NO-exposed ($NaNO_2$ or NO solution) cells were induced more than 10 times in their transcriptional levels. At the same time, we also examined the expression of *fhb2*, but its transcription level is too low to be determined if it was induced by NO stress (data not shown). These results at least suggested that *fhb*1 was respond to NO stress.

2-2-2 Construction of *fhb1* and *fhb2* disruption mutant

To study the biological roles of *fhb1* and *fhb2*, the two genes were deleted from chromosome, respectively.

In fact, the genetic analyses of *A. oryzae* is difficult because this mold has multiple nuclei in not only its vegetative cells but also its reproductive conidiospores(75). In addition, gene targeting frequency in *Aspergillus* species is very low. The DNA integration occurs predominantly through a nonhomologous end joining (NHEJ) pathway, by which the exogenous DNA integrates into chromosomes irrespective of the sequence homology (37). Two *ku* genes, namely, *ku70* and *ku80*, were reported to play a key role in NHEJ. Recently, the *ku*-disruption strains of *A. oryzae*, constructed by T. Takahashi et al., revealed a marked enhancement in gene targeting frequency without any evident phenotypic defects (73). In my study, all of the gene disruption strains were constructed from the parent strain, *A. oryzae* ΔΔ*ku70*ΔΔ*pyrG*. *pyrG* gene, encoding orotidine 5' – monophosphate decarboxylase, is often used as a selectable marker gene for transformation. Δ*pyrG* strain is a uridine/uracil auxotrophic mutant.

Historically, most gene targeting in fungi involved transformation with plasmids generated by standard cloning procedures. The construction of the transformation plasmids was time-consuming. Here I applied a Fusion-PCR mediated method to generate the gene disruption construct without the use of DNA ligase and plasmid vectors. The schematic illustration of the Fusion-PCR was described in Figure 2-2 and in the materials and methods.

Two candidate transformants for ☳*fhb1* and ☳*fhb2* were selected to be clarified the deletion of *fhb1* and *fhb2* by southern blotting, respectively (Figure 2-3).！ Then one was selected to study their phenotype for each of the single disruption strains.

2-2-3 Comparison of the phenotype of ☳*fhb1*, ☳*fhb2* and their isogenic parent strain, (☳*ku70*☳*pyrG*), in the absence of NO stress.

Like the FHb genes in *E. coli* and *S. cerevisiae* (87), both of *fhb1* and *fhb2* are not the lethal genes. *fhb1*-deletion strain (☳*fhb1*) and *fhb2*-deletion strain (☳*fhb2*) were obtained on CD medium by transforming the disruption cassette constructed by fusion PCR into *A. oryzae* ☳*ku70*☳*pyrG*.

！！ In the minimal agar medium (CD plate), under the normal conditions, the growth rate of ☳*fhb1* was obviously slower than ☳*fhb2* and their parent strain wild-type (☳*ku70*☳*pyrG*) (Figure 2-4 A). In the liquid CD medium without any external stress, unlike wild-type (☳*ku70*☳*pyrG*) and ☳*fhb2* strains, ☳*fhb1* did not form clumps any more (Figure 2-4 B,C). On the other hand, no significantly difference was found between ☳*fhb2* and wild-type(☳*ku70*☳*pyrG*). These results suggested that FHb1 affects the fungal morphology. The *S. cerevisiae* FHb (YHb) was shown not essential and its deletion mutant did not affect the growth rates and yields under both aerobic and

anaerobic conditions (87). *E. coli* FHb (HMP) was also indicated to be unessential for aerobic and anaerobic growth in LB medium or MOPS minimal medium. However, the turbidity of the *hmp* mutant cultures declined slightly during the stationary phase (49), but the possibility of the subtle effect of loss of HMP on growth under certain conditions remained unclear. On the other hand, the *Candida albicans* FHb mutant (*yhb1*) was found hyperfilamentous under nonfilamenting conditions (32). Eight genes, which had been shown to be part of the filamentous growth program in *C. albicans*, were induced greater than sixfold in the *yhb1* grown under these conditions. So *yhb1* deletion was thought to cause an inappropriately activation of the genes involved in the filamentous pathway (32). Another interesting example is that, *Dictyostelium discoideum* FHb gene deletion caused a marked increasing in cell size without affecting the growth rate or cell division (34). Together this results, it can be demonstrated that FHbs in some microbes have some relations with the cellular morphology.

On the other hand, no differences were detected between *fhb* disruption strains with wild-type when they were cultured in the nutrition rich media, DPY. So DPY medium was used to investigate the effects of *fhb* disruption on NO stress resistance.

2-2-4 Protection of *A. oryzae* against NO stress mainly by FHb1, in vivo.

To analysis of the biological functions of *fhb1* and *fhb2*, I examined the response to NO stress with the two single disruption strains. As shown in Figure 2-5 A, on plate, under the normal conditions, growth of the three strains was similar. But in the presence of the NO stress caused by 20mM $NaNO_2$, the *fhb1* was significantly more sensitive than wild-type (*ku70pyrG*), whereas *fhb2* showed no difference compared with wild-type (*ku70pyrG*). In the liquid DPY media (Figure 2-5 B), the phenotypes of

the three strains were similar to them on the plates. With the external added 20mM $NaNO_2$ or 100μM NO solution, Δ*fhb1* grew more slowly than wild-type and Δ*fhb2*. Taken together, these data indicated that *fhb1* is required to protect cells from NO stress.

As shown in chapter 1, recombinant FHb2 protein exhibits robust NO dioxygenase (NOD) activity as FHb1 in vitro. However, under this experiment conditions, no relation was found between *fhb2* and NO detoxification in vivo. The transcriptional level of *fhb2* has been identified very low, which may be the reason why *fhb2* disruption strain exhibited no obvious difference in its phenotype compared with wild type. To study the *fhb2* gene more, I constructed an FHb2 over-expression strain to see whether the role of *fhb2* could be enlarged in vivo. At the same time, *fhb1* over-expression strain and the control strain possessing a blank vector were also prepared (Figure 2-6). The over-expression vector (pPTGA) harbors an improved glucoamylase promoter (P-glaA 142), which is induced by dextrin efficiently. So when the strains were cultured in DPY medium (carbon source is dextrin) the over-expression plasmid should be activated. After the over-expression transformants were obtained, the transcription levels of fhb genes were confirmed by real-time PCR. The transcription of *fhb1* was increased 150 folds in *fhb1* over-expression strain than in the blank vector possessed strain. Meanwhile, the level of *fhb2* was increased at least 3000 folds due to the *fhb2* over-expression plasmid (data not shown). The over-expression of *fhb2* made the strain colored brown-pink. Then the over-expression strains were also examined their resistance to NO stress. However, as shown in Figure 2-7, no significantly difference was detected among the three strains, which indicated that the recombinant over-expression of *fhb1* and *fhb2* could not improve its NO stress resistance. The physiological function of *fhb2* still could not be elucidated by this experience.

2-2-5. Production of NO in mitochondria induced *fhb2* expression.

fhb2 is located in chromosome 4, and lies adjacently to a gene encoding a putative multicopper oxidase which has been identified and characterized as a dissimilatory nitrite reductase (NirK) by my predecessor, Nakanishi. NirK is putatively involved in denitrification and catalyzes the reduction of nitrite to NO. Similar to FHb2, NirK possessed a mitochondrial targeting signal sequence in its N-terminus. Additionally, NirK has been suggested to be cellular localized in mitochondria by some experiments in previous studies performed by Mr. Nakanishi. So we speculated that *fhb2* may respond to the mitochondrial NO under denitrification conditions (low O_2 plus nitrite), *in vivo*. I have investigated the transcriptional level of *fhb2* under denitrification conditions, but it is still too low to be quantitatively evaluated by real-time PCR. The mitochondrial NO produced by NirK may be minor due to the low nitrite reducase activity of the NirK *in vivo* which has been checked by Nakanishi with the crude cell extraction. A *nirk* over-expression recombinant *A. oryzae* has been constructed by Nakanishi, which showed about 6 folds higher in the denitrification ability than wild-type. Then as an intermediate of denitrification, mitochondrial NO should also be improved in cell. I investigated whether the improved mitochondrial NO would induce the expression of *fhb2*. As shown in Figure 2-8, under a special conditions (anoxia for 3 hours and then aerobiosis for 30 min), the expression of *fhb2* was obviously detected in *nirK* over-expression strains but not in the other strains. Anoxia for 3 hours was expected to induce the mitochondrial NO produced by NirK. Under anaerobic conditions, the fungal NO reductase (P450 nor) plays the role of NO detoxification by reducing NO to N_2O and FHb might be inactivated because its NO dioxygenase (NOD)

activity required O_2. So the following aerobiosis for 30 min would inactivate P450nor and possibly induce the activated FHb to detoxify the remained NO produced under the anaerobic conditions. To certify the relation between FHb2 and the mitochondrial NO more clearly, the expression patterns of *fhb2* in *nirK* over-expression strains were investigated (Figure 2-9 B) and compared with the expression of *fhb1* (Figure 2-9 A) under various conditions by Quantitative- RT-PCR. The expression pattern of *fhb1* in *nirK* over-expression strain was similar to it in wild-type (Figure 2-1), and the transcriptional level were also similar to them in wild type (data not shown). Additionally, *fhb1* was induced for about 5 folds by the O_2-limited conditions without NO_2^- addition (Figure 2-9 A). The 3 hours anaerobic incubation had increased the expression of *fhb1*, however the followed 30 min aerobic incubation made the *fhb1* expression return to the normal level (Figure 2-9 A). The denitrification condition ($NaNO_2$ + O_2 limited) robustly induced the expression of *fhb1* and after 30 min aerobic incubation its expression still kept in a high level (Figure 2-9 A). On the other hand, *fhb2* was mainly induced under the conditions that the mitochondrial NO was produced and remained (anaerobic conditions or 3 hours anaerobic incubation plus 30 min aerobic incubation.) (Figure 2-9 B). Unlike *fhb1*, the expression of *fhb2* was induced by $NaNO_2$ slightly under aerobic conditions in *nirK* over-expression strain (Figure 2-9 B).

Taken together, these results suggested that FHb2 is responding to the mitochondrial NO stress.

2-2-6 Do the two FHbs protect the cell from NO stress in a co-operative manner?

FHb1 and FHb2 are suggested to respond to the cytosol and mitochondrial NO stress, respectively. We are interesting if they act in a co-operative manner. So I

investigated that if the deletion of one *fhb* gene will affect the expression of another one. As shown in Figure 2-10, in wild type (*Δku70ΔpyrG)*, NO_2^- induced the expression of *fhb1* for about 10 folds under aerobic conditions and the 3 hours anaerobic incubation then 35 min aerobic incubation induced the expression of *fhb1* about 20 folds. These results in agreement with the results in *nirK* over-expression strain (Figure 2-9 A), suggested that anaerobic incubations increased the cytosol NO stress. In *Δfhb2*, NO_2^- induced *fhb*1 for about 14 folds (Figure 2-10), which was similar to this in wild type, whereas the *fhb2* deletion strongly enhanced the expression of *fhb1* under the " $-O_2+$ " conditions compared with it in wild type (Figure 2-10). The possible reason is that the mitochondrial NO escaped from detoxification due to the *fhb2* deletion and flow into cytosol to improve the expression of *fhb1*. I also investigated the expression pattern of *fhb2* in wild type and *Δfhb1* under these four conditions, their expression level were still too low to be quantitated accurately. (data not shown).

In the other hand, as the results discussed in 2-2-4, the presence of FHb2 could not compensate the deletion of *fhb1* under the NO stress conditions (Figure 2-5 A and B).

Taken together, these results suggested that, though *fhb2* deficiency improved the transcription of *fhb1* under NO stress conditions, FHb1 and FHb2 of *A. oryzae* do not act in a co-operative manner and they do not work in parallel.

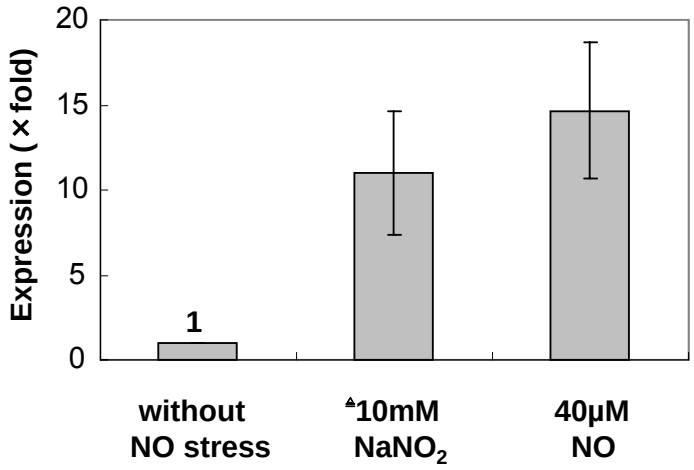

Figure 2-1 Fold induction of *fhb1* genes in response to NO stress in wild type.

The relative mRNA levels of each samples were normalized to that of γ - actin as a reference gene, firstly. Then the expression values of each samples were determined relative to it in the cells grown with no addition, which was taken as 1. Results represent the means of three independent experiments±SE.

* under acidic pH, NO_2^- can chemically converted into NO.
The pH of DPY media in this work are 5.5.

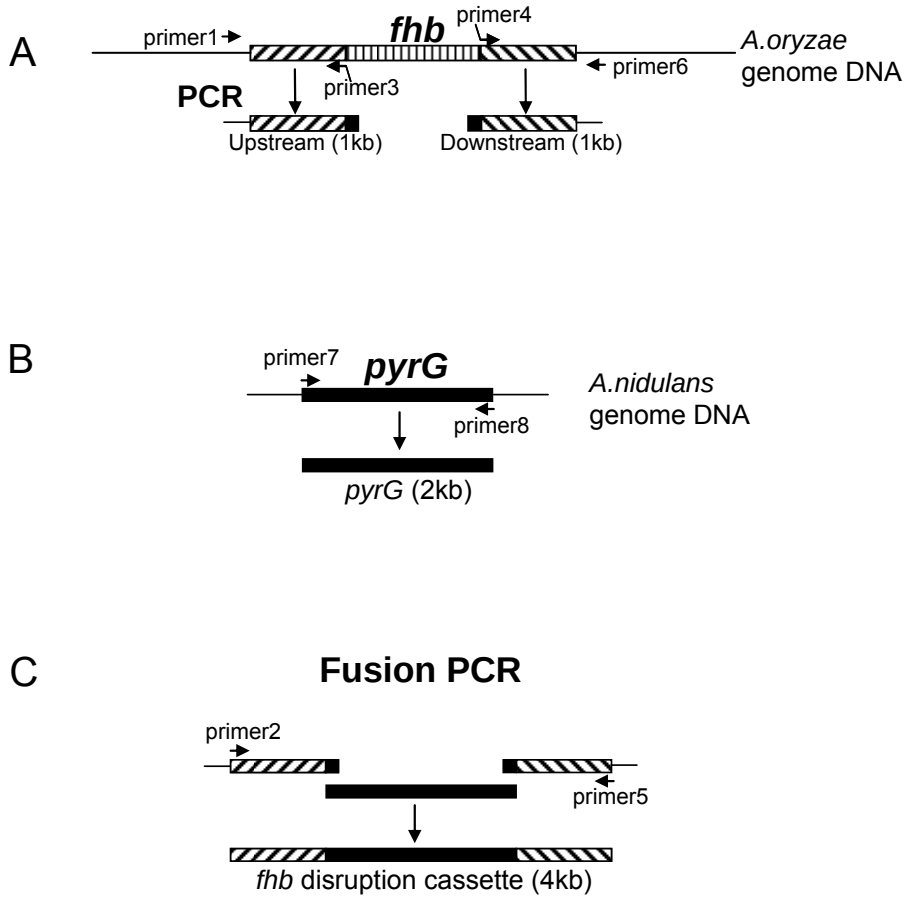

Figure 2-2 Construction of the *fhb* single disruption cassette.

A. Preparation of the upstream (1kb) and downstream (1 kb) of *fhb* by the corresponding primer pairs (primer 1+ primer 3;. Primer 4 + primer 6).
B. Preparation of the selectable marker gene, *A. nudulans pyrG* (2kb), by primer 7 and primer 8.
C. Construction of the *fhb* disruption cassette by fusion PCR with nested primers (primer 2 and primer 5).

All of the primers sequences were shown in Table 2-1.
The purified disruption cassettes were transformed into *A. oryzae ⊿ku70⊿pyrG*
to produce the *fhb* single disruption strains (*⊿fhb1* and *⊿fhb2*).

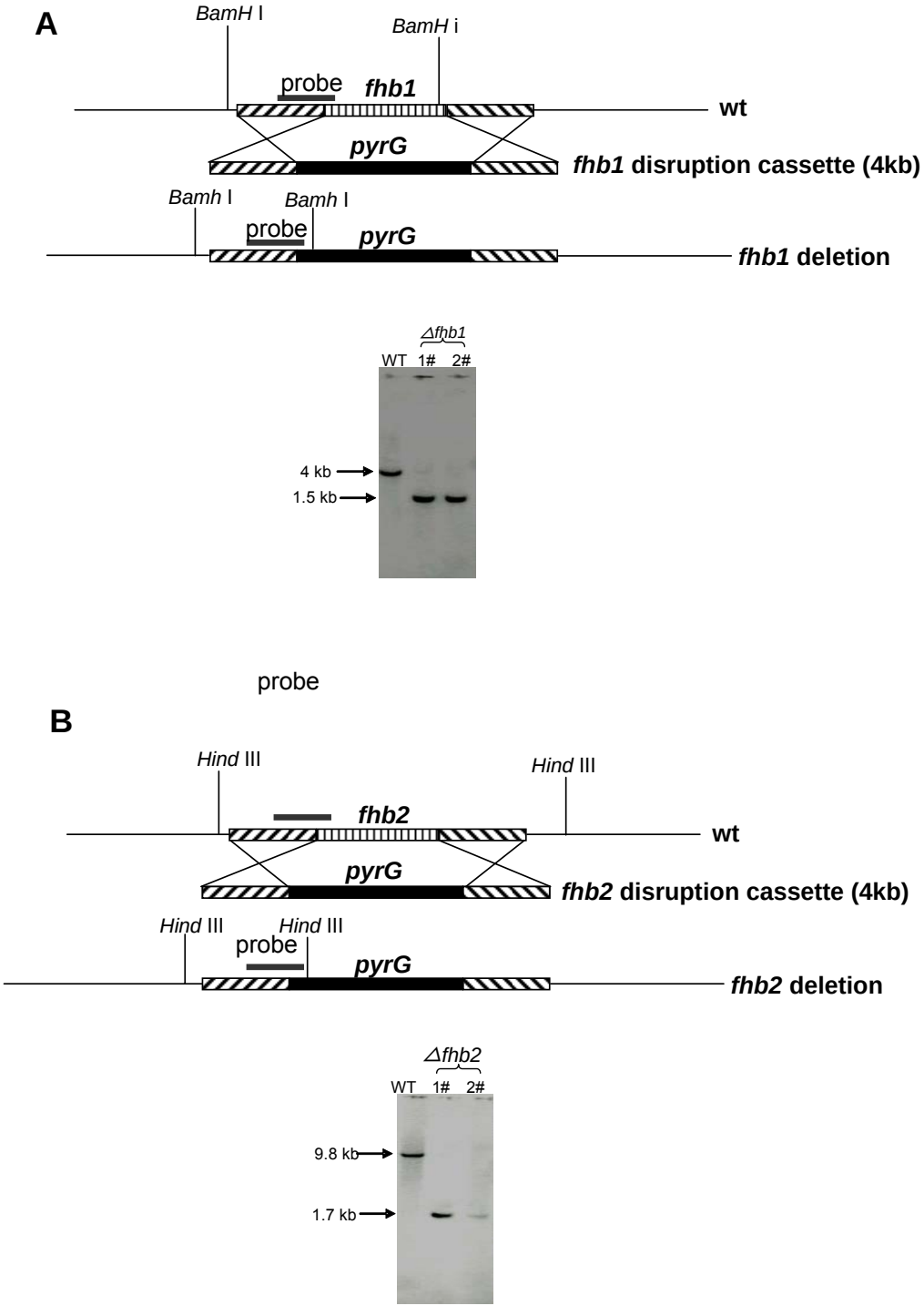

Figure 2-3 Homologous recombination occurs to delete *fhb1* (A) and *fhb2*(B) genes from chromosome and the verification of the gene disruption by southern blot.

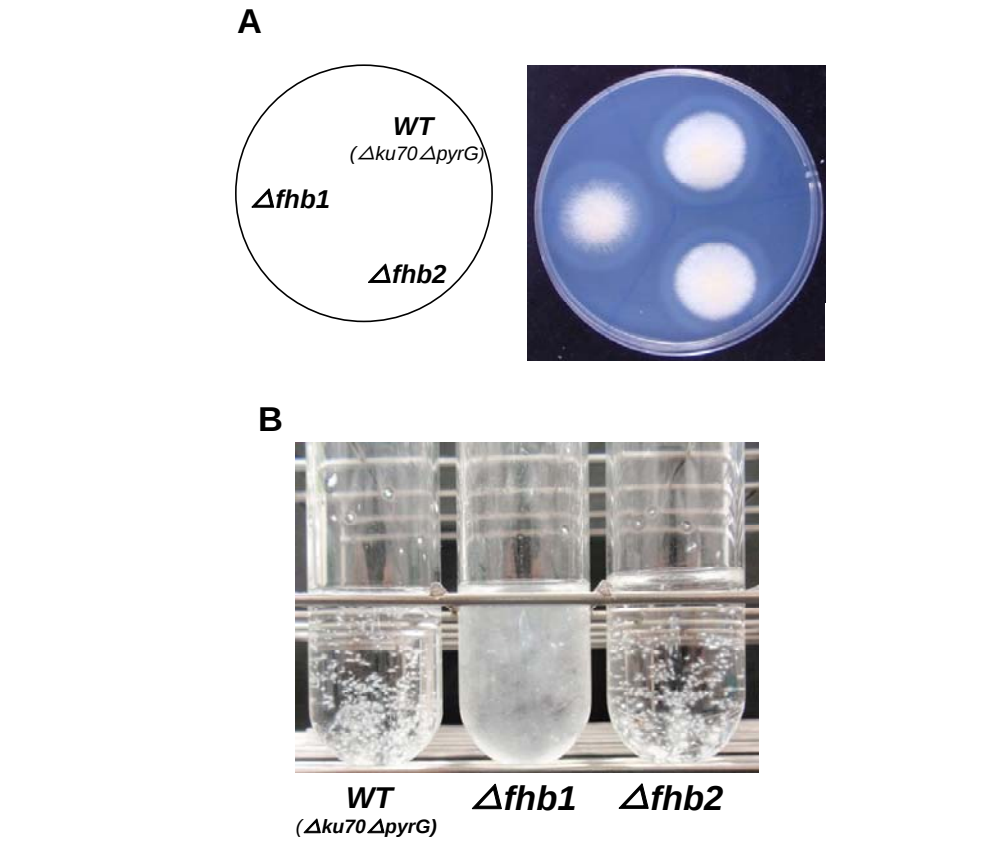

Figure 2-4 The deletion of *fhb1* affected the morphology of *A. oryzae* in minimal medium （CD + uracil + uridine) under the normal conditions.

A, 10^4 spores of wild type (*ΔKu70ΔpyrG*), *Δfhb1* and *Δfhb2* were seeded on minimal CD agar medium and incubated at 30℃ for 72 hours.
B, Spores from the three strains (10^4 spores/ml), were aerobically grown in 200 ml CD liquid media in 500 ml flasks under 30℃ for 24 hours. To compare easily, they were transferred into test tubes.
C. Morphology of fungal mycelium in the liquid minimal medium (CD) observed by microscopy (10×20).

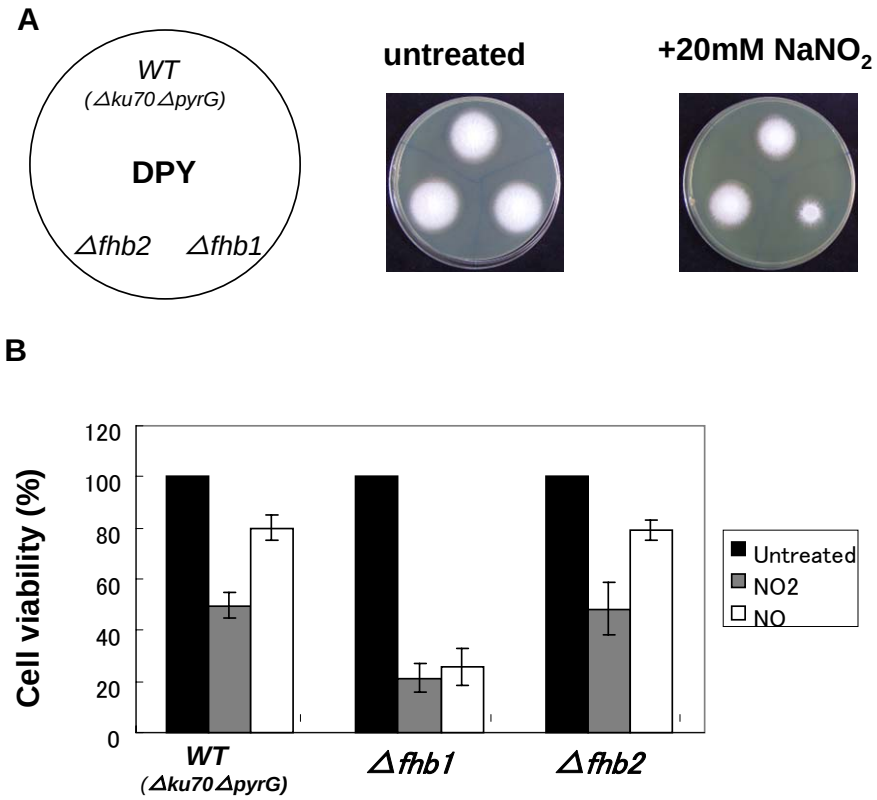

Figure 2-5. Growth impairment of the *fhb1* deletion under NO stress conditions on DPY plate (A) or in DPY liquid media (B).

A, In DPY plate (pH5.5), 20mM NaNO2 was added as the NO-generator.
10^4 spores from the three type of strains were seeded onto the plates and incubated at 30℃ for 48h.

B, After pre-culture in DPY, the three strains were seeded into the fresh liquid DPY media and incubated aerobically at 30℃ for 12 hours. 20mM $NaNO_2$ and 100 μM NO were used to cause NO stress, respectively. The cell viability was calculated by the dry weight of strains.The cell viability of the three strains in the normal medium were regarded as 100%. The data were from three independent experiments.

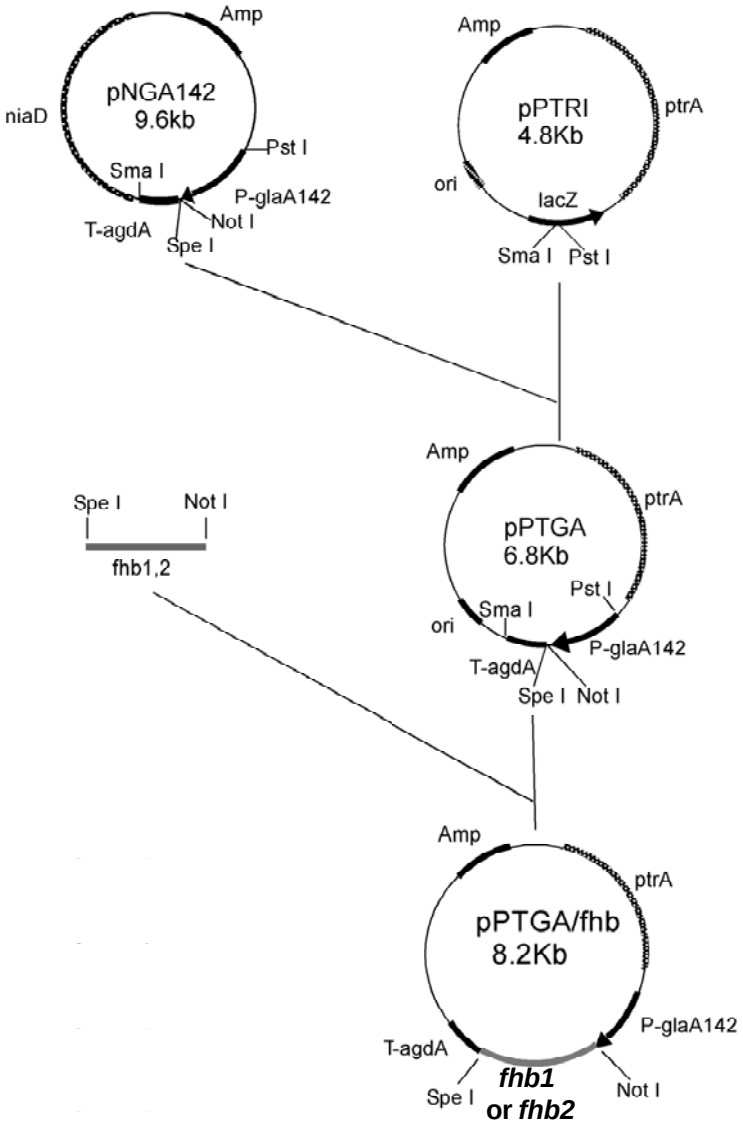

Figure 2-6 Construction of FHb1 and FHb2 over-expression plasmids.

P-glaA142: Improved glucoamylase promoter; induced by dextrin.
T-agdA: α-glucosidase terminator .
ptrA: pyrithiamine resistant marker gene.

The over-expression vector pPTGA was constructed from two vectors, p*NGA142* (possessing the promoter and terminator) and p*PTRI* (possessing the selective marker gene).

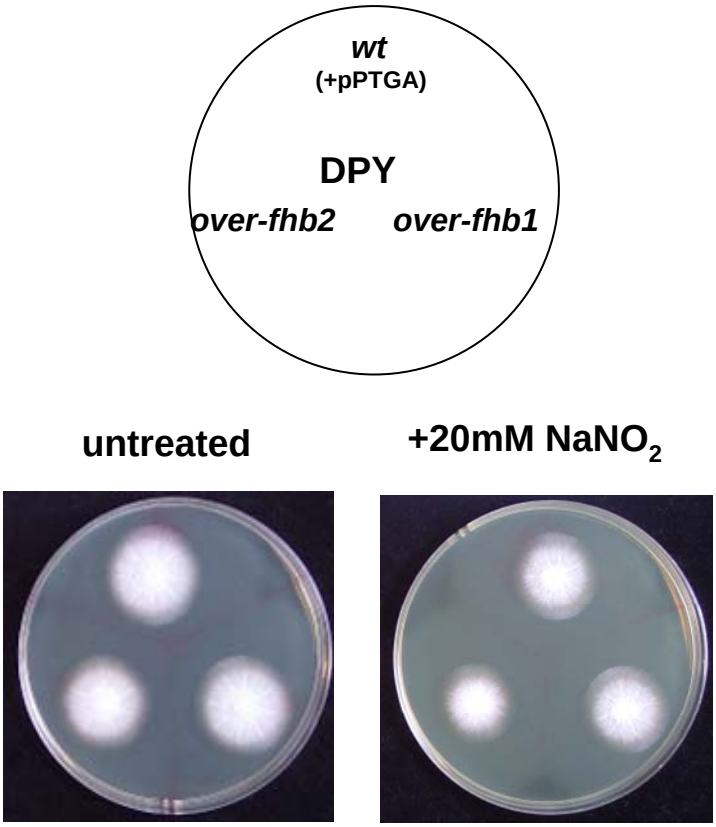

Figure 2-7. FHb over-expression unaffected the resistance to NO stress.

In DPY plate (pH5.5), 20mM $NaNO_2$ was added as the NO-generator. 10^4 spores from each of the three strains were seeded onto the plates and incubated at 30℃ for 48 h.

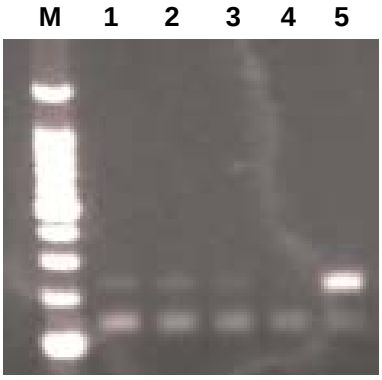

Figure 2-8 Transcription of *fhb2* was visible only in *nirK* over-expression strain

After pre-culture in DPY medium for 24 hours, the strains were anaerobically incubated in DPY medium (with or without 10mM $NaNO_2$) for 3 hours and then aerobically incubated for 30 min. The special aeration condition was interpreted in 2-2-5.

M: DNA marker;
1: wt (*⊿ku70⊿pyrG*); 2: wt (*⊿ku70⊿pyrG*) + $NaNO_2$;
3: *⊿fhb1* + $NaNO_2$; 4: *⊿fhb2* + $NaNO_2$;
5: *nirK* over-expression + $NaNO_2$
The expression patterns of *fhb2* were confirmed by RT-PCR (30 cycles).

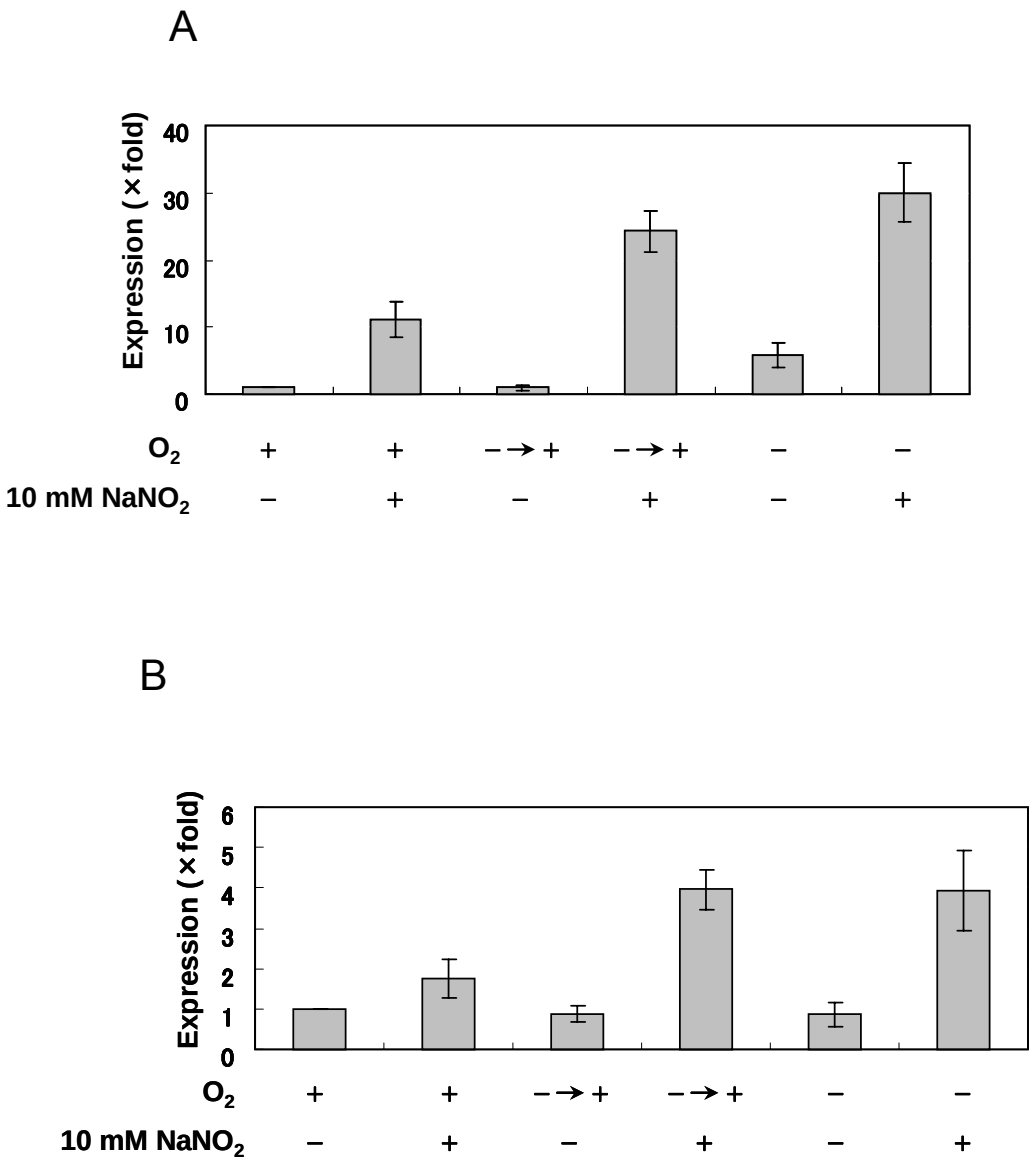

Figure 2-9 Expression patterns of *fhb*1 (A) and *fhb2* (B) in *nirK* over-expression *A .oryzae* responding to O_2 and NO_2^-.

" – →+ " means 3 hours anaerobic incubation then 35 min aerobic incubation. Details see 2-2-5

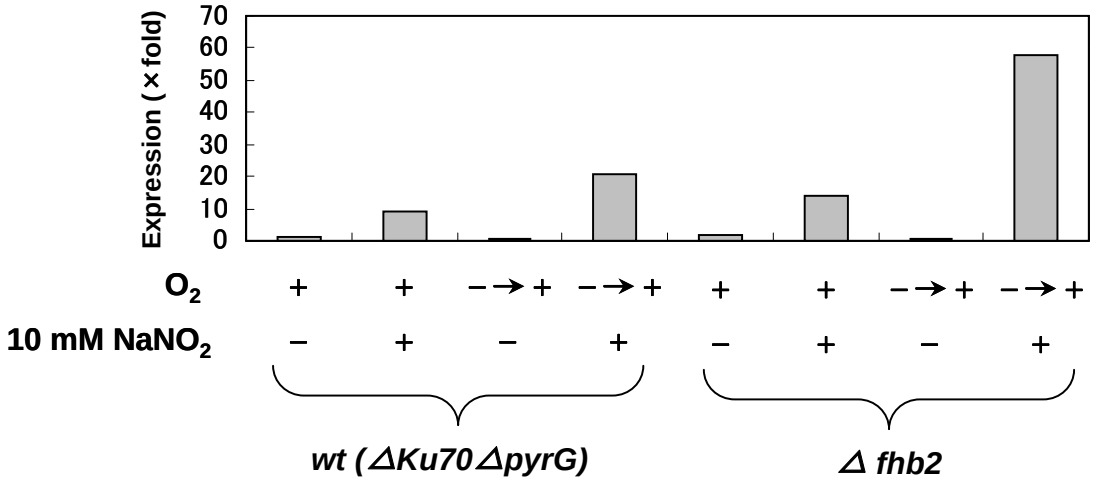

Figure 2-10 *fhb2* deletion improved the transcriptional level of *fhb1* under the mitochondrial NO remaining conditions.

" – →+ " means 3 hours anaerobic incubation then 35 min aerobic incubation.

Name	Sequnce(5'→3')
qRT-PCR-*fhb1* -F	5'-gactccctggccgagaagtac-3'
qRT-PCR-*fhb1* -R	5'-gagctccagcttgatgcgatc-3'
qRT-PCR-*fhb2* -F	5'-cgcgcggtgttctatgaag-3'
qRT-PCR-*fhb2* -R	5'-ttattcagccggagaaccg-3'
qRT-PCR-γ-*actin* -F	5'-gacccagattgtcttcgag-3'
qRT-PCR-γ-*actin* -R	5'-gtaatcggtcaaatcacggcc-3'
A.o. FHb1- F	5'-GCGGCCGCatgccgctctcccctgaac-3'
A.o. FHb1- R	5'-ACTAGTctaagcaggaacaccgccggtgc-3'
A.o. FHb2- F	5'-GCGGCCGCatgctagccaaaacaatgttc-3'
A.o. FHb2- R	5'-ACTAGTttattcagccggagaaccgaacac-3'
⊿*fhb1* primer1	5'-tggtcggactggccgaagtc-3'
⊿*fhb1* primer2	5'-cggcggtgagcgtattgtag-3'
⊿*fhb1* primer3	5'-AGGACAGGGATTGCGCCTAGggtgaagggatagtctgaag
⊿*fhb1* primer4	5'-TGGGCTGTGGTTAAGCCGGgaccatacctagaccatctg-3'
⊿*fhb1* primer5	5'-gcagaattacccctggttc-3'
⊿*fhb1* primer6	5'-cggtataccatctgaaacaccg-3'
pryG primer7	5'-CTAGGCGCAATCCCTGTCCTGG-3'
pryG primer8	5'-GCCGGCTTAACCACAGCCCAAC-3'
⊿*fhb2* primer1	5'-cgaacctaaccagctcgttcc-3'
⊿*fhb2* primer2	5'-cggatgtactaagtccgccg-3'
⊿*fhb2* primer3	5'-AGGACAGGGATTGCGCCTAGccgtggactttgcggatgg-3
⊿*fhb2* primer4	5'-TGGGCTGTGGTTAAGCCGGCacagaagaatagaagtcgg
⊿*fhb2* primer5	5'-gtgccatatccagatgag-3'
⊿*fhb2* primer6	5'-cgaagtgtggacacccag-3'
⊿*fhb1* probe F	5'-ggaagggcatcgaccaatc-3'
⊿*fhb1* probe R	5'-ccgtcggcctgcttgtacag-3'
⊿*fhb*2 probe F	5'-gctgggctagttttacctgg-3'
⊿*fhb2* probe R	5'-ctggaggagacgctggtag-3'

Table 2-1 . Nucleotide sequences of primers used in this work.

Chapter 3 *A. oryzae* FHbs promote oxidative damage of H_2O_2

S. cerevisiae FHb (YHb) had been indicated play a role in the protection against to the oxidative tress (87). Expression of YHb gene is sensitive to oxygen. The expression is optimal in hyperoxic conditions and is reduced under hypoxic conditions. The expression of YHb gene is enhanced in the presence of antimycin A, in thiol oxidants, or in strains lack superoxide dismutase. All the conditions lead to the accumulation of reactive oxygen species and promote oxidative stress. Additionally, The YHb gene deletion strains are sensitive to the oxidative conditions. Together, these findings suggested that YHb plays a role in the oxidative stress response in yeast (87). *E. coli* FHb (HMP) is also reported to be essential for response to oxidative stress (49). An *hmp* null mutant showed increased sensitivity to the redox-cycling agent, paraquat. The HMP deficient affected the superoxide dismutase synthesis in response to oxidative stress. So the protection role by HMP probably involved direct detoxification of these oxidative species and sensing of the oxidative stress (49). But another research group demonstrated a conflicting views that their results did not support a participation of *S. cerevisiae* YHb in the genetic response to oxidative stress (9). In their report, YHb gene expression was unchanged in cells challenged with antymycin A or menadione, while it decreased in cells exposed to H_2O_2. Additionally, *E. coli* HMP can generate superoxide in vitro and cause oxidative stress in vivo (51), which makes it contradicting to play the roles in protection against to the oxidative stress. So whether FHb is involved in response to oxidative stress remain unclear.

In this chapter, I investigated the response of the two *A. oryzae* FHbs to H_2O_2 to study the relations between oxidative stress and fungal FHbs.

3-1 Materials and methods

3-1-1 Strains.

Wild type (Δ*ku70*Δ*pryG*), Δ*fhb1* and Δ*fhb2* were used as the parent strain, *fhb1*-deletion strain and *fhb2*-deletion strain, respectively. wild type (pPTGA+), *fhb1*+ and *fhb2*+ were used as the blank vector containing strain, *fhb1* over-expression strain and *fhb2* over-expression strain, respectively.

3-1-2 H_2O_2 resistance assay.

10^4 spores of various strains were seeded on DPY agar media containing 0 mM, 10 mM and 15 mM H_2O_2 and incubated at 30℃ for 3 days. The colony sizes were compared to determine their resistance abilities to H_2O_2.

3-1-3 In vitro, measurements of flavin reductase activity and ferric reductase activities of FHb1 and FHb2.

Reduction of flavin was measured by monitoring the absorbance of FAD (ε =11,300 $M^{-1}cm^{-1}$) or FMN (ε =12,500 $M^{-1}cm^{-1}$) at 450 nm using V-550 spectrophotometer (Jasco). The reaction conditions were described in the legend of Figure 3-3.

Reduction of ferric iron was determined from the increasing of the absorbance at 562nm, due to the appearance of Fe^{2+} and then the formation of the Fe^{2+}-Ferene complex. Reactions were performed at 30℃ and the details were described in Figure3-4.

3-2 Results and Discussions

3-2-1 Both of FHb1 and FHb2 show deleterious effects in defense against H_2O_2.

In order to gain insight the relation of *A. oryzae* FHbs with oxidative stress, I examined the transcriptions of its genes, *fhb1* and *fhb2*, in response to H_2O_2. The transcriptional levels of the two genes were unchanged significantly in cells challenged with 15mM H_2O_2 for 1 hour in DPY medium (data not shown), which indicated that neither FHb1 nor FHb2 participated in the genetic response to H_2O_2. Following, I examined the effects of FHb gene deficiency on its tolerance to H_2O_2. As shown in Figure 3-1 A, on the DPY plate medium (added with 5mM uracil and 5mM uridine), wild type exhibited more sensitive to H_2O_2. The more concentrated H_2O_2 added, the more obvious the difference exhibited. *fhb1*-deletion and *fhb2*-deletion mutants showed higher tolerance to H_2O_2 than wild type and no obvious difference was detected between the two disruption strains. These results indicated that both of FHb1 and FHb2 were harmful in response to H_2O_2.

Next, I compared the sensitivities of wild type, *fhb1*-overexpressing strain (over-*fhb1*) and *fhb2* over-expressing strain (over-*fhb2*) to H_2O_2 on DPY medium. As shown in Figure 3-1 B, over-*fhb2* showed hypersusceptibility to H_2O_2 compared with wild type (p*PTGA*+) and *over-fhb1*, which was in agreement with the results shown in Figure 3-1 A. But it should be noted that *over-fhb1* did not show difference compared with wild-type. It may be due to the sufficient level of *fhb1* expression in wild type to suffer from the oxidative damage of H_2O_2, whereas the level of *fhb2* expression is very low and *fhb2* over expression could enhance the oxidative damage significantly. In other reports, FHb overexpressing cells of *Salmonella* and *S. cerevisiae* showed higher

susceptibility to oxidative stress than wild type, too (3, 9).

Together these results, we demonstrated that both of *A. oryzae* FHb1 and FHb2 show deleterious effects in defense against H_2O_2.

3-2-2 *A. oryzae* FHbs exhibit a flavin reductase which may be the cause for the promotion of oxidative damage.

！！ H_2O_2 is a strong oxidant which can efficiently oxidize iron-sulfur clusters and protein thiols. So when H_2O_2 are abundant, the resultant damage compromises the function of key enzymes and then inhibits metabolism (12, 68). Another significant cellular damage is likely to occur to DNA. H_2O_2 itself can not directly oxidize DNA, but it reacts metal ions to form a hydroxyl radical ($OH\cdot$), hydroxyl radicals attack both sugar and base moieties, leading to sugar fragmentation, strand scission, and base adducts (33). Oxidative DNA damage occurs in three steps (82):

$$\text{Reductant}^{red} + Fe^{3+} \nearrow \text{reductant}^{ox} + Fe^{2+} \quad (1)$$

$$Fe^{2+} + H_2O_2 \nearrow Fe^{3+} + OH\cdot + OH^- \quad \text{(Fenton reaction)} \quad (2)$$

$$OH\cdot + DNA \nearrow H_2O + \text{damage} \quad (3)$$

Reductant ^{red} and reductant ^{ox} are reduced and oxidized reductant, respectively. In equation 1, what is the iron reductant remains unclear. However, it had been reported that $FADH_2$ produced by flavin reductase (Fre) efficiently transfer electrons to Fe^{3+} in *E. coli* (82). The free reduced flavins promoted DNA damage in vivo when respiratory chain was blocked (82).

The oxidative damage of H_2O_2 to the key enzymes and the metabolism should be indistinctive to cells, which is not interpretable for the deleterious effects of FHbs in defense against H_2O_2. On the other hand, the DNA damage of H_2O_2 depending on

Fenton reaction should be responsible for it since the C-terminal portion of FHbs (redox domain) show homology to *E. coli* Fre (Figure 3-2 A and B). The identities of Fre to FHb1 and FHb2 are 25 % and 16 %, respectively. Then I examined if FHbs possessed a flavin reductase activities using the purified recombinant proteins. The internal pH in vivo is not clear, so I tested the activities under pH 5.5 and pH 7.0. As shown in Figure 3-3, compared with the controls, both of FHb1 and FHb2 exhibited obvious flavin reductase activities when NADH was used as an electron donor. FMN reductase activity of FHb2 is relatively higher than FHb1 (Figure 3-3 A), whereas there are no obvious differences detected in their FAD reductase activities (Figure 3-3 B). Next, I examined if flavin reductase activities of FHbs attribute to reduce free iron. As shown in Figure 3-4, both of the two enzymes could efficiently reduce free Fe^{3+} to Fe^{2+} in the presence of NADH and flavin under pH 5.5 or pH 7.0. No significant difference of catalyzed speed in iron reduction was found between FHb1 and FHb2 in the presence of FAD (Figure 3-4 B), but FMN improved the iron reduction activity of FHb2 obviously (Figure 3-4 A), which is consistent with the results shown in Figure 3-3 A that FMN reductase activity of FHb2 is relatively higher. Following, the resulted Fe^{2+} would reacted with H_2O_2 to produce HO· (Fenton reaction) , which should cause DNA damage efficiently.

Together these results, the possible mechanism of FHb-mediated H_2O_2 sensitivity was speculated and described in Figure 3-5. *A. oryzae* FHb play the roles in protection against NO toxicity by its NO dioxygenase (NOD) activity. But in the presence of H_2O_2, it will cause DNA damage by the free by-product, reduced flavin. FHb1 should enhance the nuclear DNA damage for its cytosol cellular localization. FHb2 localized in mitochondria should enhance the mitochondrial DNA damage.

Mitochondrial DNA is indicated more vulnerable to oxidative damage than nuclear DNA for several reasons (66, 84). Mitochondrial DNA is not covered by histones or other DNA-associated proteins, thus directly exposing to reactive oxygen species (ROS) (45). Mitochondrial DNA is an intron-less DNA with a high transcription rate, providing a high probability of oxidative modification of the coding region (43). Finally, compared with the DNA repair machinery of nuclear DNA, the repair systems of mitochondrial DNA appear to be less efficient (17, 46). Many studies have supported the notion that mitochondrial DNA is more susceptible than nuclear DNA to damage by ROS (2, 64, 84). So though the expression level of *fhb2* is very low, the effect of its deletion on mitochondrial DNA damage is still efficient.

To date, the relation between FHb and oxidative stress in yeast and bacteria is still argued. The results in this study suggested fungal FHb dose not play a role in the protection against to the oxidative stress but show a deleterious effect in defense against H_2O_2.

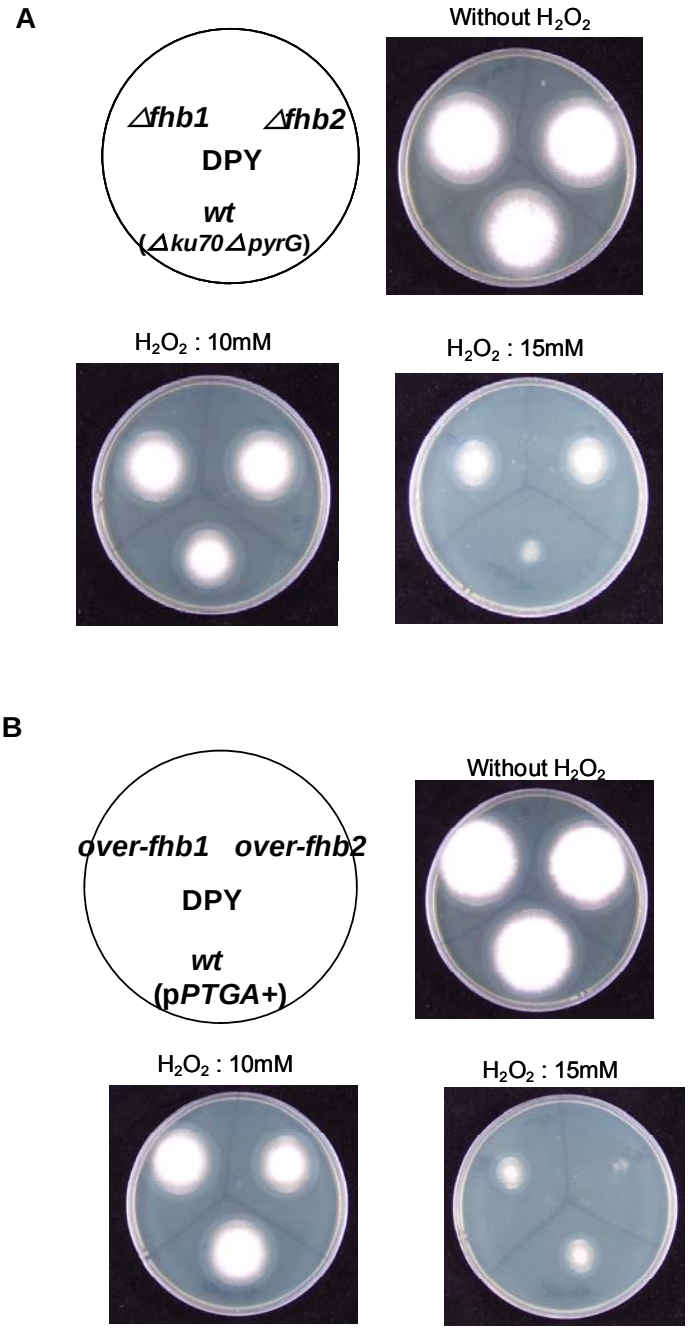

Figure 3-1 Expression of the FHbs increases *A. oryzae* suscepibility to H_2O_2.

A: Both of *fhb1* and *fhb2* deficient mutants (⊿*fhb1*,⊿*fhb2*) exhibit higher tolerance to H_2O_2 than their parent strain *wt* (⊿*ku70*⊿*pyrG*)
B: *fhb2* over-expression strain (over-*fhb2*) shows higher susceptibility to H_2O_2.

DPY medium was used in both experiments. 5mM uridine and 5mM uracil were added to maintain the growth of wt (⊿*ku70*⊿*pyrG*)
The plates were incubated at 30℃ for 3 days.

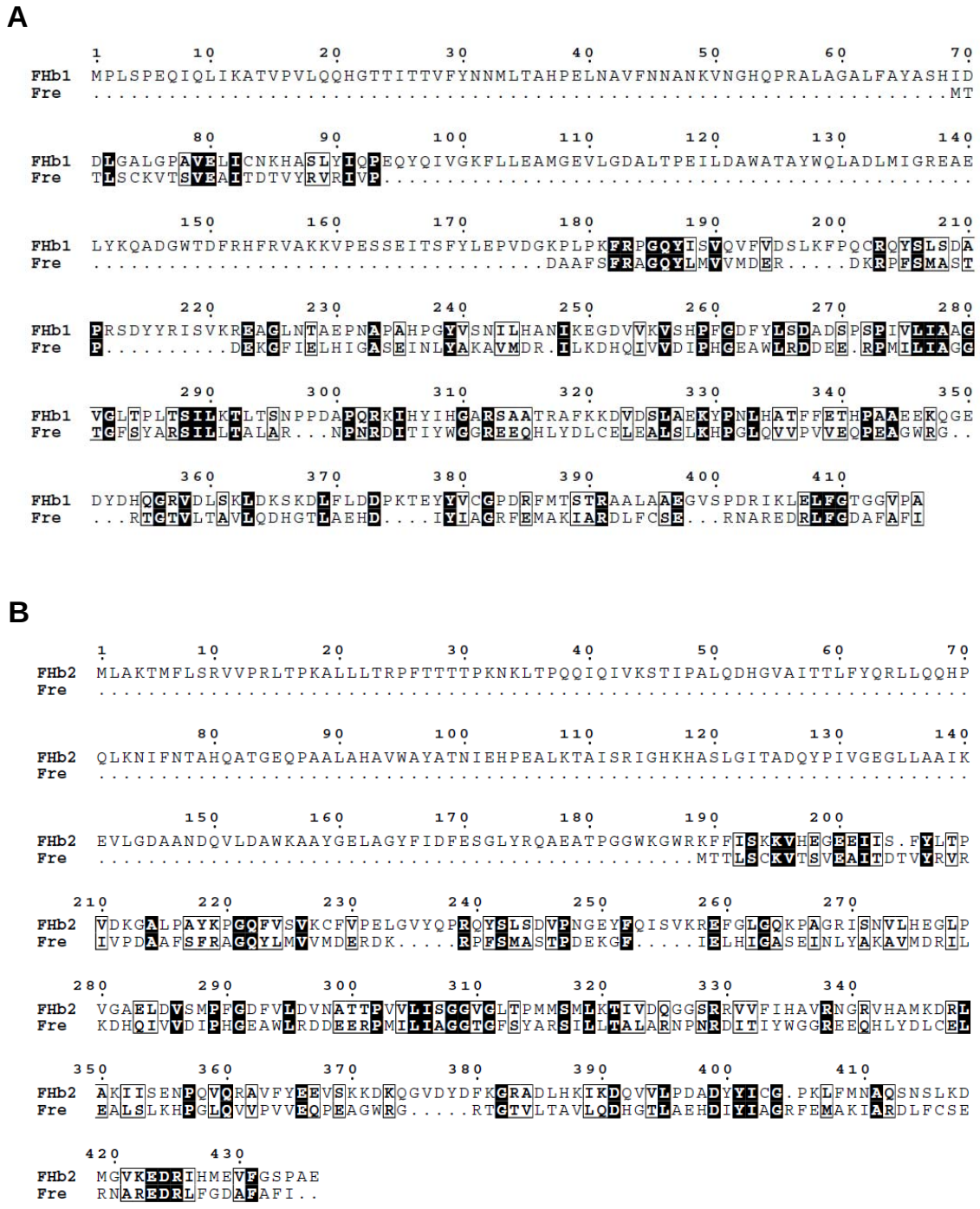

Figure 3-2 Comparison of amino acid sequences of FHb1 (A) and FHb2 (B) with *E. coli* flavin reductase (Fre).

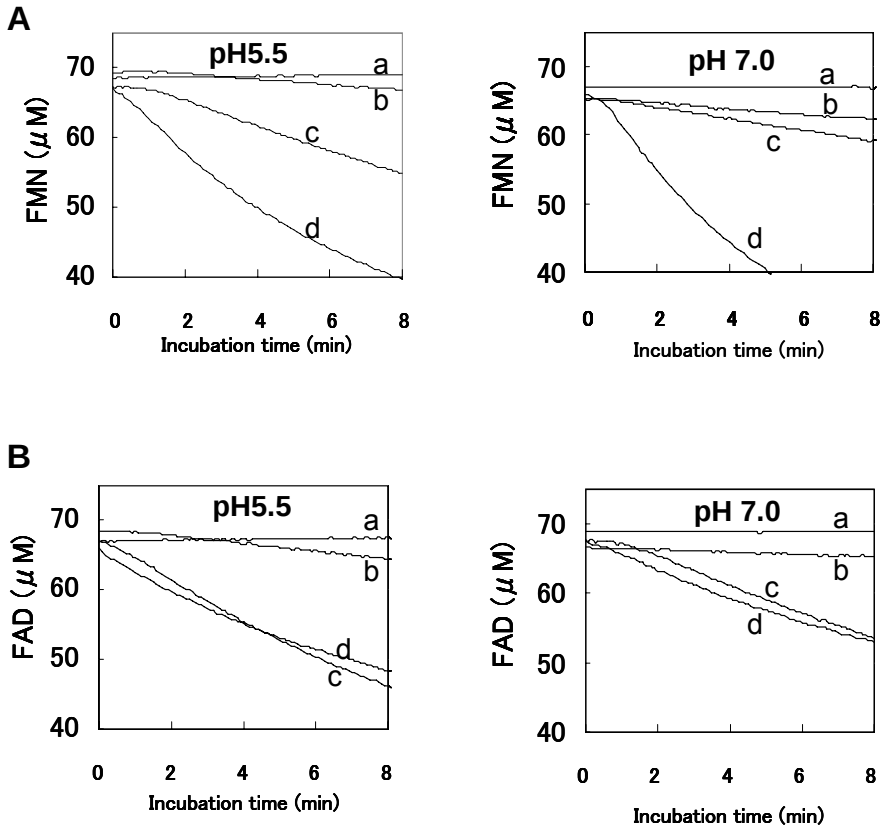

Figure 3-3 Reduction of flavin (A: FMN; B: FAD) by FHbs at pH5.5 and pH 7.0.

The reduction of Flavin was measured by monitoring the absorbance at 450nm using a spectrophotometer at 30℃ under anaerobic conditions.
The reaction solution contains 60 μM flavin(FAD or FMN), 400 μM NADH, 10mM glucose, 16 U of glucose oxidase, 260 U of catalase, 20ug FHb, in 20mM buffer (citrate buffer for pH 5.5; phosphate buffer for pH7.5, respectively).
a, control without NADH
b, control wihout FHbs
c, FHb1 (20 μg)
d, FHb2 (20 μg)

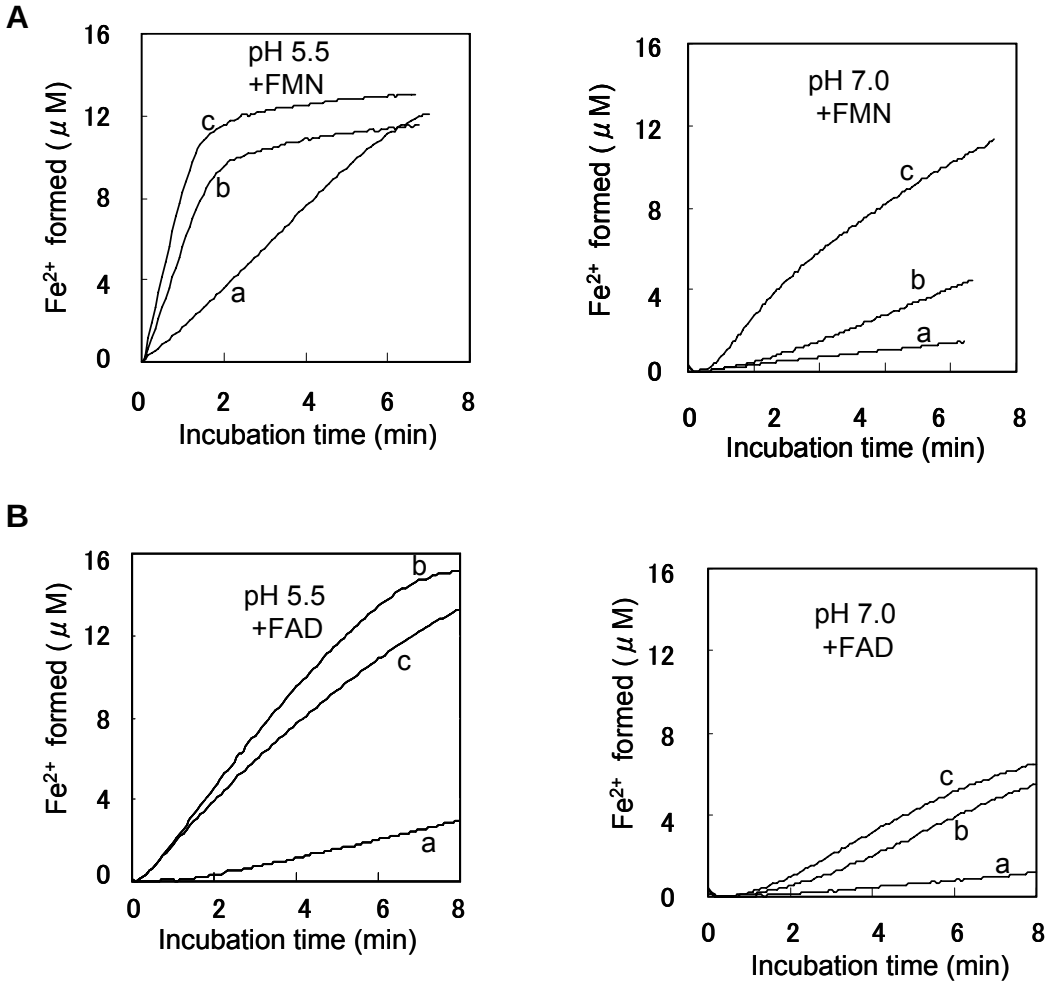

Figure 3-4 Production of ferrous iron by the reduced Flavin (A: $FADH_2$; B: $FMNH_2$) depending on FHbs at pH 5.5 and pH 7.0.

Reactions were performed at 30℃ under anaerobic conditions. They contained 20 μM ferric chloride, 400 μM NADH, 30 μM flavin (FAD or FMN), 10mM glucose, 16 U of glucose oxidase, 260 U of catalase, 20 ug FHb, 2 mM ferene, in 20mM buffer (citrate buffer for pH 5.5; phosphate buffer for pH7.5)

Ferrous iron was quatified at 562nm using an extinction coefficient of 26.6 $mM^{-1}cm^{-1}$.

a, control wihout FHbs

b, FHb1 (20 μg)

c, FHb2 (20 μg)

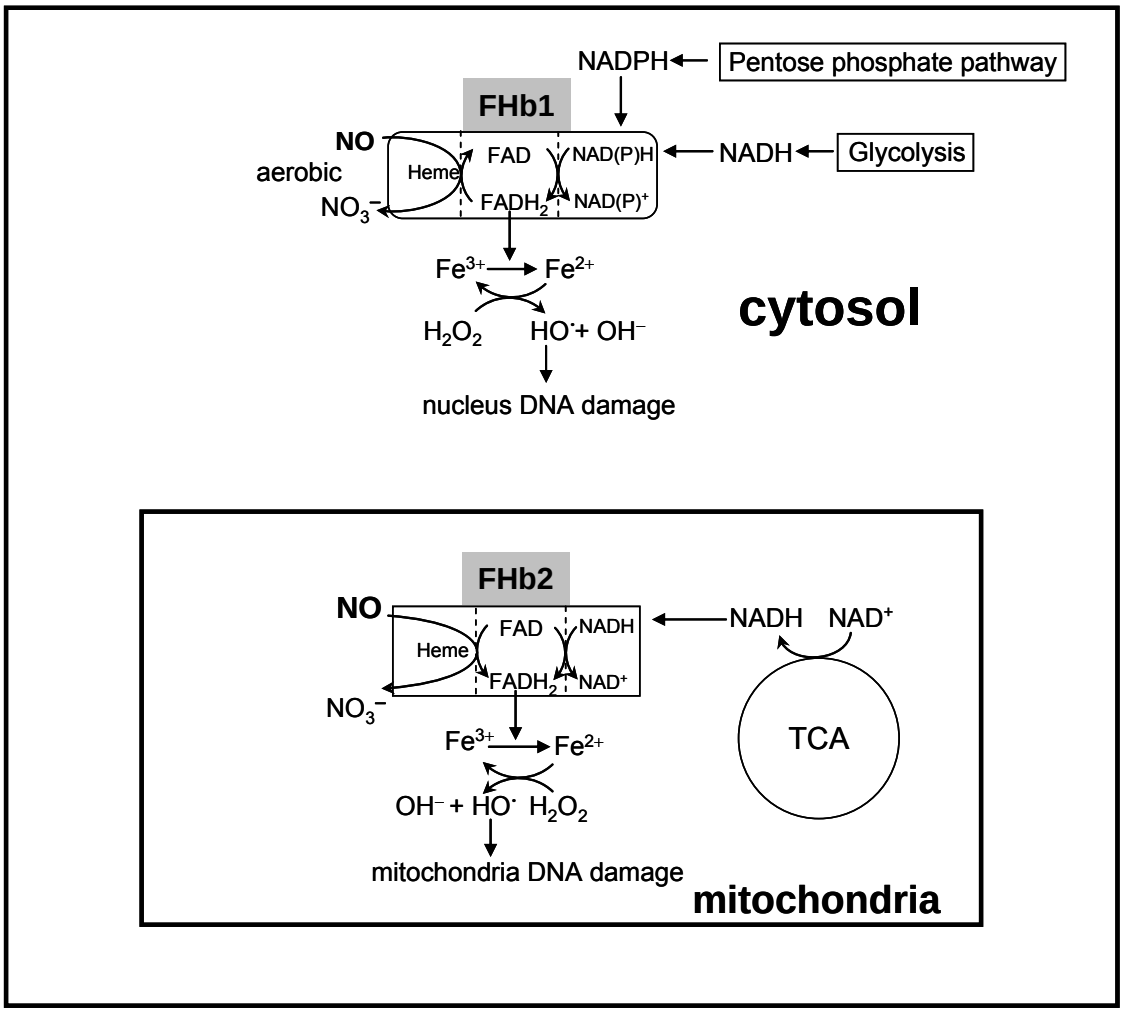

Figure 3-5 Mechanisms of the promotion of oxidative damage caused by FHb1 and FHb2.

FHb detoxifies NO to form NO_3^- via its NO dioxygenase; In the absence of NO, NAD(P)H can drive flavin reduction, leading to reduction of ferric iron and potentiation of Fenton – mediated oxidative damage in cytosol and mitochondria, respectively.

Chapter 4 Cloning of a periplasmic nitrate reductase (NapA)-like gene from *A. oryzae*.

Nitrate reduction, the most important stage of nitrogen turnover in nature, has several functions (Figure 4-1): 1) utilization of NO_3^- as a source of nitrogen (nitrate assimilation); 2) production of metabolic energy during NO_3^- utilization as terminal acceptor of electrons nitrate respiration (denitrification); and 3) dissipation of excess of reducing energy to maintain oxidation–reduction balance (nitrate dissimilation) (54).

The first, most important stage in the chain of nitrate reduction to nitrites is catalyzed by nitrate reductase (NRase). There are four types of NRases-eukaryotic assimilatory NRase (Euk-NR) (10, 11) and three different bacterial enzymes, i.e. cytoplasmic assimilatory (Nas), membrane-bound respiratory (NarG), and periplasmic dissimilatory (NapA) NRases (54) (Figure.4-1). All studied NRases share a common property – the presence of molybdenum (Mo) and molybdenum cofactor (Mo-co) in the enzyme active center. Bacterial NRases contain molybdopterin guanine dinucleotide (MGD), whereas mononucleotide is present in the active center of eukaryotic NRases (MPT) (Figure.4-2 A). Molybdenum is additionally coordinated by –S, –O, or –Se bonds of cysteine, serine, or selenocysteine residues of the polypeptide chain, as well as by accessible oxo (–O) and hydroxo (–OH) groups or by water (Figure.4-2 B) in different molybdenum enzymes (7, 19, 48). No information about Nas Mo-cofactor is available because its structure has not be resolved, yet.

Bacterial periplasmic nitrate reductase (Nap) are heterodimers consisting of a catalytic 90-kD subunit (NapA), incorporating molybdenum cofactor and one [4Fe-4S] center, and of a 13-19-kD subunit (NapB) incorporating two-heme cytochrome c (5, 23, 59) involved in electron transport onto molybdopterin (23). In many bacteria, they are involved in denitrification or dissimilatory nitrate reduction (Figure 4-1, NapA shown in red), however they are reported not to contribute directly to protons motive force (PMF)

(53).

To date, no eukaryotic dissimilatory nitrate reductase has been isolated, yet. However, by blast search on the fungal genomes, NapA-homology genes can be found in some strains. We are interested in the properties and the physiological functions of the eukaryotic NapA. In this chapter, I tried to clone and characterize a NapA-like gene from *A. oryzae*.

4-1. Materials and methods

4-1-1. Strains and plasmids and culture conditions

Wild type *A. oryzae* RIB40 was used to isolate the *napA*-like gene. *Escherichia coli* DH5α was used for DNA multiplication. *Escherichia coli* BL21 (DE3) Condon plus and *A. oryzae* niaD300 (niaD^{-}, nitrate-assimilation-defective mutant) was used as the host for expression of the recombinant NapA. pET28b (+) was used for the over-expression of N-terminal 6-His-tagged proteins and p*NGA* 142 (high-level expression vector containing an improved glucoamylase promoter) was used for expression of Nap in *A. oryzae*. *niaD* gene in pNGA was used as a selectable marker gene which compensates the nitrate-assimilation-defective mutant, *A. oryzae* niaD^{-}. *A. oryzae* was grown in DPY medium or CD agar plate. The media used in these experiments were shown in Table 1-1 in chapter 1.

4-1-2. Balst search and cloning of the the cDNAs encoding NapA-like protein.

E. coli NapA was used as a query sequence to blast search the genome database of *A. oryzae* (DOGAN). Total RNA was isolated from *A. oryzae* RIB40 grown in YPD

medium (added 10mM $NaNO_3$) at 30℃ for 24 hours, using TRIZOL Reagent (Invitrogen) following its manual. Full-length cDNAs were obtained by the method described in 1-1-2. The corresponding primers were listed in Table 4-1.

4-1-3. Subcloning, expression, and purification of the recombinant NapA protein.

I have tried expressing Nap with *E. coli* and *A. oryzae*. For *E. coli*, *napA* cDNA was subcloned using the sense primer, *napA*-ORF-F (*EcoR* I site shown in capital), and the antisense primer, *napA*-ORF-R (*Not I* site shown in capital) (Table 4-1). The construction of high expression plasmid and the methods of expression of NapA carried out as described in 1-1-3. For expression in *A. oryzae*, *napA* cDNA was subcloned with the primers of pair, nap-ORF-S (*Not* I site shown in capital) and nap-ORF-AS (*Not* I site were shown in capital and 6Ø His-tag shown in black and capital) (Table 4-1). After excised by *Not* I, the PCR product was inserted into the vector of p*NGA 142* (Figure 4-6.). Transformation of *A. oryzae* was carried out by the method described in 2-1-6. The transformants were obtained by the selectable marker gene *niaD* with CD plate medium. To induce the expression of *napA*, the transformant was incubated in DPY medium with 10 ¶M Na_2MoO_4 at 30℃ on a shaker at 150 rpm for 30 hours. The mycelium was disrupted by liquid nitrogen and suspended in 50mM phosphate-buffered (pH 7.5) added with 0.3mM PMSF and 0.5mM DTT. NapA was checked by SDS-PAGE and partially purified with HiTrap Chelating HP column (Amersham Parmacia Biotech).

4-1-4 Nitrate reductase activity

Nitrate reductase activity was assayed employing dithionite-methyl viologen (MV) system as the electron donor and by determining the amount of nitrite produced. The

reaction mixture (final, 3.0 ml) contained 50 mM phosphate buffer(pH 5.5), 10 mM $NaNO_3$, 0.1 mM MV, and appropriate amount of proteins in 15 ml volume test tube, which was sealed with a double butyl rubber stopper. The test tube was replaced with helium gas, and then the reaction was initiated by adding with a syringe 0.3 ml of 0.1 M dithionite-0.1 M $NaHCO_3$ mixture solution. The reaction was stopped by vigorously shaking the reaction mixture under atmospheric air until blue color of the mixture due to reduced MV disappeared. The produced nitrite was detected using the Griess reagents [0.02% N-(1-naphthyl) ethylenediamine and 1% sulfanilic acid in 25% HCl] at 548nm. Nitrite concentration was calculated using the slope of a linear sodium nitrite standard curve.

4-2. Results and discussions

By BLAST search on *A. oryzae* genome database (DOGAN) using *E. coli* NapA as a query sequence, a *napA*-like genes (AO090003001489) were identified, which located in chromosome 2. The full length cDNA of *nap* was cloned and sequenced. *napA*-like gene from *A. oryzae* has three introns (150-221; 333-398; 2378-2445) existing in its ORF. Figure 4-3 showed the deduced amino acids sequences. The deduced NapA consists of 990-amino acids but no putative targeting signal peptide was found at its N-terminus, whereas the N-terminal sequence of bacterial NapA is often attached with a consensus twin-arginine transfer sequence which directs the export of proteins into the periplasm by a Sec-independent pathway (65, 67, 79). The deduced *A. oryzae* NapA sequence was compared with two bacterial NapA (Figure 4-4). *A. oryzae* NapA showed 28% and 26% homology to *E. coli* and *A. eutrophus* NapA, respectively.

NapB, the electron transporter of NapA in bacteria, was also Blast searched on *A.*

oryzae and other fungal genome databases, no NapB homologous protein was found. It suggested that, though most of the bacterial Nap complex are consisted by NapA and NapB, fungal Nap is absence of NapB. NapA from *Desulfovibrio desulfuricans* is the sole bacterial monomeric NapA which has been reported to date.

To express the recombinant NapA, firstly I tried the *E. coli* expression system as described in materials and methods. Various concentrations of IPTG (0-0.5mM) were added to induce the expression at 25℃ and 30℃ (Figure 4-5). As shown in the SDS-PAGE, NapA was mostly expressed into the insoluble inclusions when induced by IPTG under either 25℃ or 30℃. In the soluble fraction, compared with the control possessed a blank vector, a weak bound matching NapA in its size (110 kDa) was also detectable under 25℃. The optimum concentration of IPTG for the induction is 20ΟM. We then investigated the nitrate reducatse of NapA under aerobic and anaerobic conditions. However, no obvious activity was detectable in both the soluble and insoluble fraction. So NapA was expressed inactivate form. The impossible reason is that *E. coli* can not synthesize the eukaryotic Mo-cofactor (MPT) which is difference from the prokaryotic Mo-cofactor (MGD) (Figure 4-2.).

We tried to express NapA in *A. oryzae* itself with the over-expression vector, pPNGA142, as described in materials and methods. To be purified easily, 6Ø His-tag was linked at the C-terminus of NapA by the primer, *napA*-ORF-AS (Table 4-1). The plasmid construction was shown in Figure 4-6. Transformants were selected by CD agar medium. As shown in Figure 4-7, six transformants were selected to check the expression of NapA. 4# transformant gave a NapA matched band in SDS-PAGE (Figure 4-7 A) and exhibited an obvious anaerobic nitrate reductase (Figure 4-7 B). So we selected 4# strains to express NapA in large scale (200 ml) and to purify it with nickel

affinity column. As shown in Figure 4-8, the expression level was very low, but the partial purified NapA (110 kDa) can be confirmed by SDS-PAGE. However, before the following purification with gel filtration chromatograph, the partially purified NapA became precipitate in solution and the nitrate reductase was lost completely. So to characterize NapA, optimization of the expression and purification conditions should be done in future.

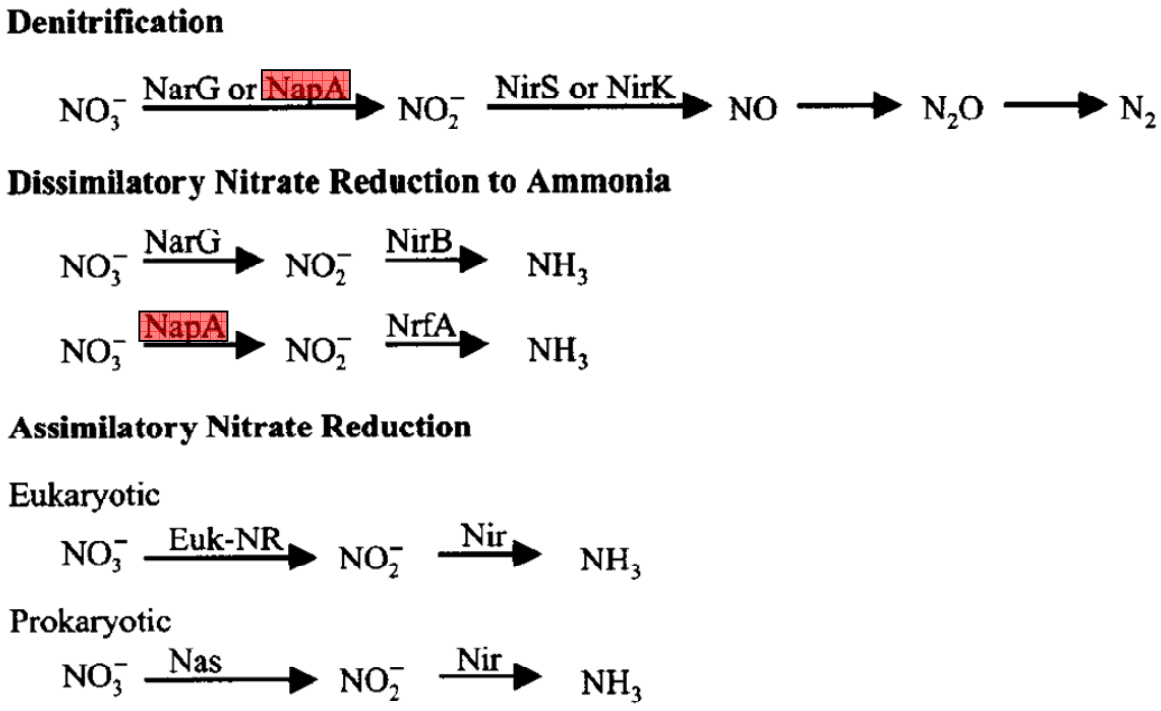

Figure.4-1. Pathways involving nitrate reduction.

NarG=membrane-bound nitrate reductase, NapA=periplasmic nitrate reductase, NirS=cytochrome cd1 nitrite reductase, NirK=copper-containing nitrite reductase, NirB=siroheme nitrite reductase, NrfA=pentaheme cytochrome c nitrite reductase. Euk NR=eukaryotic nitrate reductase (Nia, NiaD, INR, Nit), Nas=cytoplasmic nitrate reductase (NasA, NasB, NasBB, NasC, NarB), Nir=siroheme nitrate reductase (Nir, NirB, NasA, NasC, NasD). Note that both NapA and NarG can be involved in nitrate reduction leading to either dinitrogen or ammonia. In contrast, Euk-NR and Nas are involved in nitrate reduction to ammonia only.

From : Chembiochem 3, 198-206

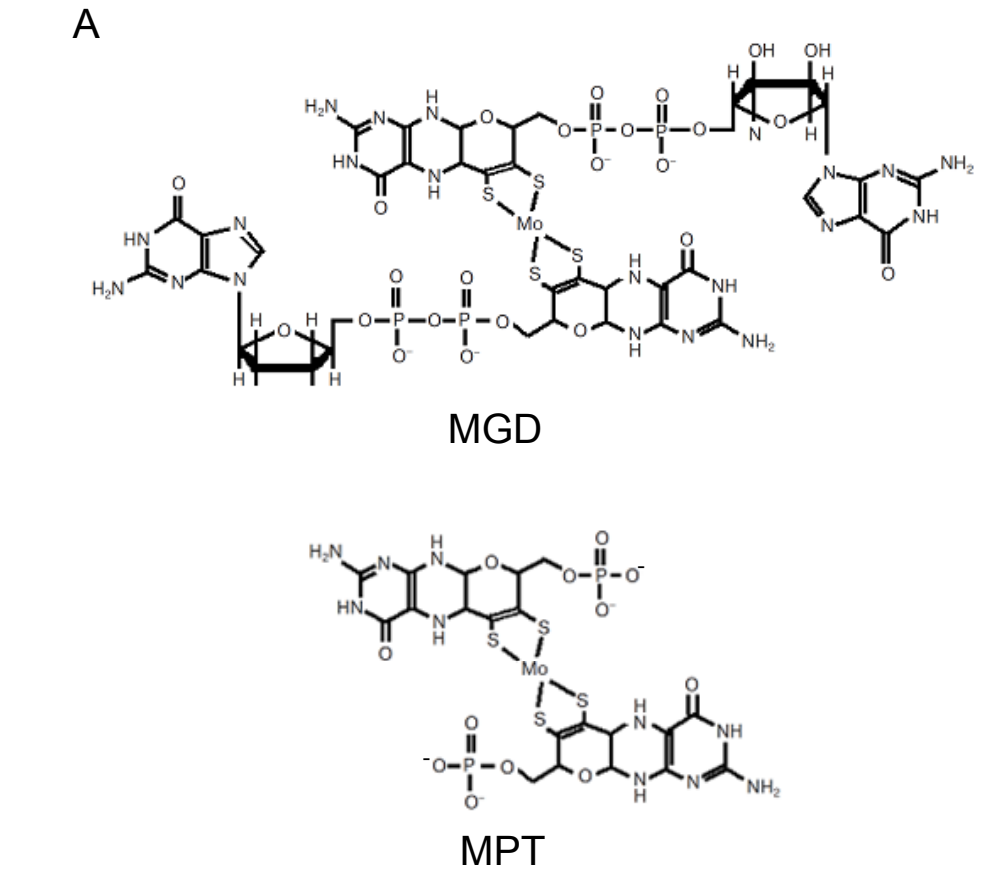

Figure.4-2. molybdenum cofactor of nitrate reductase.

A: Structure of prokaryotic molybdenum cofactor(MGD) and eukaryotic molybdenum cofactor (MPT)
B: Active site structure of NRase : I, eukaryotic (Euk-Nar); II, periplasmic (NapA);
III, membrance-bound (NarG); No information of Nas Mo-cofactor is available.

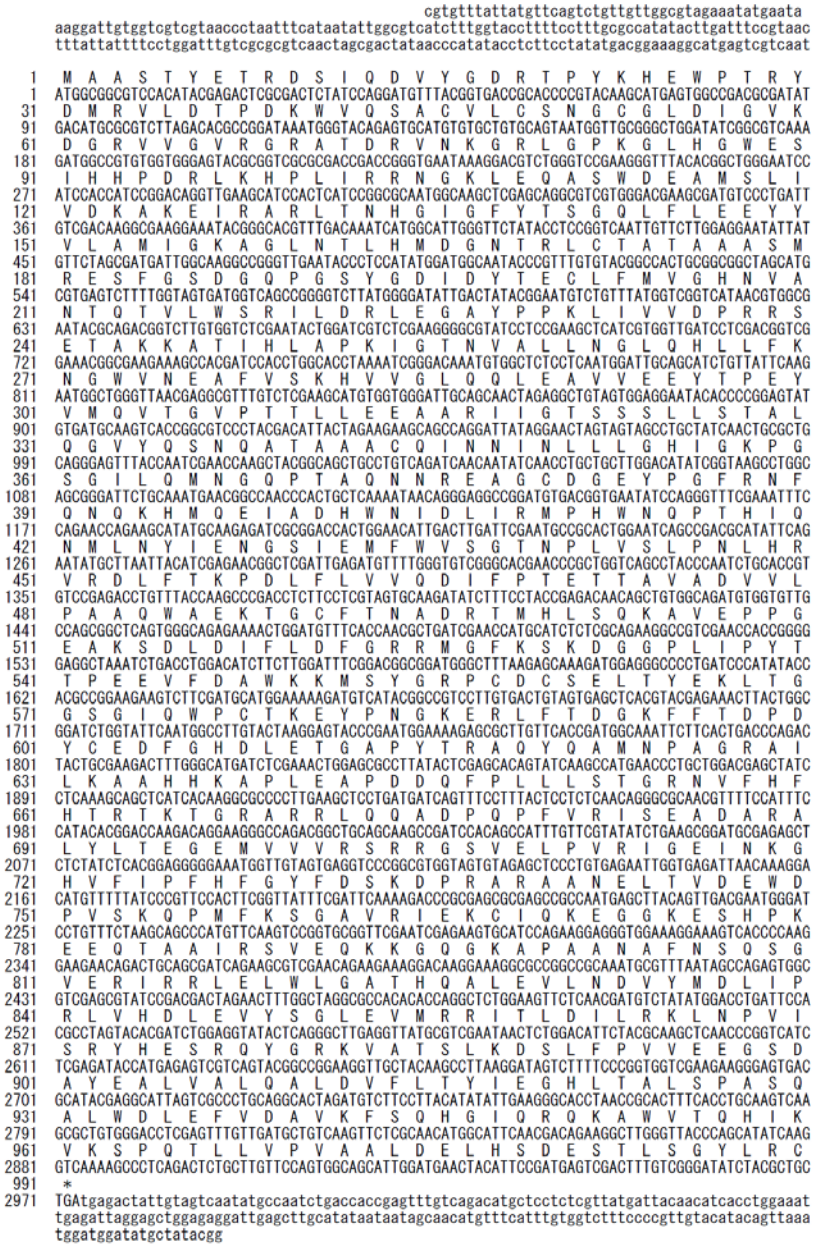

Figure 4-3. Nucleotide sequence and deduced amino acid sequence of cDNAs of *A.oryzae napA*.

The numbers on the left refer to the positions of nucleotides (bottom lines).
The number on the right refer to the position of amino acid residues (top lines)
The stop codons is indicated by asterisk.

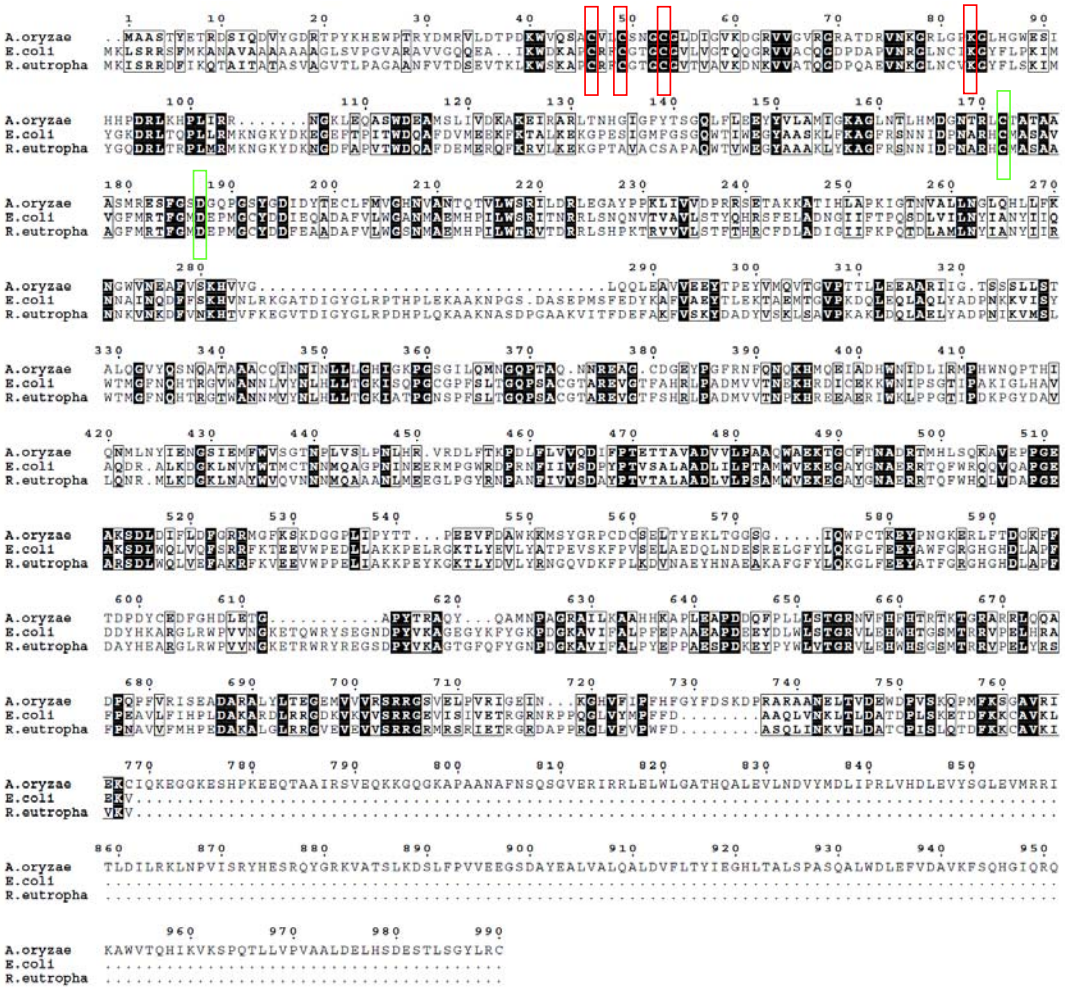

Figure 4-4. Sequences alignment of *A.oryzae* NapA with two bacterial NapA from *Escherichia coli* and *Alcaligenes eutrophus*

The cysteine-rich motif and the lysine83 highlighted in red box is predicted to bind the the 4Fe-4S cluster. The amino acids shown in green are predicted to be involved in the Mo-cofactor active site.

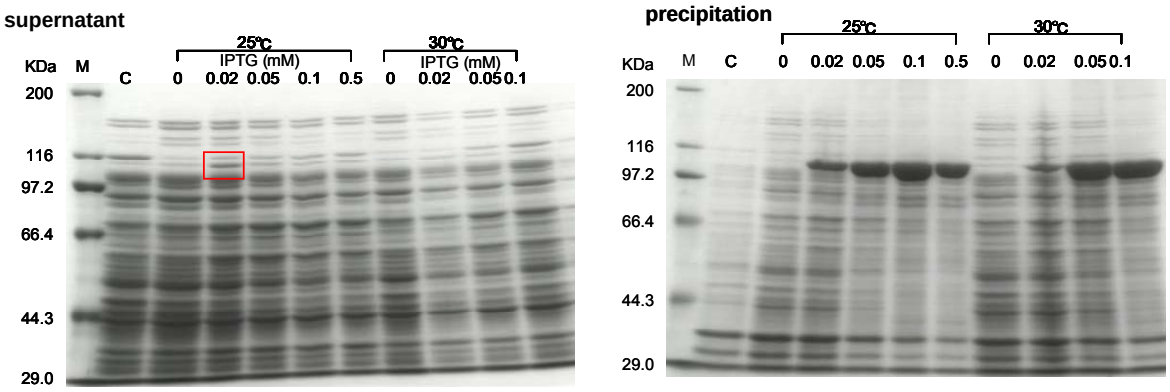

Figure 4-5 Optimization examination of NapA expressed by *E. coli*.

Gel concentration : 7.5%;
Induction period: 12 hours;
Left: supernatant of crude fraction; Right: precipitation of crude fraction
M: marker; C: control (blank vector)

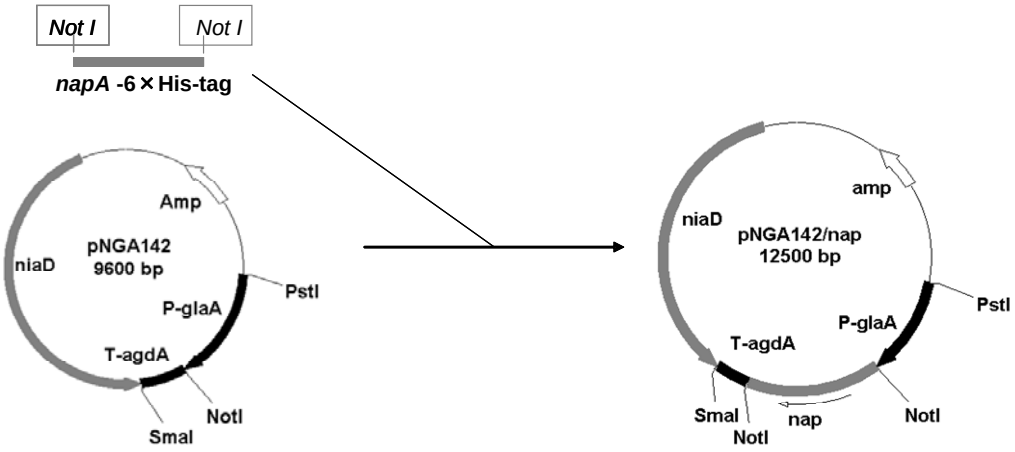

Figure 4-6. Plasmid construction for over expression of *napA* gene in *A. oryzae* niaD300.

The PCR product of *napA* from cDNA was excised by *Not* I. The *Not* I excised pNGA 142 was dealed with Bacterial Alkaline Phosphatase (BAP) before ligation with *napA*.
P-glaA: improved glucoamylase promoter (activated by dextrn)
T-agdA: α-glucosidase ternimator
niaD gene: selectable marker gene.

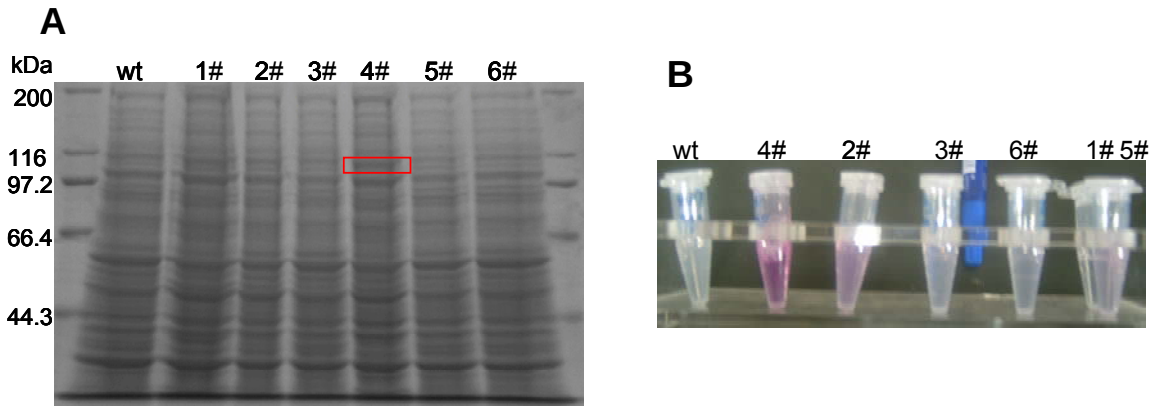

Figure 4-7 Check the NapA over-expressed in *A. oryzae* niaD300 by SDS-PAGE (A), and nitrate reductase activity (B).

A: Gel concentration : 7.5 %.
1-6 lane : Cell free from 6 transformants with the over-expression vector (p*PNGA+napA*).
wt: cell free from the tranformants with the blank vector (p*NGA*).
The band shown in red box should be NapA (110 kDa).

B: Nitrate reductase activity was assayed employing dithionite-methyl viologen (MV) as the electron donor and by determining the amount of nitrite produced under anaerobic condition. The produced nitrite will reacted with Griess reagents to form azo dye (red) which can be spectrophotomatrically quantitated based on its absorbance at 548nm.
The number on the tube is corresponding to the number shown in A.

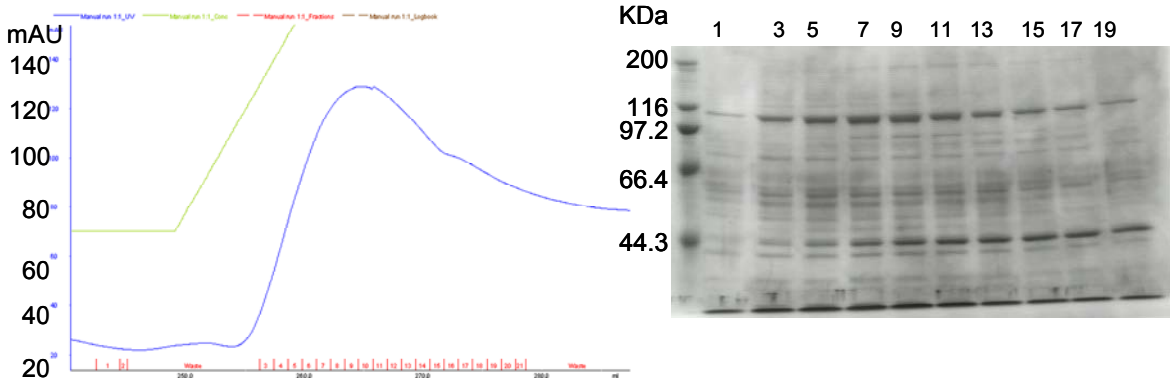

Figure 4-8. Purification of 6-His-tag NapA with nickel column and check of the purified fraction by SDS-PAGE.

Name	Segunce (5' → 3')
napA reverse GSP primer	cctccactacagcctctagttgctgc
napA reverse GSP nested primer	gagggtattcaacccggccttgccaatc
napA forward GSP primer	atggcggcgtccacatacgagactcgc
napA forward GSP nested primer	tgggtacagagtgcatgtgtgctgtgc
napA-ORF-F	GAATTCatggcggcgtccacatacgagac
napA- ORF-R	GCGGCCGCtcagcagcgtagatatcccg
napA-ORF-S	GCGGCCGCatggcggcgtccacatacgag
napA- ORF-AS	GCGGCCGC**TCAGTGGTGGTGGTGGTGGTG**gcagcgtagatatcccgac

Table.4-1. Nucleotide sequences of primers used in this work.

Restriction endonuclease cleavage sites are shown in capital.

Chapter 5 Study on the enzymes involved in denitrification of *A. oryzae*

Denitrification had been considered to be an exclusive process of bacteria until the fungal denitrification was discovered by Shoun *et al.* firstly at 1991. Unlike bacteria, fungi do not seem to have N_2O-reducing activity, and thus the final product of the fungal denitrification is N_2O. To date, though the denitrification of fungus has been extremely studied, no gene involved in this pathway was identified except p450nor. To well understand the denitrification of fungi, the molecular genetic analysis are required.

A. oryzae is a denitrifier, which can reduce NO_2^- to N_2O under O_2-limited conditions. My predecessor, Nakanishi, had cloned and characterized the nitrite reductase (*nirk*) gene involved denitrification from *A. oryzae* at the first time. In this study, I will revise and supplement some data for the previous study of NirK. Moreover, I will study the genes involved in denitrification of *A. oryzae*.

5-1 Materials and methods

5-1-1 Fungal strains and media.

Wild-type *Aspergillus oryzae* RIB40 was used to isolation the flavoHb genes.! The RIB40 Δ*ku70*Δ*pryG* was used as the parent strain to construct *nirK*-deletion strain (Δ*nirK*) and p450nor-disruption strain (Δ*CYP55A5*). The cultivation, media were described in chapter 1 and chapter2.

5-1-2 Denitrifying conditions

The fungal spores (10^4 / ml) were aerobically incubated at 30˚C for 24 h in 200ml DPY medium (pre-culture). Mycelia from 30 ml of pre-culture was collected by filtration with the MIRACULOUS (CALBIOCHEM) and washed twice with 0.7%

NaCl, and then inoculated into 500-ml Erlenmeyer flask with baffles containing 200 ml of DPY medium supplemented with 5 mM $NaNO_2$. When examine the denitrification of *nirK* over-expression strain, 0.3% of trace element (Table 5-3) was requirement. After inoculation, the medium was degassed and the head space of flask was replaced with helium gas and the flask was sealed with a rubber stopper (anaerobic conditions).

5-1-3 Gas analysis

An aliquot (usually 40μl) of the upper-space gas in the flasks was collected with a syringe through the side arm, and analyzed by GCMS.

5-1-4 Determination of the full length of *nirK* cDNA.

Total RNA was isolated from *A. oryzae* cells grown for 16 h under denitrifying conditions, using TRIZOL Reagent (Invitrogen) following its manual. Full-length cDNAs were obtained by 5'-3' RACE using the GeneRacer™ Kit (Invitrogen) following the supplier's protocol. To obtain 5' ends, cDNA was amplified using *nirK* reverse gene specific primer (reverse GSP primer), GeneRacer™5' primer and then using the nested primers, nirK reverse gene specific nested primer (reverse GSP nested primer) and GeneRacer 5' nested primer (Table 5-1). To obtain 3' ends, cDNA was amplified using *nirK* forward gene specific primers (Forward GSP primer), GeneRacer™ 3' primer and then the nested primers, forward gene specific nested primer (*nirK* forward GSP nested primer) and the GeneRacer 3' nested primer (Table 5-1). Amplified 5'- and 3'- RACE DNA was cloned using pT7Blue T-Vector (TaKaRa), respectively. The sequencing reaction were performed with CEQ Dye Terminator Cycle Sequencing with Quick Start Kit (BECKMAN COULTER), and sequenced with a

sequencer (CEQ2000XL; BECKMAN COULTER).

5-1-5 Expression of NirK in *E. coli* and purification of the recombinant protein

See the master theme of Nakanishi.

5-1-6 Disruption of *nirK* and p450nor gene, respectively.

The disruption cassettes for deletion of *nirK* and p450nor gene (*CYP55A5*) from the chromosomal DNA of *A. oryzae* were constructed by fusion PCR as described in chapter 2. The used primers were shown in Table 5-1.

5-1-9 Southern blot analysis

The primers used for probes synthesis were listed in Table 5-1. The methods were described in chapter 2.

5-1-10 Transformation of *A. oryzae*.

See chapter 2.

5-1-11 Quantitative Real-time PCR analysis

See chapter 2. The corresponding primers were shown in Table 5-1.

5-1-12 Enzyme activity

Nitrite reductase activity was assayed employing dithionite-methyl viologen (MV) system as the electron donor and by determining the amount of nitrite remaining after the reaction. The reaction mixture (final, 3.0 ml) contained 50 mM MES buffer (pH 5.5),

1.0 mM $NaNO_2$, 0.1 mM MV, and appropriate amount of dNir in 15 ml volume test tube, which was sealed with a double butyl rubber stopper. The test tube was replaced with helium gas, and then the reaction was initiated by adding with a syringe 0.3 ml of 0.1 M dithionite-0.1 M $NaHCO_3$ mixture solution. The reaction was stopped by vigorously shaking the reaction mixture under atmospheric air until blue color of the mixture due to reduced MV disappeared. Residual nitrite was detected using the Griess reagents [0.02% N-(1-naphthyl) ethylenediamine and 1% sulfanilic acid in 25% HCl] at 540nm.

5-2 Results and discussions

5-2-1 Optimization of denitrification condition of *A. oryzae*.

My predecessor, Nakanishi, had confirmed the potentiality of denitrification by *A. oryzae*. He had demonstrated *A. oryzae* is a denitrifier fungus that can reduce NO_2^- to N_2O. However, the denitrification is very weak compared with other denitrifying fungi such as *Fusarium oxysporum* et al. In this study, I have optimized the denitrifcation conditions, and found that the more nutrition rich medium, DPY plus 5mM NO_2^-, gave a denitification ability about 5 times higher than it tested by Nakanishi with Glycerol-peptone medium (Table 5-2) plus 10mM NO_2^-. (Figure 5-1). Then DPY medium was used for denitrification experiments throughout this work.

5-2-2 Determination of the Full-length *nirK* cDNA

The *nirK*-homologue gene was found in the database of *A. oryzae* RIB40 genome by Nakanishi using the Blast homology search. Then he directly cloned the *nirK* cDNA according to the database. However it may cause a mistake in determining the

translation start sites of the *nirK* ORF. So I confirmed the full-cDNA sequence of *nirK* by 5'-3' RACE using the GeneRacer^{TM} Kit. The full cDNA and the deduced amino acid sequences were shown in Figure 5-2. It is lucky that real ORF determined by the full length of cDNA is in agreement with it cloned by Nakanishi.

5-2-3 Characterization of the *nirK* over-expression strain of *A. oryzae*.

Nakanishi had expressed and characterized the recombinant NirK. The purified NirK exhibited robust anaerobic nitrite reductase and the properties similar to bacterial NirKs.

The most interesting job done by Nakanishi was the construction of a *nirK* over-expression strain of *A. oryzae*, which possessed a high potential denitrification ability of denitrification. He had demonstrated the over-expression strain showed about 600 times higher than wild type in denitrification ability. But in my experimental condition, they showed only 6 times difference between the over-expression and Wild type strain (Figure 5-3 A). The possible reason is the richer medium in this experiment promoted the Wild type significantly in denitrifying, which decreased the deference between the two strains. I have compared the amounts of mRNA and nitrite reducatse activities between the two type strains (Figure 5-3 B,C), which suggested that high denitrification ability can be attributed to the high expression of *nirK* gene. The NirK was over-expressed as a membrane bound protein under aerobic conditions. In this work, I gained the similar result under denitrifying condition (Figure 5-3 D). These results strongly suggested that *A. oryzae* NirK is a membrane-anchored enzyme.

5-2-4 Transcriptional response of *nirK* to denitrification conditions.

Next, I investigated if the *nirK* gene is really involved in fungal denitrification. As shown in Figure 5-4, *nirK* gene does not expressed under aerobic condition regardless of the presence of NO_2^- or not. *nirK* was slightly expressed under anaerobic condition. The externally added 5mM NO_2^- under anaerobic condition (denitrificiaction condition) induced the expression level about 25 times higher than it under the condition absence the NO_2^-. These results suggested that *nirK* is involved in denitrification.

5-2-5 Effects of deletions of *nirK* and p450 nor gene on denitrification

I disrupted *nirK* gene (Figure 5-5) to investigate the effect of *nirK* gene deficiency on *A. oryzae* denitrification. To our surprising, no difference in denitrification was found between the Wild type and the *nirK* deficient strain (Figure 5-7 A). Our denitrification experiment is done at pH5.5. It had been reported NO_2^- is chemically converted into NO at acidic pH. The chemically produced NO may abate the role of NirK. So I also compared the denitrification levels of the two strains under a relatively high pH (pH7.3). The denitrifications were suppressed in both of the strains because of the non-optimal pH for fungi, but the denitrification could still be detectable and no obvious distinct between the two strains was found (data not shown). So the denitrification of *A. oryzae* is not pH dependent, though pH will affect its activity. It has been reported that plant nitrate reductase (52, 63, 85, 86) and yeast mitochondrial cytochrome oxidase are also involved in NO production (13). These two enzymes are also existing in *A. oryzae*. So it is possible that there also exist some NO producing enzyme substitutes NirK to reduce NO_2^- to NO in the *nirK* deficient mutant.

I also constructed a p450nor deficient mutant (Δ*CYP55A5*) (Figure 5-6) to investigate if there are also some substitution genes encoding for NO reductase. As

shown in Figure 5-7 B, p450nor is vital to denitrification.

These results indicated that though *nirK* gene is response to denitrification, it is not vital to denitrification. On the other hand, p450nor is the sole NO reductase in *A. oryzae* under denitrifiaction condition.

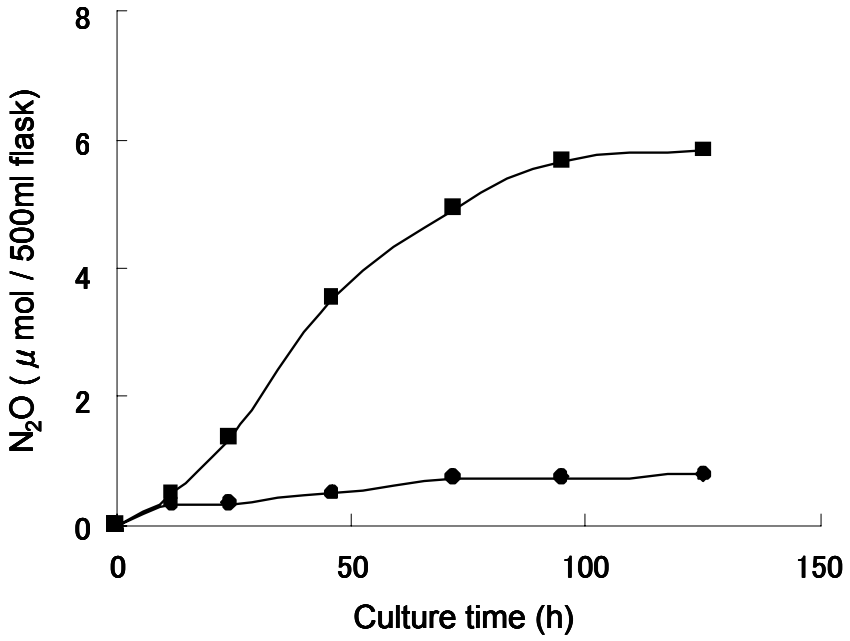

Figure 5-1 Denitrification by *A. oryzae*.
N_2O generation during incubation of *A. oryzae* in YPD medium with 5mM nitrite under anaerobic conditions.
■,*Aspergillus oryzae* RIB40
●,control (without strains)

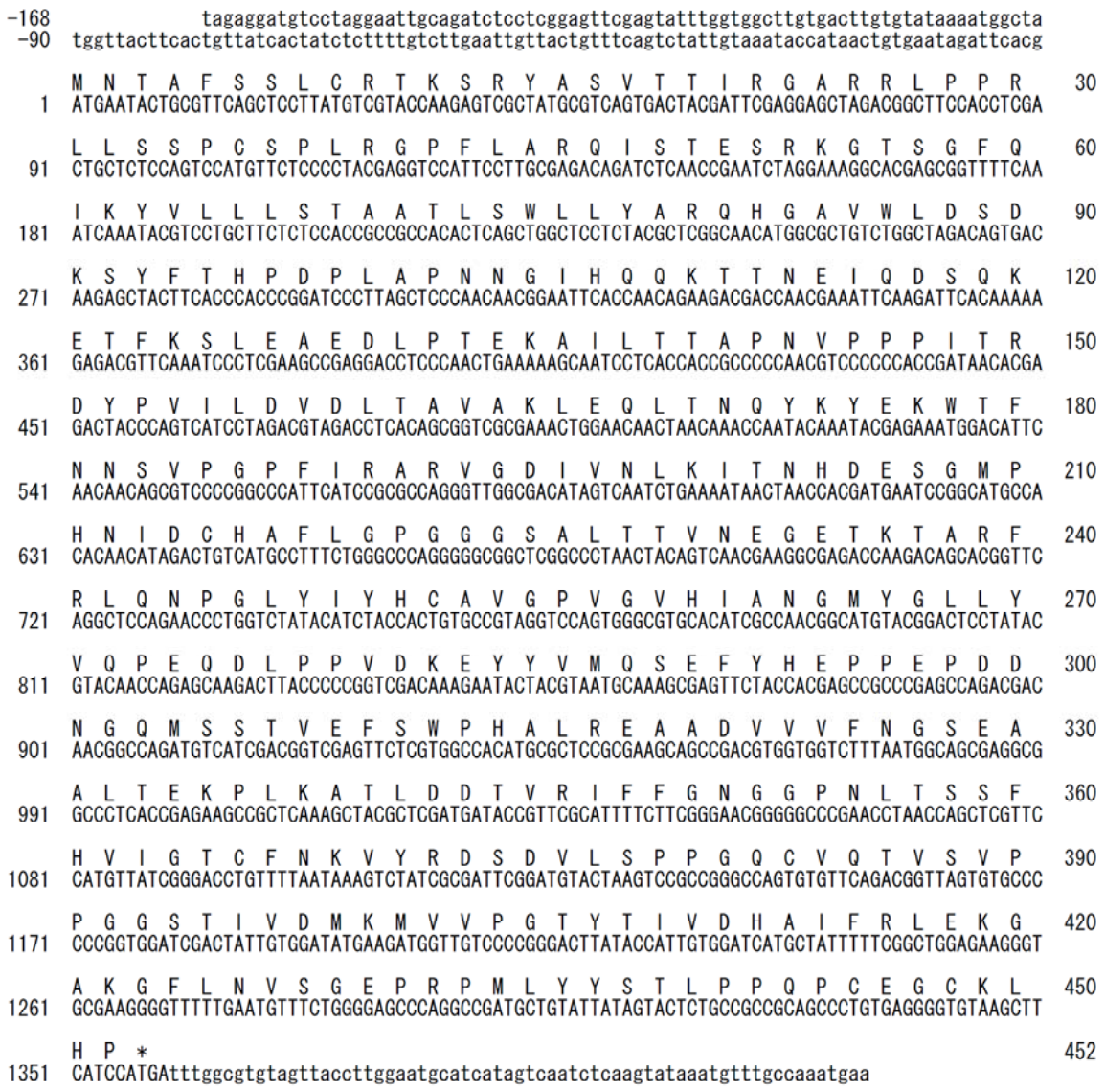

Figure 5-2 Nucleotide sequence of the full length *nirK* cDNA and the deduced amino acid sequences.

The deduced amino acid sequence is indicated above the nucleotide sequence.
The translation start site ATG was defined as position 1.
The stop codon is marked as ∗.

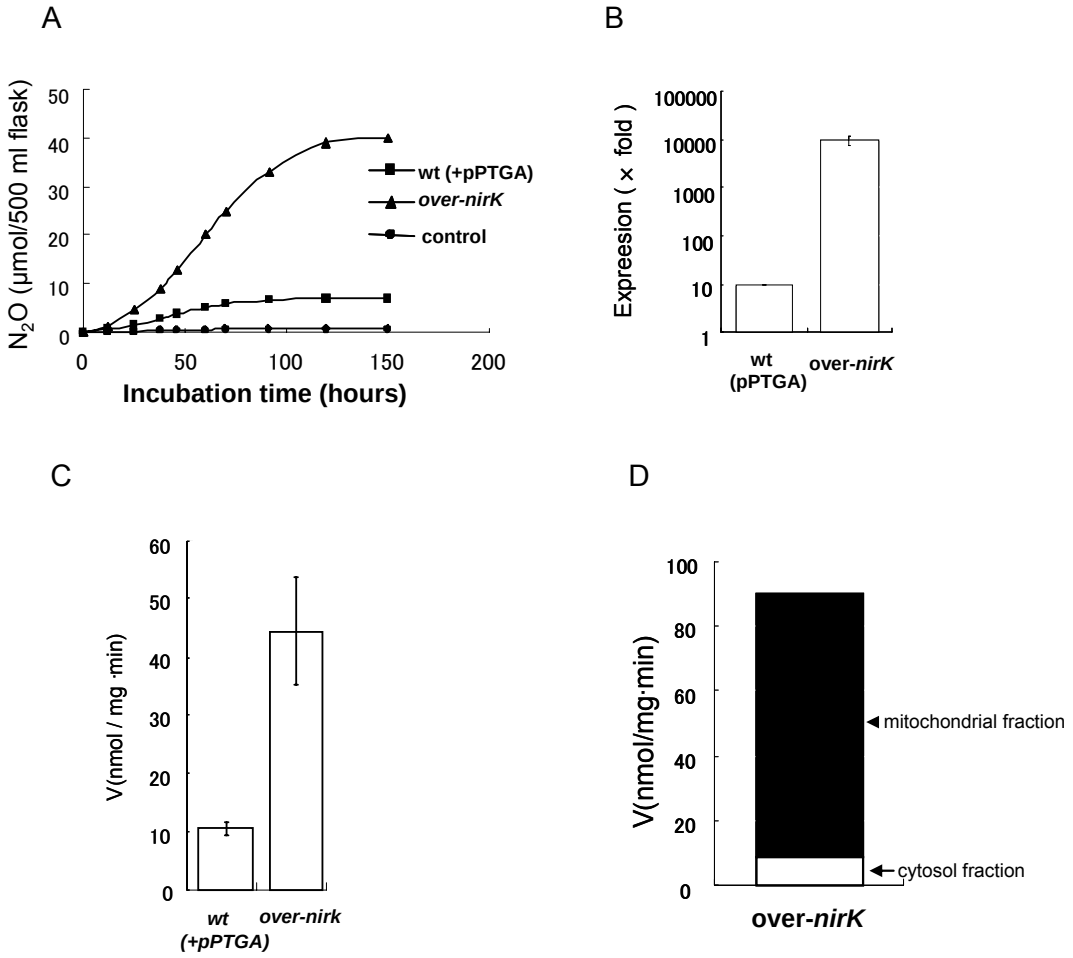

Figure 5-3. Characterization of the *nirK* over-expression strain of *A. oryzae*.

A, Comparison of the denitrification of wild type (pPTGA possessing) and *nirK* over-expression(over-*nirK*) strain. The medium without strains was shown as control.

B, Comparison of mRNA level of *nirk* in wild type (pPTGA+) and *nirK* over-expression (over-*nirK*) strain under denitrification conditions.

C, Nitrite reductase activity of the cell homogenate proteins from wild type (pPTGA+) and *nirK* over-expression (over-*nirK*) strain incubated under denitrifications.

D, Distribution of anaerobic nitrite reductase among sub-cellular fraction of *nirK* over-expression strain. The activity of soluble fraction is shown in blank, and the activity of mitochondria fraction was shown in black. Denitrifying cells were disrupted by grinding in a mortar with liquid N2 and Tris-HCl buffer (50mM, pH8.0) containing Protease Inhibitor Mixture. After the centrifugation of the homogenate at 1,500 × g for 15 min, the cell wall and undisrupted were removed. The supernatant was future centrifuged at 10,000 × g for 60 min. Then the resulting supernatant and precipitate were respectively used as the soluble fraction and mitochondria fraction.

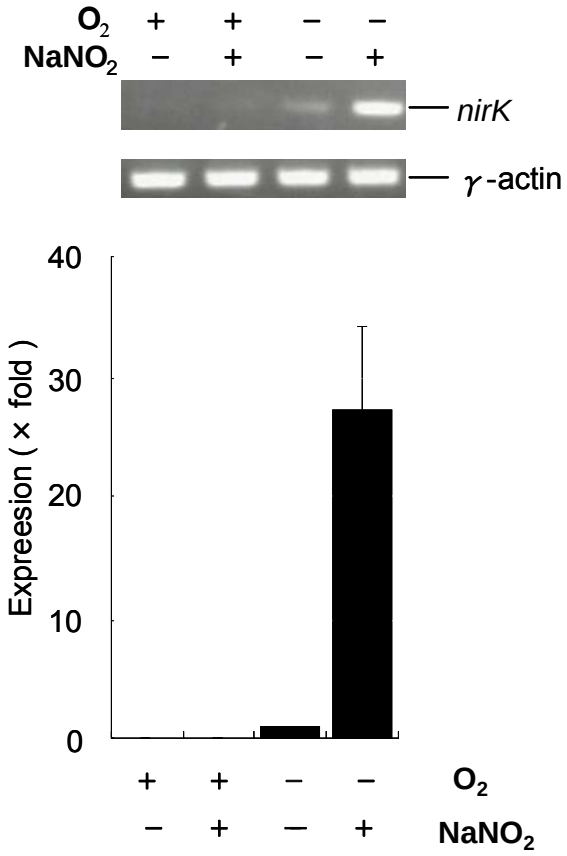

Figure 5-4 Transcription of *nirK* gene is response to denitrification

All the cultures were grown in DPY medium for 12 hours.
Transcriptional levels of *nir*K response to O_2 and NO_2^- were measured by RT-PCR and Quantitative-RT-PCR.
Measured values were normalized to transcriptional level of housekeeping γ*-actin* mRNA.
Data are representative of three independent experiments.

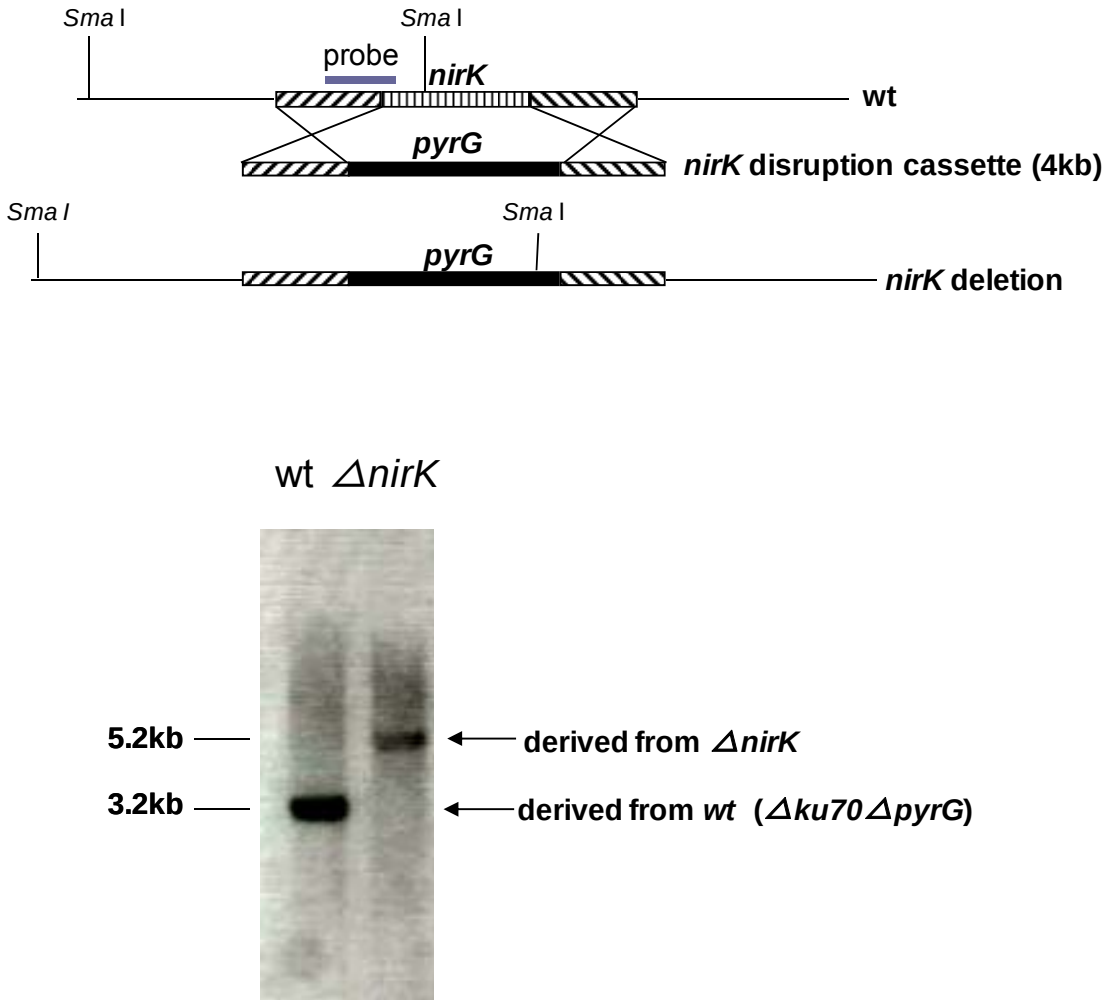

Figure 5-5 Construction of *nirK* deletion mutant (⊿*nirK*)

A. Strategy of *nirK* gene deletion
B. Deletion verification by Southern blotting analysis.

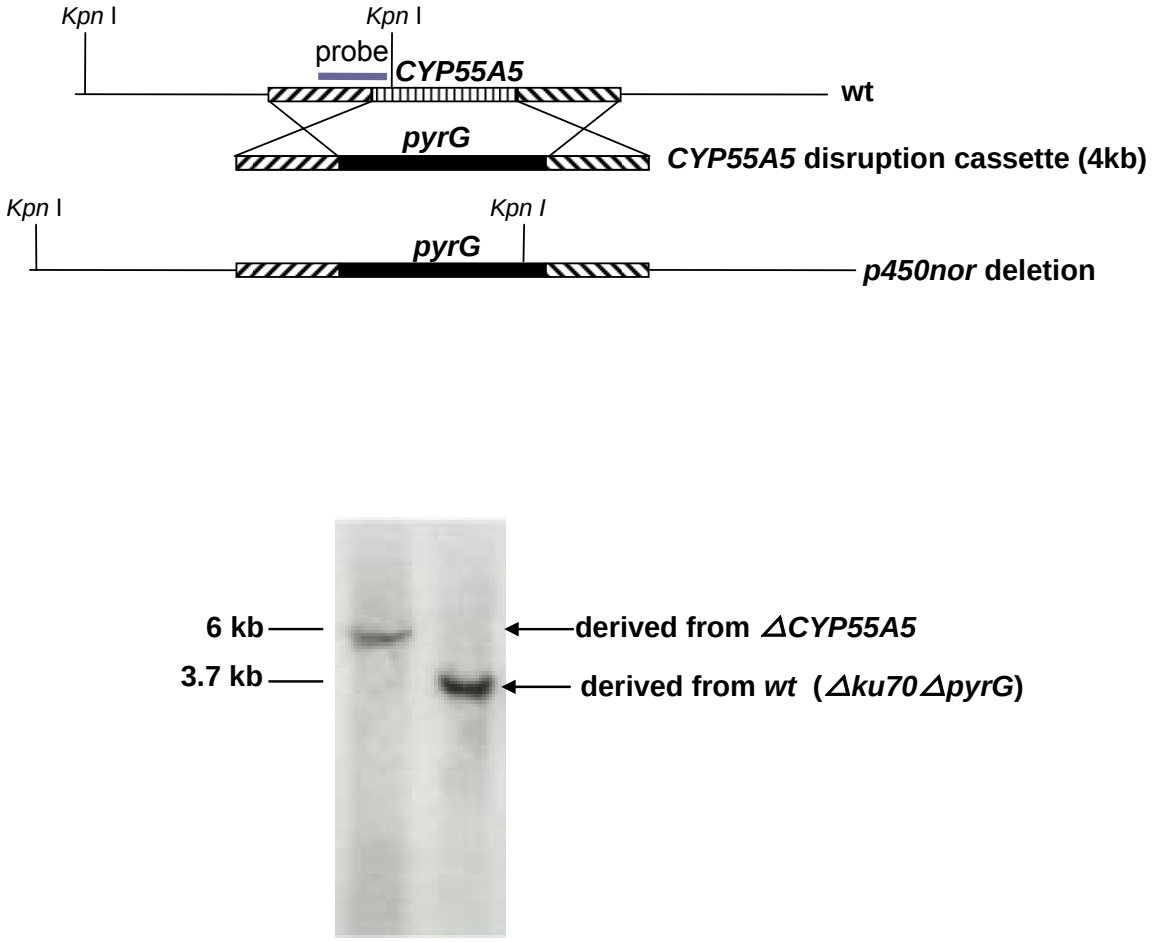

Figure 5-6 Construction of p450nor disruption mutant (*ΔCYP55A5*).

A. Strategy of *p450nor* gene deletion
B. Deletion verification by southern blotting analysis.

Cytochrome P450nor gene : *CYP55A5*

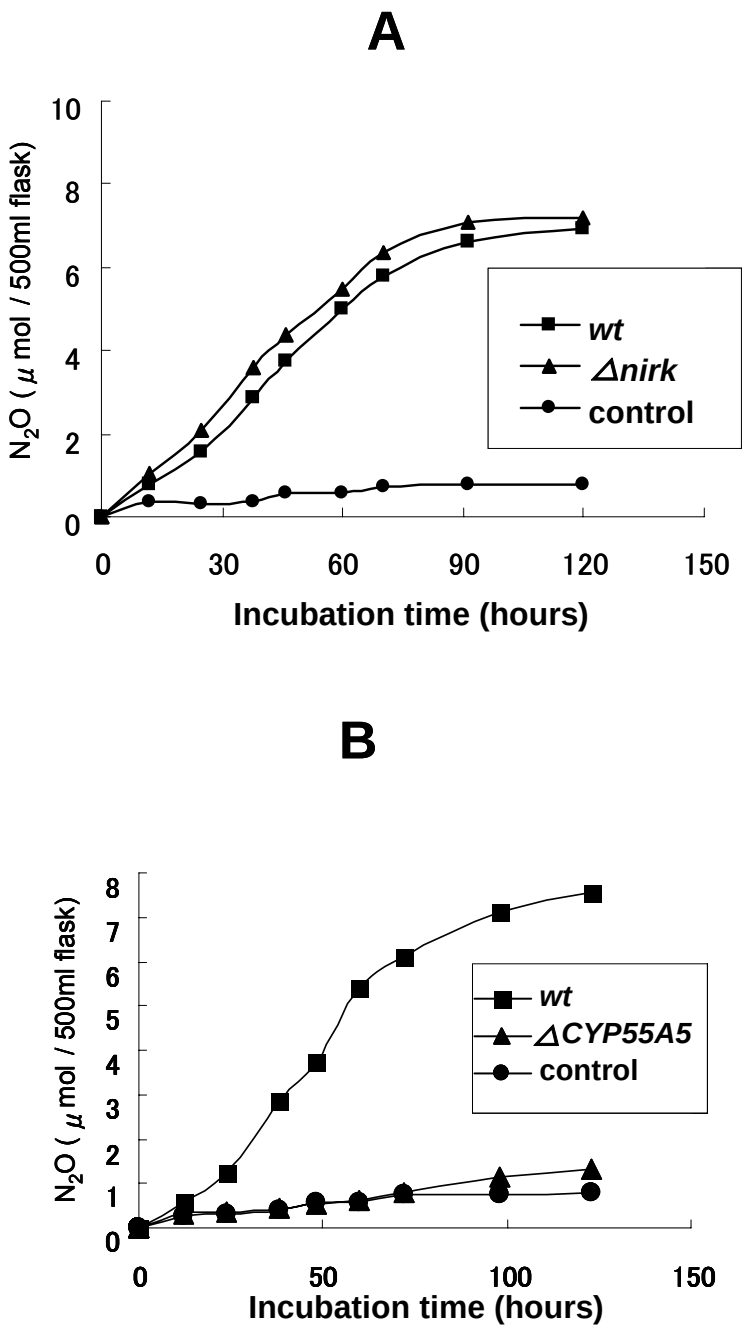

Figure 5-7 Effects of deletion of *nirK* (A) and p450nor gene (*CYP55A5*) (B) on denitrification.

Control: without strains.

	Name	Sequnce
	nirK reverse GSP primer	5'-tcatggatgaagcttacac-3'
	nirK reverse GSP nested primer	5'-cggcggcagagtactataatac-3'
	nirK forward GSP primer	5'-atgaatactgcgttcagctcc-3'
	nirK forward GSP nested primer	5'-gtcgctatgcgtcagtgactacg-3'
	qRT-*nirK*-F	5'-gtcgctatgcgtcagtgactacg-3'
	qRT-*nirK*-R	5'-gtctagccagacagcgccatgttg-3'
	qRT-γ-*actin*-F	5'-ctcgaagacaatctgggtc-3'
	qRT-γ-*actin*-R	5'-gtaatcggtcaaatcacggcc-3'
	ΔnirK-1	5'-cagggccattccattgggacc-3'
	ΔnirK-2	5'-gatcgtctcggcctgccg-3'
	ΔnirK-3	5'-AGGACAGGGATTGCGCCTAGcagtgaagtaaccatagcc-3'
	ΔnirK-4	5'-TGGGCTGTGGTTAAGCCGGCtttggcgtgtagttaccttgg-3'
	ΔnirK-5	5'-gcgacgccgtggtcttggag-3'
	ΔnirK-6	5'-gatgttcttgagctgcgg-3'
	pyrG-F	5'-CTAGGCGCAATCCCTGTCCTGG-3'
	pyrG-R	5'-GCCGGCTTAACCACAGCCCAAC-3'
*	*ΔCYP55A5*-1	5'-tatcactggcctcggccac-3'
	ΔCYP55A5-2	5'-cctcggcggatacgacgtac-3'
	ΔCYP55A5-3	5'-AGGACAGGGATTGCGCCTAGgttagcatgaaaggccagg-3'
	ΔCYP55A5-4	5'-TGGGCTGTGGTTAAGCCGGCggaggacgaggcgtatttg-3'
	ΔCYP55A5-5	5'-cgagtgtctagctggttcg-3'
	ΔCYP55A5-6	5'-caccgcggatcttgatacg-3'
	ΔnirK probe F	5'-cctccacagacagtcaatggcc-3'
	ΔnirK probe R	5'-cttgtcactgtctagccagacag-3'
	ΔCYP55A5-probe F	5'-tccctgactcaagagtccacac-3'
	ΔCYP55A5-probe R	5'-gtctcgttgacgaacctgcg-3'

* *CYP 55A5*: *A. oryzae* p450nor gene

Table 5-1 . Nucleotide sequences of primers used in this work.

Glycerol	30 g
POLYPEPTON	2 g
KH_2PO_4	1.36 g
$MgSO_4 \cdot 7H_2O$	0.2 g
Trace Element Solution	1 ml
DW	1000 ml
	pH 6.5

Table. 5-2. Glycerol-Peptone(GP) medium

$FeSO_4 \cdot 7H_2O$	10 g
$FeCl_3 \cdot 6H_2O$	10 g
$ZnCl_2$	2 g
$CuSO_4 \cdot 5H_2O$	1 g
$Na_2MoO_4 \cdot 2H_2O$	0.5 g
$CoCl_2 \cdot 6H_2O$	0.2 g
$MnCl_2 \cdot 4H_2O$	0.1 g
H_3BO_3	0.1 g
Citric acid	10 g
DW	1000 ml

Table. 5-3. Trace Element Solution

Chapter 6 Conclusion

In this work, I studied the enzymes involved in NO detoxification, denitrification and dissimilatory nitrate reduction in *Aspergillus oryzae*.

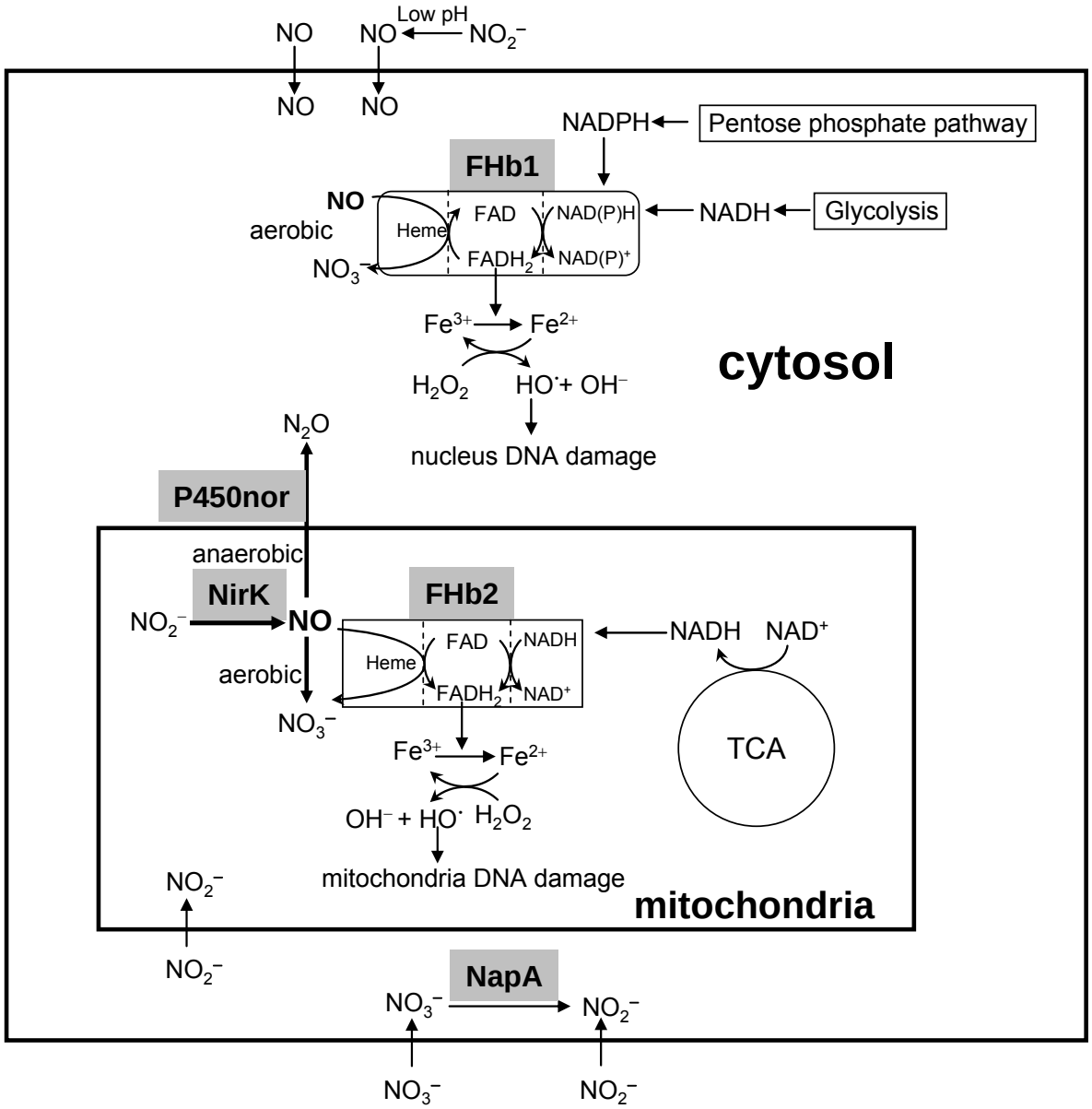

Enzymes studied in this work were shown in gray.

！ Flavohemoglobin (FHb) is demonstrated to play the role of NO detoxification under aerobic conditions in bacteria and yeast. Multiple FHb genes are found in some fungal genomes. I cloned two FHb genes (*fhb1*, *fhb2*) from *A. oryzae* and characterized the fugal FHbs in vitro and in vivo. Both of the recombinant FHbs exhibited robust NO dioxygenase activity. By the specificities against the electron donors (NADH or NADPH), FHb1 and FHb2 were suggested to be localized in cytosol and mitochondria, respectively. The transcription of *fhb1* is response to the external NO stress and FHb1 play a critical role in protecting the cells from NO toxicity. *fhb2* is only response to the mitochondrial NO.

In the presence of H_2O_2, both FHb1 and FHb2 showed deleterious effects on the growth of *A. oryzae*. Both of FHb1 and FHb2 share homology to flavin reductase. Like flavin reductase, FHbs can used the electrons offered by NAD(P)H to reduce FAD to $FADH_2$. $FADH_2$ can in turn act as a ferric iron reductant and then drive the Fenton reaction to generate hydroxyl radical ($HO\cdot$) which can cause DNA damage. So *A. oryzae* FHbs promote the oxidative stress of H_2O_2 probably depending on Fenton reaction in cytosol and mitochondria, respectively.

NirK, a dissimilatory nitrite reductase, was suggested to be cellular localized in *A. oryzae* mitochondria. Its transcription was response to denitrification conditions and the recombinant NirK exhibited robust anaerobic nitrite reductase activity. So *nir*K was suggested to involve in denitrification. However, *nirK*-deletion strains still kept the denitrification ability comparable to wild type. It suggested that there may be some isoenzyme existing in *A. oryzae*. On the other hand, p450nor was demonstrated to be vital to denitrification.

Nothing was known about the eukaryotic dissimilatory nitrate reductase. A gene encoding NapA-homology was isolated for the first time from *A. oryzae*. The recombinant NapA showed an anaerobic nitrate reductase activity. Unlike bacterial NapA, no typical targeting signal for transportation was found in *A. oryzae* NapA. Further characterization of NapA protein and its gene are underway.

Reference

1. **Averill, B. A.** 1996. Dissimilatory nitrite and nitric oxide reductases. Chemical Reviews **96:**2951-2964.
2. **Ballinger, S. W., B. Van Houten, G. F. Jin, C. A. Conklin, and B. F. Godley.** 1999. Hydrogen peroxide causes significant mitochondrial DNA damage in human RPE cells. Experimental Eye Research **68:**765-772.
3. **Bang, I. S., L. M. Liu, A. Vazquez-Torres, M. L. Crouch, J. S. Stamler, and F. C. Fang.** 2006. Maintenance of nitric oxide and redox homeostasis by the *Salmonella* flavohemoglobin Hmp. Journal of Biological Chemistry **281:**28039-28047.
4. **Beckman, J. S., T. W. Beckman, J. Chen, P. A. Marshall, and B. A. Freeman.** 1990. Apparent Hydroxyl Radical Production by Peroxynitrite - Implications for Endothelial Injury from Nitric-Oxide and Superoxide. Proceedings of the National Academy of Sciences of the United States of America **87:**1620-1624.
5. **Berks, B. C., D. J. Richardson, A. Reilly, A. C. Willis, and S. J. Ferguson.** 1995. The Napedabc Gene-Cluster Encoding the Periplasmic Nitrate Reductase System of *Thiosphaera-Pantotropha*. Biochemical Journal **309:**983-992.
6. **Bonamore, A., and A. Boffi.** 2008. Flavohemoglobin: Structure and reactivity. Iubmb Life **60:**19-28.
7. **Boyington, J. C., V. N. Gladyshev, S. V. Khangulov, T. C. Stadtman, and P. D. Sun.** 1997. Crystal structure of formate dehydrogenase H: Catalysis involving Mo, molybdopterin, selenocysteine, and an Fe4S4 cluster. Science **275:**1305-1308.
8. **Brown, G. C.** 1999. Nitric oxide and mitochondrial respiration. Biochimica Et Biophysica Acta-Bioenergetics **1411:**351-369.
9. **Buisson, N., and R. Labbe-Bois.** 1998. Flavohemoglobin expression and function in *Saccharomyces cerevisiae* - No relationship with respiration and complex response to oxidative stress. Journal of Biological Chemistry **273:**9527-9533.
10. **Campbell, W. H.** 1999. Nitrate reductase structure, function and regulation: Bridging the gap between biochemistry and physiology. Annual Review of Plant Physiology and Plant Molecular Biology **50:**277-+.
11. **Campbell, W. H.** 2001. Structure and function of eukaryotic NAD(P)H: nitrate reductase. Cellular and Molecular Life Sciences **58:**194-204.
12. **Carlioz, A., and D. Touati.** 1986. Isolation of Superoxide-Dismutase Mutants in *Escherichia coli* - Is Superoxide-Dismutase Necessary for Aerobic Life. Embo Journal **5:**623-630.

13. **Castello, P. R., P. S. David, T. McClure, Z. Crook, and R. O. Poyton.** 2006. Mitochondrial cytochrome oxidase produces nitric oxide under hypoxic conditions: Implications for oxygen sensing and hypoxic signaling in eukaryotes. Cell Metabolism **3:**277-287.

14. **Cooper, C. E.** 1999. Nitric oxide and iron proteins. Biochimica Et Biophysica Acta-Bioenergetics **1411:**290-309.

15. **Cramm, R., R. A. Siddiqui, and B. Friedrich.** 1994. Primary sequence and evidence for a physiological function of the flavohemoprotein of *Alcaligenes eutrophus*. Journal of Biological Chemistry **269:**7349-7354.

16. **Crawford, M. J., and D. E. Goldberg.** 1998. Role for the *salmonella* flavohemoglobin in protection from nitric oxide. Journal of Biological Chemistry **273:**12543-12547.

17. **Croteau, D. L., and V. A. Bohr.** 1997. Repair of oxidative damage to nuclear and mitochondrial DNA in mammalian cells. Journal of Biological Chemistry **272:**25409-25412.

18. **de Jesus-Berrios, M., L. M. Liu, J. C. Nussbaum, G. M. Cox, J. S. Stamler, and J. Heitman.** 2003. Enzymes that counteract nitrosative stress promote fungal virulence. Current Biology **13:**1963-1968.

19. **Dias, J. M., M. E. Than, A. Humm, R. Huber, G. P. Bourenkov, H. D. Bartunik, S. Bursakov, J. Calvete, J. Caldeira, C. Carneiro, J. J. G. Moura, I. Moura, and M. J. Romao.** 1999. Crystal structure of the first dissimilatory nitrate reductase at 1.9 angstrom solved by MAD methods. Structure **7:**65-79.

20. **Drapier, J. C., and J. B. Hibbs.** 1996. Aconitases: A class of metalloproteins highly sensitive to nitric oxide synthesis. Nitric Oxide, Pt B **269:**26-36.

21. **Fang, F. C.** 1997. Mechanisms of nitric oxide-related antimicrobial activity. Journal of Clinical Investigation **99:**2818-2825.

22. **Ferguson, S. J.** 1994. Denitrification and Its Control. Antonie Van Leeuwenhoek International Journal of General and Molecular Microbiology **66:**89-110.

23. **Flanagan, D. A., L. G. Gregory, J. P. Carter, A. Karakas-Sen, D. J. Richardson, and S. Spiro.** 1999. Detection of genes for periplasmic nitrate reductase in nitrate respiring bacteria and in community DNA. Fems Microbiology Letters **177:**263-270.

24. **Gardner, P. R.** 2005. Nitric oxide dioxygenase function and mechanism of flavohemoglobin, hemoglobin, myoglobin and their associated reductases. Journal of Inorganic Biochemistry **99:**247-266.

25. **Gardner, P. R., G. Costantino, and A. L. Salzman.** 1998. Constitutive and adaptive detoxification of nitric oxide in E*scherichia coli* - Role of nitric-oxide dioxygenase in the protection of aconitase. Journal of Biological Chemistry **273:**26528-26533.

26. **Gardner, P. R., A. M. Gardner, L. A. Martin, and A. L. Salzman.** 1998. Nitric oxide dioxygenase: An enzymic function for flavohemoglobin. Proceedings of the National Academy of Sciences of the United States of America **95:**10378-10383.

27. **Gliszczynska, A., and A. Koziolowa.** 1998. Chromatographic determination of flavin derivatives in baker's yeast. J Chromatogr A **822:**59-66.

28. **Gomi, K., Y. Iimura, and S. Hara.** 1987. Integrative Transformation of *Aspergillus oryzae* with a plasmid containing the *Aspergillus nidulans* argb Gene. Agricultural and Biological Chemistry **51:**2549-2555.

29. **Goretski, J., O. C. Zafiriou, and T. C. Hollocher.** 1990. Steady state nitric oxide concentrations during denitrification. Journal of Biological Chemistry **265:**11535-11538.

30. **Hasan, S. M., and J. B. Hall.** 1975. Physiological Function of nitrate reduction in *Clostridium perfringens*. Journal of General Microbiology **87:**120-128.

31. **Hausladen, A., A. J. Gow, and J. S. Stamler.** 1998. Nitrosative stress: Metabolic pathway involving the flavohemoglobin. Proceedings of the National Academy of Sciences of the United States of America **95:**14100-14105.

32. **Hromatka, B. S., S. M. Noble, and A. D. Johnson.** 2005. Transcriptional response of *Candida albicans* to nitric oxide and the role of the *YHB1* gene in nitrosative stress and virulence. Molecular Biology of the Cell **16:**4814-4826.

33. **Hutchinson, F.** 1985. Chemical changes induced in DNA by ionizing radiation. Progress in Nucleic Acid Research and Molecular Biology **32:**115-154.

34. **Iijima, M., H. Shimizu, Y. Tanaka, and H. Urushihara.** 2000. Identification and characterization of two flavohemoglobin genes in *Dictyostelium discoideum*. Cell Structure and Function **25:**47-55.

35. **Iijima, M., H. Shimizu, Y. Tanaka, and H. Urushihara.** 2000. Identification and characterization of two flavohemoglobin genes in *Dictyostelium discoideum*. Cell Struct Funct **25:**47-55.

36. **Ilari, A., A. Bonamore, A. Farina, K. A. Johnson, and A. Boffi.** 2002. The X-ray structure of ferric *Escherichia coli* flavohemoglobin reveals an unexpected geometry of the distal heme pocket. Journal of Biological Chemistry **277:**23725-23732.

37. **Kanaar, R., J. H. J. Hoeijmakers, and D. C. van Gent.** 1998. Molecular mechanisms of DNA double-strand break repair. Trends in Cell Biology **8:**483-489.

38. **Keilin, D., and A. Tissieres.** 1953. Haemoglobin in moulds *Neurospora crassa* and *Penicillium notatum*. Nature **172:**393-394.

39. **Kim, S. O., Y. Orii, D. Lloyd, M. N. Hughes, and R. K. Poole.** 1999. Anoxic function for the *Escherichia coli* flavohaemoglobin (Hmp): reversible binding of nitric oxide

and reduction to nitrous oxide. Febs Letters **445:**389-394.

40. **Kitamoto, K.** 2002. Molecular biology of the Koji molds. Advances in Applied Microbiology, Vol 51 **51:**129-153.
41. **Kobayashi, M., Y. Matsuo, A. Takimoto, S. Suzuki, F. Maruo, and H. Shoun.** 1996. Denitrification, a novel type of respiratory metabolism in fungal mitochondrion. Journal of Biological Chemistry **271:**16263-16267.
42. **Kudo, T., N. Takaya, S. Y. Park, Y. Shiro, and H. Shoun.** 2001. A positively charged cluster formed in the heme-distal pocket of cytochrome P450nor is essential for interaction with NADH. J Biol Chem **276:**5020-6.
43. **Liang, F. Q., and B. F. Godley.** 2003. Oxidative stress-induced mitochondrial DNA damage in human retinal pigment epithelial cells: a possible mechanism for RPE aging and age-related macular degeneration. Experimental Eye Research **76:**397-403.
44. **Liu, L. M., M. Zeng, A. Hausladen, J. Heitman, and J. S. Stamler.** 2000. Protection from nitrosative stress by yeast flavohemoglobin. Proceedings of the National Academy of Sciences of the United States of America **97:**4672-4676.
45. **Ljungman, M., and P. C. Hanawalt.** 1992. Efficient protection against oxidative DNA damage in chromatin. Molecular Carcinogenesis **5:**264-269.
46. **Mandavilli, B. S., J. H. Santos, and B. Van Houten.** 2002. Mitochondrial DNA repair and aging. Mutation Research-Fundamental and Molecular Mechanisms of Mutagenesis **509:**127-151.
47. **Marletta, M. A.** 1993. Nitric oxide synthase - Function and Mechanism. Faseb Journal **7:**A1129-a1129.
48. **McAlpine, A. S., A. G. McEwan, and S. Bailey.** 1998. The high resolution crystal structure of DMSO reductase in complex with DMSO. Journal of Molecular Biology **275:**613-623.
49. **Membrillo-Hernandez, J., M. D. Coopamah, M. F. Anjum, T. M. Stevanin, A. Kelly, M. N. Hughes, and R. K. Poole.** 1999. The flavohemoglobin of *Escherichia coli* confers resistance to a nitrosating agent, a "nitric oxide releaser," and paraquat and is essential for transcriptional responses to oxidative stress. Journal of Biological Chemistry **274:**748-754.
50. **Membrillo-Hernandez, J., M. D. Coopamah, A. Channa, M. N. Hughes, and R. K. Poole.** 1998. A novel mechanism for upregulation of the *Escherichia coli* K-12 *hmp* (flavohaemoglobin) gene by the 'NO releaser', S-nitrosoglutathione: nitrosation of homocysteine and modulation of MetR binding to the *glyA-hmp* intergenic region. Molecular Microbiology **29:**1101-1112.

51. **MembrilloHernandez, J., N. Ioannidis, and R. K. Poole.** 1996. The flavohaemoglobin (HMP) of *Escherichia coli* generates superoxide in vitro and causes oxidative stress in vivo. Febs Letters **382:**141-144.

52. **Modolo, L. V., O. Augusto, I. M. G. Almeida, J. R. Magalhaes, and I. Salgado.** 2005. Nitrite as the major source of nitric oxide production by *Arabidopsis thaliana* in response to Pseudomonas syringae. Febs Letters **579:**3814-3820.

53. **Moreno-Vivian, C., P. Cabello, M. Martinez-Luque, R. Blasco, and F. Castillo.** 1999. Prokaryotic nitrate reduction: Molecular properties and functional distinction among bacterial nitrate reductases. Journal of Bacteriology **181:**6573-6584.

54. **Morozkina, E. V., and R. A. Zvyagilskaya.** 2007. Nitrate reductases: Structure, functions, and effect of stress factors. Biochemistry-Moscow **72:**1151-1160.

55. **Mukai, M., C. E. Mills, R. K. Poole, and S. R. Yeh.** 2001. Flavohemoglobin, a globin with a peroxidase-like catalytic site. Journal of Biological Chemistry **276:**7272-7277.

56. **Mukhopadhyay, P., M. Zheng, L. A. Bedzyk, R. A. LaRossa, and G. Storz.** 2004. Prominent roles of the NorR and Fur regulators in the *Escherichia coli* transcriptional response to reactive nitrogen species. Proceedings of the National Academy of Sciences of the United States of America **101:**745-750.

57. **Nakahara, K., T. Tanimoto, K. Hatano, K. Usuda, and H. Shoun.** 1993. Cytochrome P-450 55A1 (P-450dNIR) acts as nitric oxide reductase employing NADH as the direct electron donor. J Biol Chem **268:**8350-5.

58. **Omura, T., and R. Sato.** 1964. The Carbon monoxide binding pigment of liver microsomes. Ii. Solubilization, Purification, and Properties. J Biol Chem **239:**2379-85.

59. **Philippot, L., A. ClaysJosserand, R. Lensi, I. Trinsoutreau, P. Normand, and P. Potier.** 1997. Purification of the dissimilative nitrate reductase of *Pseudomonas fluorescens* and the cloning and sequencing of its corresponding genes. Biochimica Et Biophysica Acta-Gene Structure and Expression **1350:**272-276.

60. **Poole, R. K., M. F. Anjum, J. MembrilloHernandez, S. O. Kim, M. N. Hughes, and V. Stewart.** 1996. Nitric oxide, nitrite, and *fnr* regulation of *hmp* (Flavohemoglobin) gene expression in *Escherichia coli* K-12. Journal of Bacteriology **178:**5487-5492.

61. **Poole, R. K., N. Ioannidis, and Y. Orii.** 1994. Reactions of the *Escherichia coli* Flavohaemoglobin (Hmp) with oxygen and reduced nicotinamide adenine dinucleotide - Evidence for oxygen switching of flavin oxidoreduction and a mechanism for oxygen sensing. Proceedings of the Royal Society of London Series B-Biological Sciences **255:**251-258.

62. **Radi, R., J. S. Beckman, K. M. Bush, and B. A. Freeman.** 1991. Peroxynitrite

induced membrane lipid peroxidation - the cytotoxic potential of superoxide and nitric oxide. Archives of Biochemistry and Biophysics **288:**481-487.

63. **Rockel, P., F. Strube, A. Rockel, J. Wildt, and W. M. Kaiser.** 2002. Regulation of nitric oxide (NO) production by plant nitrate reductase in vivo and in vitro. Journal of Experimental Botany **53:**103-110.

64. **Salazar, J. J., and B. Van Houten.** 1997. Preferential mitochondrial DNA injury caused by glucose oxidase as a steady generator of hydrogen peroxide in human fibroblasts. Mutation Research-DNA Repair **385:**139-149.

65. **Santini, C. L., B. Ize, A. Chanal, M. Muller, G. Giordano, and L. F. Wu.** 1998. A novel Sec-independent periplasmic protein translocation pathway in *Escherichia coli*. Embo Journal **17:**101-112.

66. **Santos, J. H., L. Hunakova, Y. M. Chen, C. Bortner, and B. Van Houten.** 2003. Cell sorting experiments link persistent mitochondrial DNA damage with loss of mitochondrial membrane potential and apoptotic cell death. Journal of Biological Chemistry **278:**1728-1734.

67. **Sargent, F., E. G. Bogsch, N. R. Stanley, M. Wexler, C. Robinson, B. C. Berks, and T. Palmer.** 1998. Overlapping functions of components of a bacterial Sec-independent protein export pathway. Embo Journal **17:**3640-3650.

68. **Seaver, L. C., and J. A. Imlay.** 2001. Hydrogen peroxide fluxes and compartmentalization inside growing *Escherichia coli*. Journal of Bacteriology **183:**7182-7189.

69. **Shiro, Y., M. Fujii, T. Iizuka, S. Adachi, K. Tsukamoto, K. Nakahara, and H. Shoun.** 1995. Spectroscopic and kinetic studies on reaction of cytochrome P450nor with nitric oxide. Implication for its nitric oxide reduction mechanism. J Biol Chem **270:**1617-23.

70. **Shoun, H., D. H. Kim, H. Uchiyama, and J. Sugiyama.** 1992. Denitrification by fungi. FEMS Microbiol Lett **73:**277-81.

71. **Shoun, H., and T. Tanimoto.** 1991. Denitrification by the fungus *Fusarium oxysporum* and involvement of cytochrome P-450 in the respiratory nitrite reduction. J Biol Chem **266:**11078-82.

72. **Stevanin, T. M., N. Ioannidis, C. E. Mills, S. O. Kim, M. N. Hughes, and R. K. Poole.** 2000. Flavohemoglobin hmp affords inducible protection for *Escherichia coli* respiration, catalyzed by cytochromes bo ' or bd, from nitric oxide. Journal of Biological Chemistry **275:**35868-35875.

73. **Takahashi, T., T. Masuda, and Y. Koyama.** 2006. Enhanced gene targeting frequency in *ku70* and *ku80* disruption mutants of *Aspergillus sojae* and *Aspergillus oryzae*.

Molecular Genetics and Genomics **275:**460-470.

74. **Ullmann, B. D., H. Myers, W. Chiranand, A. L. Lazzell, Q. Zhao, L. A. Vega, J. L. Lopez-Ribot, P. R. Gardner, and M. C. Gustin.** 2004. Inducible defense mechanism against nitric oxide in *Candida albicans*. Eukaryotic Cell **3:**715-723.

75. **Ushijima, S., and T. Nakadai.** 1987. Breeding by Protoplast Fusion of Koji Mold, *Aspergillus sojae*. Agricultural and Biological Chemistry **51:**1051-1057.

76. **Usuda, K., N. Toritsuka, Y. Matsuo, D. H. Kim, and H. Shoun.** 1995. Denitrification by the fungus *Cylindrocarpon tonkinense* - Anaerobic cell growth and 2 isozyme forms of cytochrome P450Nor. Applied and Environmental Microbiology **61:**883-889.

77. **Wakabayashi, S., H. Matsubara, and D. A. Webster.** 1986. Primary sequence of a dimeric bacterial hemoglobin from *Vitreoscilla*. Nature **322:**481-483.

78. **Watsuji, T. O., N. Takaya, A. Nakamura, and H. Shoun.** 2003. Denitrification of nitrate by the fungus *Cylindrocarpon tonkinense*. Biosci Biotechnol Biochem **67:**1115-20.

79. **Weiner, J. H., P. T. Bilous, G. M. Shaw, S. P. Lubitz, L. Frost, G. H. Thomas, J. A. Cole, and R. J. Turner.** 1998. A novel and ubiquitous system for membrane targeting and secretion of cofactor-containing proteins. Cell **93:**93-101.

80. **Wink, D. A., K. S. Kasprzak, C. M. Maragos, R. K. Elespuru, M. Misra, T. M. Dunams, T. A. Cebula, W. H. Koch, A. W. Andrews, J. S. Allen, and L. K. Keefer.** 1991. DNA deaminating ability and genotoxicity of nitric oxide and its progenitors. Science **254:**1001-1003.

81. **Wittenberg, J. B., and B. A. Wittenberg.** 1990. Mechanisms of Cytoplasmic Hemoglobin and Myoglobin Function. Annual Review of Biophysics and Biophysical Chemistry **19:**217-241.

82. **Woodmansee, A. N., and J. A. Imlay.** 2002. Reduced flavins promote oxidative DNA damage in non-respiring Escherichia coli by delivering electrons to intracellular free iron. Journal of Biological Chemistry **277:**34055-34066.

83. **Wu, G. H., L. M. Wainwright, and R. K. Poole.** 2003. Microbial globins. Advances in microbial physiology, Vol 47 **47:**255-310.

84. **Yakes, F. M., and B. VanHouten.** 1997. Mitochondrial DNA damage is more extensive and persists longer than nuclear DNA damage in human cells following oxidative stress. Proceedings of the National Academy of Sciences of the United States of America **94:**514-519.

85. **Yamasaki, H., and Y. Sakihama.** 2000. Simultaneous production of nitric oxide and peroxynitrite by plant nitrate reductase: in vitro evidence for the NR-dependent formation of active nitrogen species. Febs Letters **468:**89-92.

86. **Yamasaki, H., Y. Sakihama, and S. Takahashi.** 1999. An alternative pathway for nitric oxide production in plants: new features of an old enzyme. Trends in Plant Science **4:**128-129.

87. **Zhao, X. J., D. Raitt, P. V. Burke, A. S. Clewell, K. E. Kwast, and R. O. Poyton.** 1996. Function and expression of flavohemoglobin in *Saccharomyces cerevisiae* - Evidence for a role in the oxidative stress response. Journal of Biological Chemistry **271:**25131-25138.

88. **Zumft, W. G.** 1997. Cell biology and molecular basis of denitrification. Microbiology and Molecular Biology Reviews **61:**533-616

Acknowledgments

I would like to express my sincere gratitude to professor, Hirofumi Shoun, who supported and directed my doctor theme. I also appreciate his care in my life.

Sincere thanks are also for associate professor Takayoshi Wakagi and Dr. Shinya Fushinobu, who gave me many instructions and advances benefited me greatly.

I thank associate professor Hiroyuki Horiuchi (Laboratory of Cellular Genetics) and Dr. Jun-ichi Maruyama (Laboratory of Microbiology) who provided the necessary plasmid and gave me many technical supports.

I must thank Mr. Yoshito Nakanishi who gave me very great aids especially at the beginning of my study in this lab when the help was instant. I thank Dr. Sangwan Kim and Dr. Hiroshi Nishimasu who gave me many good advices and help me to solve the problems in my experiments. I am grateful for the care of Mio Fujimoto in my study and life. I also thank my classfellow and friend Noriyuki Ogawa and Lianhua Xu who also gave me many helps in my study. In additional, I thank the other members of my lab who had made a pleased atmosphere to do research.